Adsorption of hydrocarbons in porous materials: a computational study

Joseph Fox

Thesis submitted for the degree of Doctor of Philosophy

School of Physics

University of Edinburgh

January 17, 2005

Abstract

Porous materials, such as zeolites and mesopores, are widely used and have many industrial and domestic applications. One of the most lucrative uses is in the petrochemical industry where crude oil is refined to form products such as petrol. Petrol consists of a mixture of many different types of hydrocarbons, some more valuable than others. Porous materials play a vital role in altering the composition of the mixture to increase its value and performance as a fuel. The porous materials can be used as both molecular sieves which separate mixtures of different molecules and catalysts which convert one molecular type to another. Both of these functions rely on hydrocarbon molecules moving inside the material, and adsorbing onto its internal surface, deep within the porous network. However, the efficiency of the porous materials can be greatly reduced by a build up of adsorbed molecules which may block the path of other molecules through the porous network. It is therefore important to know how mixtures of hydrocarbons behave inside porous materials and where in the pores they are able to adsorb.

In this work, Monte Carlo computer simulations are used to study hydrocarbon molecules (linear, branched and cyclic) within the pores of four different porous materials: three zeolites (silicalite-1, $AlPO_4$-5 and ITQ-22) and one mesopore (MCM-41). The three zeolites have different compositions and pore structures and include an extremely well known and widely used structure (silicalite-1), a recently synthesised zeolite with a complex pore structure (ITQ-22) and a zeolite with a simple, one dimensional pore structure ($AlPO_4$-5). The mesopore, MCM-41, has pores which are an order of magnitude larger than the zeolites and can therefore accommodate many more hydrocarbons within its porous network.

The adsorption characteristics of the three hydrocarbons in the zeolites are simulated and compared with the available experimental data. Binary and ternary mixtures of the hydrocarbons are also studied and the temperature dependence of the selectivity of each zeolite is discussed and an explanation given for any reversal in selectivity at high temperature. Ideal Adsorption solution Theory is used to predict the behaviour of mixtures in zeolites and the results of the theory are compared with the simulations.

A new computational model for MCM-41 is introduced and used to study the adsorption of hydrocarbons within its pores. The results are compared with experiments (where possible) and the structure of the adsorbed molecules is investigated. Possible refinements to the model are proposed and their affect on the adsorption properties discussed.

Declaration

I declare that this thesis and the work described therein was carried out by the author and has not been submitted to any other degree or professional qualification.

Joseph Paul Fox

January 17, 2005

Acknowledgements

I would like to thank my supervisor and friend, Simon Bates, for his help, guidance, enthusiasm, friendship and rowing competitions! Thanks also to Prof Lovat Rees, Dr Lijuan Song and Christian Schumacher for useful discussions on zeolites and mesopores. A special thanks to Vincent Rooy who patiently guided me through the code and answered all of my (stupid) questions. I must also thank my friends for making sure that I don't always think about my PhD. Thanks to Julie for putting up with my moods and helping and supporting me through the course of this work.

Thanks to my brother, Paddy, for always having the right answers and for getting me through every physics exam I have ever taken!

However, I could never have undertaken this work if it were not for the love, support and generosity of my parents. This thesis is dedicated to them.

Contents

Chapter 1

Introduction

This chapter aims to introduce the reader to porous materials and their interaction with molecules within their pores. The first two sections will familiarise the reader with the structure and uses of porous materials along with their synthesis. Next, a brief introduction to the hydrocarbon molecules used in this work will be given. The interaction between the porous materials and the hydrocarbons will be discussed, along with the ways in which this interaction can be probed. A brief summary of previous simulation work will then be given followed by the outline and scope of this thesis. This introduction is not intended to be exhaustive but is designed to give the reader sufficient background to understand the motivation for this work.

1.1 Zeolites and mesopores as porous materials

Porous materials are those which allow gases or liquids to move through their voids by way of pores. This description covers a wide range of substances including trees, sponges, carbon nanotubes, celery, foam, and some rocks. However, for the purposes of this work, the term 'porous materials' will refer to *zeolites* and *mesopores*.

There are many different types of zeolites, both naturally occurring (around 40 types) and synthetic (more than 150 types) and were first discovered, in their natural form, by the Swedish mineralogist Baron Cronstedt in the 18^{th} century. Zeolites are microporous aluminium silicate materials whose crystalline structure can also include cations of sodium, potassium, calcium,

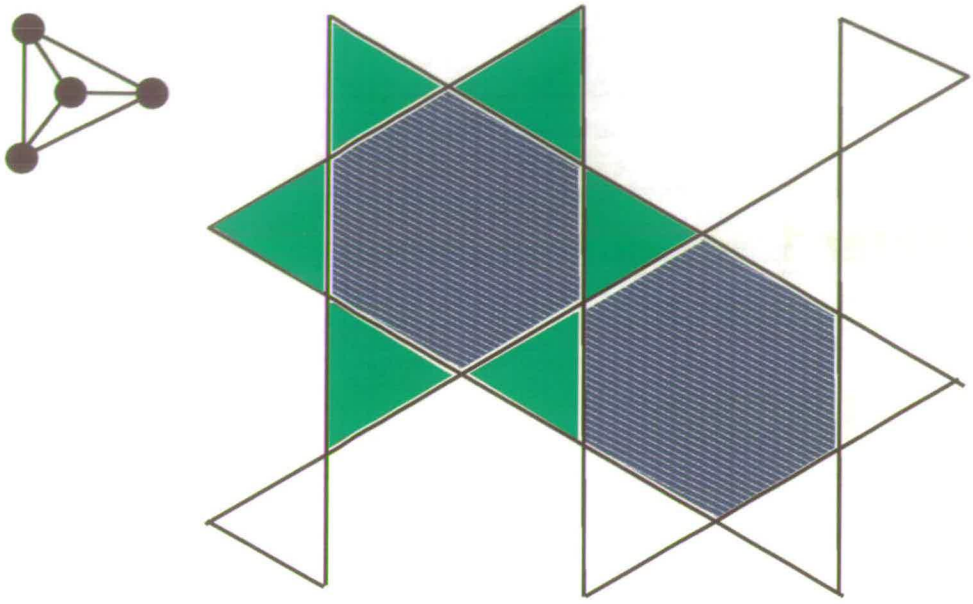

Figure 1.1: A schematic representation of a zeolite structure. In this example, channels (complete channels are highlighted in blue) are formed by connecting 6 tetrahedral building blocks. The secondary building unit is highlighted in green and contains 6 corner connected tetrahedra. A single building block is shown on the left: the black circles represent the oxygen atoms.

strontium, hydrogen or barium. They have pores whose diameters range from 3 to 10Å which connect together in regular, crystalline patterns which can form 3-dimensional interconnected networks. Zeolites may permit molecules to enter the network but only if the molecules are small enough to negotiate the pores - large molecules will not fit and are therefore excluded from the zeolite porous network. In this way, zeolites can be used to *sieve* and separate mixtures of different molecules.

Although zeolites have complex structures they are all based on a simple XO_4 tetrahedral building block where X stands for silicon or aluminium[1]. These relatively simple building blocks link together, via their corners, to form more complicated secondary building units (SBUs) as shown in Figure 1.1. SBUs can contain different numbers of tetrahedra in many different orientations which can connect to form structures which have cavities and pores. The connectivity of the network of cavities and pores can range from straight, unconnected channels to complex 3-dimensional interconnected networks. The example shown in Figure

[1] or phosphorous in the case of the aluminophosphate, $AlPO_4$-5

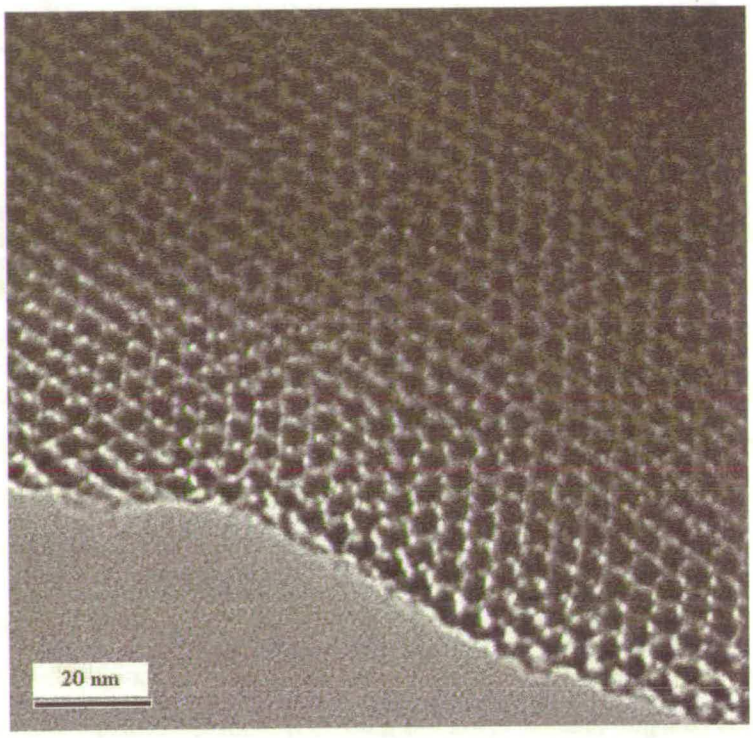

Figure 1.2: A Transmission Electron Microscopy image of MCM-41 from reference [1].

1.1 is a simplified 2-dimensional representation of a zeolite, in reality the structures are more complicated with the tetrahedra connecting in 3-dimensions and the SBUs enclosing volumes and not simply areas as seen in Figure 1.1. The variety of different zeolite topologies and the different atoms which can be used to construct the tetrahedra, result in many distinct zeolites with varying pore networks which exhibit particular properties and may be suited to particular applications.

In principle, zeolites have a perfectly crystalline structure. However, in practice a zeolite will contain non-crystalline defects such as pore blockages or the regions where two crystals join. The boundary between two crystals of a zeolite will result in a pore blockage since the pores of the two crystals will not, in general, align. These defects can affect the way guest molecules (molecules within the porous network) behave by reducing their mobility and restricting the ease with which they are able to negotiate their way though the zeolite.

Unlike zeolites, which are crystalline materials, mesopores are non-crystalline and do not have

well defined atomic positions. They do, however, have a regular structure comprising (in the case of MCM-41 [2], the mesopore used in this study) a hexagonal array of straight pores, whose diameter is much larger than those of a zeolite, typically tens of Angstroms, surrounded by an amorphous silicon and oxygen structure (see Figure 1.2). Since MCM-41 is not crystalline, the usual techniques used to determine the exact structure, such as x-ray diffraction, cannot accurately predict the atomic coordinates. X-ray diffraction can only determine the atomic positions if there are distinct peaks in the diffraction pattern - this would indicate a repeated, periodic structure in the substance, i.e. a crystalline structure. Since there is no repeated pattern (other than the arrangement of the pores) in MCM-41, x-ray diffraction cannot be used to detect the atomic positions. As is the case for zeolites, there will be imperfections in MCM-41 and experimentally one would expect these to lead to pore constrictions and blockages.

The understanding of the complex structure of zeolites and mesopores has been the topic of many experimental and simulation studies. These studies aim to not only determine and categorise the porous structure but also to attempt to design (both theoretically and experimentally) new materials with novel pore structures. It is the porous structure of zeolites and mesopores which makes them widely used in many different applications, some of which will now be explored.

Zeolites have a wide variety of uses both industrial and domestic with world consumption (in 2000) reaching almost 4 Million tons. Domestically, they are used in detergents, cat litter, shoe deodorisers, catalytic converters, soil conditioners and beer keg coolers [3, 4]. These applications make use of the zeolite as a selective adsorber (in the case of cat litter and shoe deodorisers), an ion exchanger (in soil conditioners and detergents, where, for example, the calcium in the water is replaced by sodium within the zeolite), a catalyst (in a catalytic converter where harmful exhaust products are removed) and finally as a coolant in the beer keg cooler where the zeolite is used to quickly adsorb water vapour - resulting in a drop in temperature due to evaporation.

In industry, zeolites are used as filters for ammonia in kidney-dialysis machines, supplements in animal diets, pollution control and, perhaps the most important, in the refining of crude oil

[2] MCM-41 stands for *M*obil *C*omposition of *M*atter and was first synthesised [2] in 1992.

to form petrol. These applications make use of the zeolite as an adsorber (dialysis machines, feed supplements - where ammonia is adsorbed to control levels of urea in the animal - and pollution control) and as both a molecular sieve and a catalyst in the petrochemical industry.

Mesopores are less widely used but still play an important role in many applications such as drug delivery [5, 6], catalysis [7], nuclear waste removal [8], removal of sulphur and aromatics from diesel fuel [9] and have potential uses such as biological hosts [5] and magnetic storage media [10]. These applications make use of the adsorption and catalytic properties of MCM-41 whilst its potential use as a magnetic storage material would require the confinement of ferromagnetic material within the pores of MCM-41.

Whilst all of the uses of zeolites and mesopores are of great benefit[3], it is the use in the petrochemical industry which is arguably the most valuable. In this role, a zeolite is used to improve the quality of fuel by altering the fraction of each type of hydrocarbon within the fuel mixture - this will be discussed in more detail later in this chapter.

1.2 Synthesis

Some porous materials are naturally occurring whereas others are synthesised. Zeolite synthesis involves clustering a solution of silicon and oxygen around organic template molecules to form primary building units which then aggregate and grow to form crystals - eventually leading to zeolite crystals (once the organic templates have been removed) as shown in Figure 1.3. This process normally occurs at high temperature, around 700K and takes many days to complete[4].

The synthesis of mesopores involves using micelles (a submicroscopic aggregation of organic molecules) as a template for the pores. In the synthesis of MCM-41, hexagonal arrays of cylindrical micelles are surrounded by a silicon and oxygen aqueous solution which, when the micelles are removed by calcination (i.e. heating), form a material with a regular array of pores.

[3] some more so than others, see reference [4] for details of beer keg coolers

[4] although recently, Cooper *et al.* [11] have shown how synthesis can be achieved at much lower temperatures - less than 450K

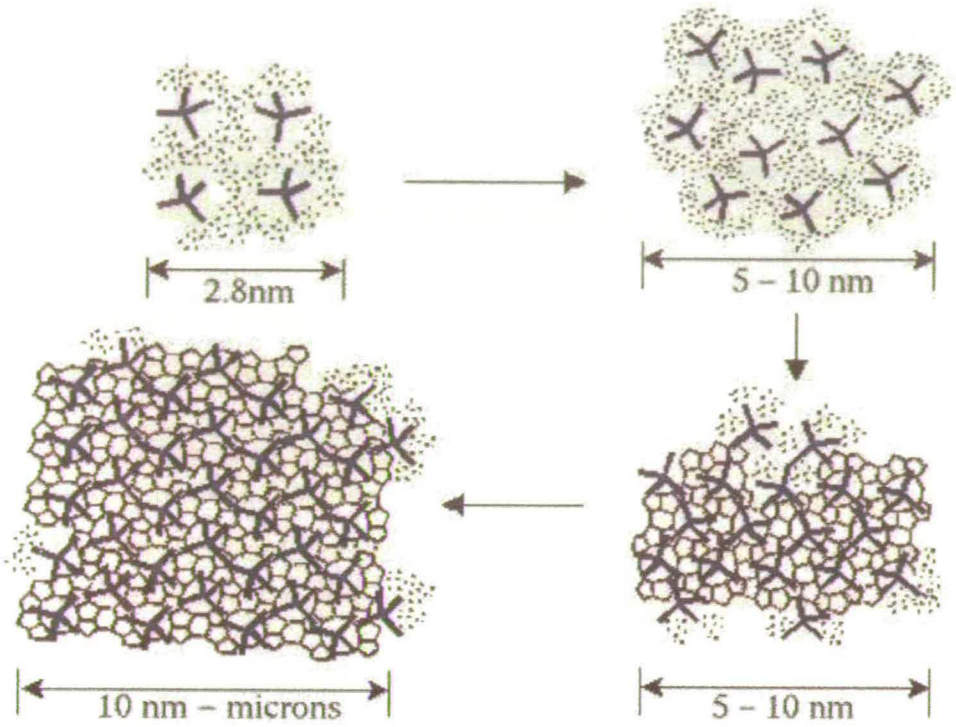

Figure 1.3: A schematic of the synthesis of a zeolite. Blue crosses represent the organic template and the black dots represent the silicon and oxygen solution. The molecules cluster and the clusters grow (indicated by the arrows) and form crystals on the micron scale. After growth, the organic templates are removed to leave the zeolite structure. The image is based on reference [12].

Again this process requires high temperatures (around 700K) and takes many days to produce the completed mesopores.

Zeolites and mesopores may have acidic sites within their structure formed, for example, by replacing one of the silicon atoms with an aluminium atom, and compensating for the resulting charge imbalance by adding a hydrogen to one of the oxygen atoms (the bridging oxygen - which is bonded to the aluminium atom). These acidic sites play a vital role in the ability of the zeolite to act as a catalyst and there is a great deal of effort spent attempting to control the location (which affects the strength of the acid site) and quantity (which affects activity of the zeolite/mespore) of the acidic sites.

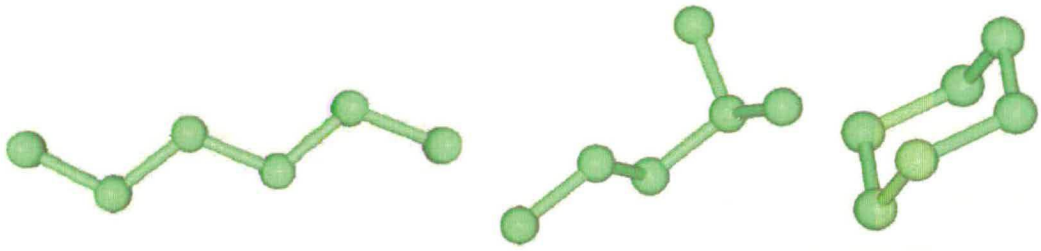

Figure 1.4: Schematic representation of the structure of (from left to right) hexane, 2-methylpentane and cyclohexane. For clarity, only the carbon atoms are shown.

1.3 Hydrocarbons

Crude oil is a mixture of many different types of hydrocarbons; linear, branched, cyclic, both saturated (no double bonds) and unsaturated. Not all of the components of crude oil are useful in petrol and so the process of refining crude oil aims to decrease the concentration of these less important molecules. Typically, petrol consists of linear hydrocarbons ranging in size between 4 and 8 carbon atoms, branched hydrocarbons between 5 and 10 carbon atoms and cyclic hydrocarbons between 5 and 9 carbon atoms. The hydrocarbons used in this study are typical of those found in both crude oil and petrol and comprise linear, branched and cyclic alkanes with 6 carbon atoms, namely; hexane, 2-methylpentane, and cyclohexane which are shown schematically in Figure 1.4. Whilst all of these molecules consist of the same number of carbon atoms, their structures are very different giving each molecule unique properties and, since the ease with which a molecule moves through a zeolite depends on its size, each molecule may behave very differently in a zeolite. The size[5] of each of the molecules varies from 4.3Å for hexane to 5.4Å for 2-methylpentane and 6.0Å for cyclohexane. The three molecules also have very different octane numbers [13], ranging from 25 for hexane to 83 for cyclohexane and 73 for 2-methylpentane: the octane number of a hydrocarbon is a measure of its potency as a fuel, for example, an octane number of 100 is indicative of a hydrocarbon which will give excellent performance whilst a smaller octane number (such as 0 for heptane) indicates lower levels of performance.

The properties of hydrocarbons have been well studied both experimentally and using com-

[5]in this case, the 'size' is actually the critical diameter which is the diameter of the smallest cylinder that circumscribes the molecule

puter simulations to model their fluid properties [14–21]. The 'fluid properties' include how a mixture of the hydrocarbon in its vapour and liquid state will behave. This is an important step in the simulation of pure hydrocarbons and will be discussed in further detail in Chapter 2.

Although the study of hydrocarbons is an important field, it is the behaviour of the molecules within porous materials which is of special interest.

1.4 Hydrocarbons within porous materials

It is important to investigate the interaction between porous materials and hydrocarbons from both an academic and industrial viewpoint. Academically, the behaviour of hydrocarbons within the pores presents a excellent opportunity to probe the subtle forces which dictate the energetic landscape of the hydrocarbon-porous material interaction. From an industrial perspective, further understanding of the processes involving both hydrocarbons and zeolites/mesopores could improve the efficiency of the industrial techniques - even a small increase in efficiency could result in major financial benefits.

The role of zeolites and mesopores in industry is varied but, as the next few paragraphs will show, it is the adsorption of molecules within their pores which is particularly important to both catalysis and molecular sieving.

There are several distinct steps in the process of zeolite/mesopore catalysis. The guest molecule must *diffuse* through the pore before it can *adsorb* onto the surface and undergo a *reaction* with the catalyst. Once this reaction is complete the products then *desorb* from the surface and *diffuse* through and out of the porous network. In the petrochemical industry, it is common for pores of the catalyst to become blocked (fouled) with products of a reaction which adsorb onto the internal surface and reduce the efficiency of the catalyst. It is therefore vital to know where in the zeolite a molecule will adsorb, so that steps can be taken to reduce the fouling of the catalyst. Furthermore, since the molecules which foul the catalyst are constituents of a mixture, it is necessary to know how different molecules in a mixture of many species behave within the porous network.

Porous materials are also used as molecular sieves, whereby mixtures of different molecular

types can be separated. This may be achieved by selective adsorption of one type of molecule over another - thus the porous material fills with one type of molecule and correspondingly its concentration in the mixture decreases. Knowing where a particular molecule prefers[6] to adsorb within the porous network is vital when determining how a mixture should be separated (if both molecules are found to adsorb at similar sites or in similar quantities then it may be necessary to use a different method to separate a mixture comprising the two species).

In small pores (relative to the size of the adsorbed molecules) the interaction between the molecule and the pore is the dominant factor controlling the adsorption: the interaction between the adsorbed molecules is less important because the molecules are few in number and, in general, do not come into close proximity with one another due to the tight fit within the pores. However, the adsorbate-adsorbate interaction will influence the adsorption in a mesopore, such as MCM-41, to a much larger extent than in a zeolite since in a mesopore the pores are much larger and are able to accommodate more adsorbates which will come into contact with one another more readily than in a zeolite.

It is important to understand the behaviour of different molecules within the porous network, but what is the best way to investigate the adsorbate-adsorbent interaction?

1.4.1 Simulations versus experiments

The adsorption of hydrocarbons in certain zeolites can be a very slow process, especially if the molecule finds it difficult to manoeuvre through the porous network. Indeed, it can take weeks for the adsorption process to reach equilibrium if the molecule is particularly cumbersome - if its size is close to that of the pore diameter. Performing an experiment to investigate the adsorption properties of hydrocarbons in porous materials not only suffers from this problem of long duration but it becomes very difficult to find accurate data on the adsorption of mixtures. This is because not only must the experiment be allowed to equilibrate but the different adsorbed species must be distinguished from one another to determine the quantity of each adsorbed component of the mixture. Furthermore, experiments at very low pressures (which are

[6]Every molecule has a preference for the lowest energy site - the location of this site depends on the interaction between the molecule and its surroundings, which may include other molecules, as well as the porous material.

important when determining the Henry coefficient, see Chapter 2) are easily disrupted by slight changes in pressure and so it is vital that the (very low) pressure be kept constant. These difficulties present great challenges to the experimentalist who must be able to accurately maintain pressures for long periods of time and be able to analyse the adsorbed components.

One challenge of understanding hydrocarbon adsorption is to determine *where* in the porous materials a particular molecule prefers to adsorb. Analysing the adsorption locations of mixtures of different molecules increases the complexity since these molecules must be identified *in situ* - raising further problems for experimentalists.

An alternative to performing laboratory experiments may be to use computer simulations. The 'computer experiment' is not designed to replace the conventional laboratory experiment but is, instead, a complementary technique. There are many different techniques available to the simulator - each one is particularly suited to certain situations but may be less efficient (or worse, wrong) in other situations. Thus it is important to choose the simulation method correctly and to set up the simulation precisely. In the same way as an laboratory experiment can be ruined by poor apparatus set up, so too can a computer experiment be ruined by poor set up of the components, such as the model, potential parameters (see Chapter 2 and 3 for details) or input files. Both the laboratory experimentalist and computer simulation practitioner must know how their 'apparatus' works to be able to make the best use of it. Knowledge of the the strengths and limitations of the different simulation techniques can allow for the correct choice, enabling accurate computer experiments.

Laboratory experiments frequently reveal *macroscopic* information such as the mass of molecules which adsorb within a porous material, or the average speed of diffusion in a particular direction through the pores. However, computer simulations allow an extra level of information to be analysed; it is possible to predict not only the total mass of molecules which adsorb but also their preferred adsorption location and the orientation of a molecule at a particular site in the porous network. It is also possible to perform simulations that reveal information that would be impossible to obtain using conventional laboratory experiments; making use of the interaction potential between a molecule and a porous material, it is possible to build up a detailed picture of the energetic landscape that a molecule would encounter as it moves through the porous

network. This 'picture' of the adsorbate-zeolite/mesopore interaction is made possible by the *microscopic* information available from the computer simulation - the potential energy can be determined at every point. With the extra detail available from computer simulations it is possible to analyse the adsorption of molecules in porous materials from both the macroscopic and microscopic level.

Care must be taken when making predictions based on the microscopic information from computer simulations to ensure that every possible comparison with experiment is made. If these comparisons are made (and the two methods compare favourably) then it is possible to use the model to predict *new* features of the adsorption process and, more importantly, to have confidence in these predictions. If the simulations do not agree with the available experimental data then it is difficult to make predictions with any authority.

Many new porous materials are synthesised, each with its own unique structure and pore network. Each new porous material may have the potential to be used in a variety of different industrial or domestic applications. Using laboratory experiments to investigate every new porous material to determine its properties, such as adsorption or catalysis, may take a significant length of time and may result in no useful properties being found. To speed up this process, it is possible to perform simulations of newly synthesised porous materials (as has been done in this work) to determine their properties in a much shorter time than the equivalent laboratory experiments. However, care must be taken to ensure that the correct techniques and forcefields are used in the simulation of new porous materials - such forcefields may not exist in which case the 'quick' simulation of the new material would not provide accurate results and work would be needed to determine a new forcefield suitable for the new porous material.

Computer simulations are not only used to explore the properties of existing and newly synthesised zeolites, but can also be used to predict structures of hypothetical zeolites which may then be synthesised in a laboratory. Such simulations [22–24] often predict many hundreds of zeolites structures, the synthesis of which may not be possible. However, by computationally modelling the zeolite structures, the hypothetical networks may be interrogated to determine their energetics and thus predict which structures it is possible to synthesise in a laboratory. Simulations of hypothetical zeolites have resulted in the synthesis of new zeolites with struc-

tural properties which match those of the computational predictions [22].

1.4.2 Computer simulations of hydrocarbons and porous materials

Computers have been used for decades as simulation tools to model physical and chemical systems. The concepts of computer simulation have not changed greatly over the decades - the task is still to perform calculations at discrete time intervals and adjust the properties of the components of the simulation based on the results of the calculations. This vague description captures all different types of simulation from those focusing on the atomic structure of a single molecule to those attempting to simulate the movement of weather fronts on a global scale or those modelling the trajectory of planets far into the future. Although the concepts have not changed significantly over the decades, the accuracy, precision[7], speed, size and duration of the simulations have increased with the increase in power of computers.

There are many different techniques available to the simulator, these are discussed in Chapter 2, with simulations of atoms and molecules most frequently making use of one of the following: Molecular Dynamics; Monte Carlo; Kinetic Monte Carlo simulation. Each technique has its strengths and weaknesses and care must be made when choosing the simulation method to ensure that it is accurate and of a suitable length and time scale to capture the relevant physics.

Each simulation technique relies on models which approximate the system that is being studied. For example, it is possible to model a hydrocarbon molecule in a number of different ways: keeping track of the position of all of the electrons and nuclei (quantum mechanical approach); approximating the nucleus and electrons as a single atom (classical approach); approximating several atoms as one 'pseudo atom' - more on this in chapter 3 (again, a classical approach but with further approximation); approximating the whole molecule as a single entity. Ideally, every simulation would use the most detailed technique - which includes electrons and nuclei. However, it is currently not computationally feasible to attempt a simulation of a porous material with many thousands of atoms using quantum mechanical simulations. It is possible to

[7] accuracy and precision are slightly different concepts. For example, several decades ago the density of water at 9.48 degrees Celsius (value is defined as $1 kg/m^3$) found via simulation may have been $1.0001 kg/m^3$ whilst today the same quantity may be $1.0000001 kg/m^3$. Both the accuracy and the precision of today's value are improvements on that of yesteryear. In the general context of this work, accuracy and precision mean rigour of the theoretical model and reproducibility of known, often experimental, data.

model small portions of a zeolite/mespore using quantum mechanical simulations but these do not allow for the prediciton of (for example) diffusion properties since the length of time that such simulations cover is not sufficient. Since it is not possible to use the most accurate method (quantum mechanical simulations), classical models are used whereby the level of detail, and therefore computational requirements, are less.

Computer simulations have been used to investigate many different aspects of porous materials and hydrocarbons, with the majority of the work focusing on zeolites, rather than mesopores (simply because the study of mesopores is a younger field). The forcefields used to control the interaction between the different components of the simulation (the hydrocarbons and the porous materials) are described in Chapter 3 and each forcefield requires many parameters which stipulate the strength of the interactions. There have been many simulations presenting potential parameters to model linear, branched and cyclic hydrocarbons. In references [14, 15, 18, 20, 25–31] different potential parameters which are used to model linear hydrocarbons are discussed and the simulations are compared to experimental macroscopic data (see Chapter 2 for details of such comparisons). Potential parameters for models used to describe branched hydrocarbons are outlined in references [16, 21, 32, 33] although some of the potentials for linear hydrocarbons may be used to model many of the properties of branched hydrocarbons. Potential models for cyclic molecules, or molecules with 'special' requirements (such as those with internal flexibility) are featured in references [19, 34–40]. Special techniques, such as the Configurational Bias Monte Carlo method [41], have been developed to allow the routine simulation of large, flexible molecules within the relatively narrow pores of a zeolite. Such techniques are discussed in detail in Chapter 2 and have vastly increased the scope of computer simulations in this field which are able to model the behaviour of very large molecules [42, 43] as they negotiate the narrow pores of a zeolite.

When attempting to simulate the interaction between hydrocarbons and porous materials, it is vital to be able to simulate not only the hydrocarbons but also the porous material. Whilst most simulations use a rigid model for the porous material (see Chapter 3 for more details of this approximation) there have been some computational studies of only zeolites (i.e. no adsorbates or diffusing molecules) performed using a flexible model [44–53]. The benefits and limitations of rigid and flexible models of the porous material are described in Chapter 3 where the rigid

model approximation is discussed and its computational time saving benefits outlined.

Combining the hydrocarbon models with both rigid and flexible models of the zeolite allow many different types of simulation to be carried out. Diffusion of molecules though the pores of a zeolite is carried out using classical Molecular Dynamics simulations, using a forcefield which treats molecules as a set of bonded atoms, and has been a popular field for study for determining the rate at which molecules move through a zeolite [54–72]. The classical Molecular Dynamics technique is particularly suited to determining the diffusion coefficient of molecules through the pores of a zeolite. However, the diffusion may be extremely slow (for example, cyclohexane has a diffusion coefficient of $10^{-15}cm^2/s$ in silicalite-1 [73]) and so simulations are required to run for long enough to be able to capture data on this time sale. Such simulations demand significant computer resources particularly if a flexible zeolite model is used. Due to the slow diffusion of large molecules within the pores, Molecular Dynamics simulations are not well suited to investigating the adsorption properties in zeolite because the length of time a molecule may take to explore the zeolite sufficiently to find its preferred adsorption location may be prohibitively large. Techniques exist to allow simulations to proceed in such situations, allowing the molecule to explore parts of the structure which it would not otherwise be able in the duration of a 'normal' Molecular Dynamics simulation. Information on these techniques (such as Transition State Theory) can be found in references [74] and [75].

Using quantum mechanical simulations to probe the chemical reaction between adsorbates and the zeolite is another well used technique [76, 77], although simulations in this area are limited in size by the complexity of the techniques used. Quantum mechanical simulations proceed by moving atoms based upon calculations determining the force on each atom - a function of the position of all of the nuclei and electrons of all the atoms. Such levels of detail result in simulations that consume large quantities of computing resources and can therefore be run for only a short time and for a small number of atoms (relative to classical simulations). These simulations are particularly suited to analysing chemical interactions between molecules, such as the catalytic activity of a small portion of a zeolite, since it is possible to model the creation and destruction of chemical bonds (because the positions of the electrons are known).

The adsorption of hydrocarbons in porous materials is usually studied using the Monte Carlo

technique. This technique is described in detail in Chapter 2 and relies on following not the physical path that a diffusing molecule would take through the zeolite but, instead, jumping between different positions in the porous network. In this way, the preferred adsorption site can be found more quickly than if the simulation were to follow the true path of the molecule (as is the case in Molecular Dynamics).

The adsorption of molecules on the internal surface of zeolites has been an extremely well studied area and the simulations in this field are numerous. Simulations range from those of single component adsorption [41–43, 70, 78–104] to the adsorption and separation of mixtures of different molecules [105–119]. Whilst there have been many simulation studies focusing on the adsorption characteristics of mixtures of linear and branched molecules, the adsorption of mixtures of linear and cyclic and branched and cyclic molecules have not been studied using computer simulations. From an academic viewpoint it is important to improve the understanding of the adsorption of molecules in porous materials and performing simulations of mixtures is an important step. The adsorption of a mixture of different hydrocarbons (all with 6 carbon atoms) provides an excellent opportunity to explore the interaction between the molecules and to determine the adsorption selectivity of each zeolite. Furthermore, these mixtures play an important role in the petrochemical industry where molecular sieving and zeolite catalysis can be greatly affected by the build up of adsorbed molecules. Thus, an understanding of hydrocarbon adsorption in zeolites is a key step in further improving the efficiency of petrol production.

Simulation studies of adsorption in mesopores have been restricted to very small molecules, such as nitrogen, argon, methane and ethane [120–128]. The behaviour of larger molecules in mesoporous materials has not been studied, despite a number of experimental studies [5, 6, 9, 129–138] of larger hydrocarbons in MCM-41. Mesopores are the focus for numerous research studies which have resulted in many potential industrial uses being proposed (including use in the petrochemical industry). Increasing the understanding of hydrocarbon adsorption within their pores is vital to the further development of mesopore as a potentially useful industrial substance.

1.5 Outline of this work

This thesis presents work on the Monte Carlo simulation of the adsorption of 3 different hydrocarbons (hexane, 2-methylpentane, and cyclohexane) in three different zeolites: silicalite-1, $AlPO_4$-5 and ITQ-22 as well as introducing a new model for the adsorption of these molecules in the mesopore MCM-41. The layout of the thesis is as follows: first, the theory of computer simulations and adsorption will be presented (in Chapter 2), followed by a description of the model used in zeolite adsorption (in Chapter 3). Next, in Chapter 4 the single component adsorption of the three species in the three zeolites will be discussed and comparisons made with both experimental and simulation work. The adsorption of binary and ternary mixtures of the three molecules at different temperatures and partial pressure in the three zeolites will then be discussed (in Chapter 5). Next, in Chapter 6, the adsorption in the mesopores MCM-41 will be introduced, along with the model used. An analysis of the structure of the adsorbed molecules will also be given. Finally, in Chapter 7, the conclusions will be presented and topics for further work will be suggested.

Chapter 2

Theory

This section aims to describe the theory of adsorption within zeolites and mesopores as well as discussing some of the technical details of Monte Carlo simulations. It will also briefly explain the Ideal Adsorption Solution Theory, vapour liquid coexistence curves and the visualisation techniques used in this work. It is not intended as a complete theoretical background to either adsorption processes or Monte Carlo simulations but simply to highlight some of the aspects of both topics which are relevant to this work. More detailed discussions can be found in references [41,74,79,139,140].

2.1 Adsorption in microporous and mesoporous materials

When a hydrocarbon moves through the pores of a zeolite or mesopore, it can adsorb onto the internal surface. There are two types of adsorption; chemisorption and physisorption. Chemisorption involves the formation of chemical bonds between the adsorbate and adsorbent and thus normally only one layer of adsorbates can form in a given region of adsorbent surface. In contrast, physisorption does not involve the creation of chemical bonds and relies on the van der Waals' forces between the adsorbate and adsorbent. A physisorbed molecule can, in general, be more easily removed than a chemisorbed molecule and, unlike chemisorption, is characterised by multiple layers of adsorbate on the adsorbent surface. The build up of physisorbed molecules can cause blockages within a zeolite (and to a lesser extent mesopores)

and prevent the movement of catalytically important molecules, thus reducing the catalytic efficiency of the zeolite/mesopores. This work focuses exclusively on the physisorption of both single components and mixtures of different hydrocarbons in zeolites and mesoporous materials.

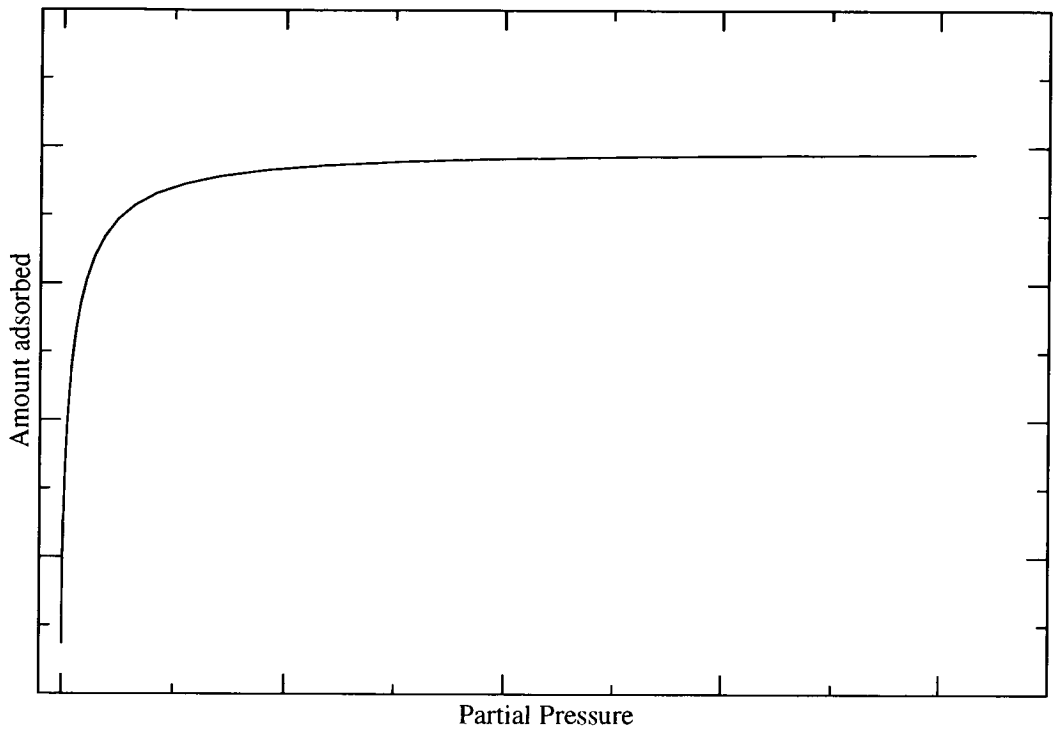

Figure 2.1: A typical adsorption isotherm.

At very low pressure, the number of molecules adsorbed within a zeolite/mesopore is proportional to its Henry Coefficient, K_H,

$$N_{ads} = K_H P \tag{2.1}$$

where N_{ads} is the number of adsorbed molecules per unit volume and P is the external pressure. The heat of adsorption of a molecule is defined as the difference in energy between the molecule when it is in its ideal gas state and when it is adsorbed on the internal surface of a zeolite/mesopore at very low pressure. Combining the Henry coefficient and heat of adsorption can give a good indication of how readily a particular molecule can adsorb within a

zeolite/mesopore. However, the Henry coefficient is only defined at very low pressure (i.e. at zero coverage - no molecules adsorbed) and the heat of adsorption will change with a change in pressure and coverage. Therefore, to get a complete picture of the adsorption process, the full adsorption isotherm must be found. The adsorption isotherm is simply a measure of the quantity of molecules adsorbed over a pressure range at a constant temperature. However, it is a vital measure of the adsorption capacity of a porous material and, coupled with knowledge of the location of the adsorbates within the porous network it is possible to build up a detailed picture of adsorption within the pores of a zeolite/mesopore. Figure 2.1 shows a typical adsorption isotherm which can be fitted using the Langmuir equation which relates the loading at a given pressure (N) to the maximum possible loading (N_{max}),

$$N = \frac{N_{max} P}{1 + N_{max} P} \tag{2.2}$$

The Langmuir model is only applicable if the following assumption are true:

- Adsorption takes place only at specific sites on the adsorbent surface. If all of these sites are occupied then no further adsorption can take place.
- There is only a single layer of adsorbed molecules.
- The temperature is constant throughout the adsorption process.
- No phase transition occurs during the adsorption process.
- There is no interaction between the adsorbed molecules.[1]

These assumptions are, in general, true in the case of adsorption in zeolites. However, adsorption in mesopores is characterised by multi-layer adsorption with strong adsorbate-adsorbate interactions. These features of mesopore adsorption require the use of different methods [141] to fit the adsorption isotherms.

The Langmuir fit can be used in conjunction with the Ideal Adsorption Solution Theory (Section 2.5) to predict the adsorption of mixtures of different species in zeolites.

[1] if adsorbate-adsorbate interactions need to be considered then the Fowler or Hill-de Boer approximations can be used. See reference [141]

2.2 Simulations in general

Computer simulations are a widely used tool in many different areas. With the steady increase in computing power, the maximum size, speed and accuracy of the simulations can also increase. However, all simulations, regardless of the system they aim to study, are governed by one basic rule:

$$\text{Rubbish In} = \text{Rubbish Out} \tag{2.3}$$

Indeed, not only does the input have to be carefully prepared but also the simulation technique which is used to model the system must be chosen correctly. The length scale and time scale over which the simulation runs can immediately narrow the range of choices of applicable techniques. For example, if the aim of the simulation is to model the movement of air from the equator to the poles then a quantum mechanical simulation using a femtosecond timestep is impractical. On the other hand, a simulation of the ionization of certain greenhouse gases demands a length and time scale which makes it a good candidate for an *ab initio* quantum mechanical simulation.

On the length and timescale of a simulation of adsorption of guest molecules within microporous and mesoporous materials there are three different techniques that could be employed; *ab initio* quantum mechanical (QM) simulation, classical Molecular Dynamics (MD) and classical Monte Carlo (MC) simulations. The first of these is the most accurate and consequently the most computationally expensive. Attempting to perform a QM simulation of the thousands of atoms which make up a zeolite/mesopore is prohibitively slow and thus it is not practical to study adsorption by using these techniques since the length of time that QM simulation can model is not sufficient to capture the physics of adsorption in zeolites/mesopores. However, there have been a few studies using QM simulations, but these have mainly focused on the reaction between the guest molecule and zeolite/mesopore and have not been used to predict the adsorption properties. These QM simulations do not attempt to model the entire porous network[2], instead only a small portion of the zeolite/mesopore is used - it is 'cut out' from the bulk structure and the small section is simulated. In this way the computational task becomes

[2]Quantum mechanical simulations of entire zeolites *are* possible for only the very smallest of zeolites (ones whose unit cell contains only tens of atoms). Indeed, Shah *et al.* have performed many simulations [142–144] investigating the properties of molecules in Chabazite, a zeolite with only 36 atoms in its unit cell.

tractable but at a cost - the simulation is no longer of a zeolite/mesopore but instead of only a very small section of its internal surface.

Classical Molecular Dynamics simulations aim to mimic the path of an atom or molecule as it moves through a zeolite/mesopore. The force that the molecule experiences as it interacts with the zeolite/mesopore is used to determine the direction of movement at each time step. Thus, MD simulations can determine the diffusivity of a molecule within a zeolite/mesopore and, if run for sufficiently long, the most likely adsorption sites. However, the diffusion of large molecules, whose kinetic diameter is commensurate with that of the pore, is extremely slow with laboratory experiments often taking weeks to equilibrate. Attempting to simulate the diffusion of these large molecules using MD is a fruitless task since the molecule will try to follow its true path through the porous network, which will require a simulation that lasts for weeks - far beyond the typical nanosecond simulations which are currently possible.

Thus a compromise is necessary - a simulation which allows molecules to explore the different sites within a zeolite/mesopore without being restricted by the slow diffusion though its narrow pores. Monte Carlo simulations provide such a compromise and are a widely used tool in the investigation of the adsorption properties of porous materials. Monte Carlo simulations use non physical 'jumps' between different sites within the zeolite/mesopore, thus avoiding the prohibitively slow journey though the pores and allowing for the quick, accurate determination of the most probable adsorption sites. By using suitable acceptance rules to determine if a jump between locations is permitted, MC simulations can allow a molecule to explore not just the minimum energy sites but, given sufficient time, all sites within the porous structure. The MC method is described in more detail in the next section.

2.3 Monte Carlo simulations and ensembles

Adsorption isotherms (see Section 2.1) are measured experimentally by allowing a zeolite/mesopore to come into contact with a reservoir containing molecules. The two are then allowed to equilibrate (which can take up to several weeks) and the change in mass of the zeolite/mesopore is measured. In this way, the mass of adsorbed molecules can be determined. As discussed in the

previous section, Molecular Dynamics simulations are not suitable to model on this timescale and instead, Monte Carlo simulations are used. Monte Carlo simulations rely on the fact that whilst a substance may be in *macro*scopic equilibrium, *micro*scopically it may be in constant change. For example: macroscopically, a beaker of water at room temperature is stationary - it does not spontaneously move across the bench or jump out of the beaker - it is static. However, on the microscopic scale, the water is dynamic - the molecules are in constant motion, in fact there are many different ways in which the molecules of the beaker of water can be arranged without altering the macroscopic properties of the water. This powerful concept is the basis of Monte Carlo simulations. It implies that in order to simulate the macroscopic properties of the water it is sufficient to simulate a much smaller microscopic section (microstate) of the water and use the average of the values of the microscopic simulation to predict the macroscopic values of the beaker of water. This is summed up in the following equation,

$$A_{\text{macrostate}} = \langle A \rangle_{\text{microstates}} = \lim_{N \to \infty} \sum_{i=1}^{N} A_i P_i \tag{2.4}$$

where A is the property that is being measured and P_i is the probability of finding the system in microstate A_i. Small changes in the positions of the molecules in the microstate allow the system to explore more of its phase space and, as the number of microstates explored increases, the accuracy with which $A_{\text{macrostate}}$ can be measured also increases.

An ensemble is a microstate with well defined constant properties such as pressure or volume or the number of molecules in the system. There are three different ensembles used in this work: Gibbs (constant NVT - two simulation boxes), Grand Canonical (constant μVT) and canonical (constant NVT). (N, V, T, and μ stand for number of molecules, volume, temperature and chemical potential.) The Gibbs ensemble is used to simulate the vapour-liquid coexistence - without having to focus the majority of the computational resources on the interface between the two phases. The Grand Canonical ensemble (illustrated in Figure 2.2) is used to simulate the adsorption of molecules. An imaginary reservoir of molecules with equal chemical potential and temperature is in 'contact' with the zeolite/mesopore and molecules can transfer between the two. Again, this approach is used to avoid the problem of simulating the interface between the reservoir and the porous structure which would dominate the computational effort. The canonical ensemble is used to determine the Henry coefficient of the adsorbates.

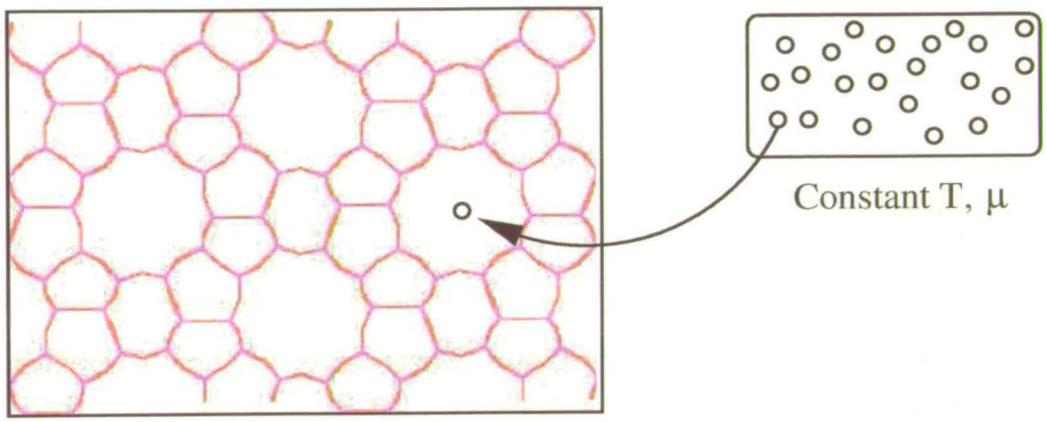

Figure 2.2: Schematic of the Grand Canonical Ensemble. The box on the left represents a zeolite within the simulation cell and the box on the right represents the reservoir of molecules (the circles) held at constant temperature and chemical potential.

A Monte Carlo simulation uses a variety of techniques to explore different microstates. These include translation, rotation, insertion, removal, volume change and regrowth - all of which are described in the next section. The generic procedure for a Monte Carlo simulation is as follows:

- Choose at random from the list of possible moves
- Choose at random a molecule to apply the move to (or which box in the case of the Gibbs ensemble volume change)
- Try to perform the selected action on the molecule (or box)
- Accept the move according to the prescribed acceptance criteria (see next section) which are based on the change in energy of the system caused by the move
- save useful data (such as pressure or number of molecules adsorbed)

The energy of the system is defined as the sum of the internal molecular energy and the external energy of the interaction between the molecule and its surroundings. If the acceptance criteria are carefully chosen so that they do not introduce a bias (i.e. they satisfy detailed balance) then the simulation will sample microstates and data can be used to determine the average value

of the properties of the microscopic ensemble that is then used to predict the macroscopic properties of the system.

2.4 Monte Carlo moves

The ensemble in which the simulation is carried out determines the choice of possible Monte Carlo 'moves' that may take place at each step. All possible moves (for all ensembles) are:

- Translate
- Rotate
- Add
- Remove
- Swap
- Volume change
- Configurational Bias regrow

The volume change and swap move applying to only the Gibbs ensemble and the add and remove to only the Grand canonical ensemble. Each move will now be discussed in detail.

2.4.1 Translate and Rotate

The translation and rotation moves are relatively straightforward, in each case a new position for the molecule is chosen - based on a direct translation or a rotation about the centre of mass of the molecule. The energy of the system with the molecule in the new location is determined and the translation or rotation is accepted using the following acceptance rule:

$$acc(\text{old} \rightarrow \text{new}) = min(1, \exp\{-\beta(E_{new} - E_{old})\}) \tag{2.5}$$

where $\beta = \frac{1}{k_B T}$ where k_B is the Boltzmann constant and T is the temperature. E_{old} is the energy of the system with the molecule in its old location. Similarly E_{new} represents the energy of the system with the molecule in its new location. The acceptance rule simply means that if the new energy is less than the old energy then the move is accepted, otherwise, a random number between zero and one is chosen and the move is accepted if that random number is less than the exponential term in equation 2.5. Using this acceptance rule, changes to the system which raise the total energy can be accepted thus allowing the system to explore not only its local but also its global minimum energy state. This is achieved by the small probability that

a molecule will leave its local minimum energy level and explore the higher energy region. Since the probability of 'escaping' a region increases with increasing energy, the molecule will be more likely to 'escape' a relatively small local energy minimum that it would a large (or global - the largest) energy minimum; in this way, a sufficiently long simulation will allow the molecule to explore both the local and global energy minima.

2.4.2 Addition / Removal

The addition and removal of a molecule are the defining moves of the Grand canonical ensemble. In both cases a molecule is chosen at random and is either added or removed from the simulation cell. The additional molecule is accepted according to the energy and the chemical potential, μ, as follows:

$$acc(\text{add}) = min\left[1, \frac{V}{\Lambda^3(N+1)} \exp\{\beta[\mu - E_{N+1} + E_N]\}\right] \tag{2.6}$$

where N is the number of molecules in the system at the start of the move and Λ is the thermal de Broglie wavelength ($\sqrt{\frac{h^2}{2\pi m k_B T}}$, h is Planck's constant and m is the mass of the molecule). Once again, the move is accepted if the exponential term is greater than one, otherwise a random number is chosen and the move is accepted if that random number is less than the exponential term.

The acceptance rule for the removal of a molecule is as follows:

$$acc(\text{remove}) = min\left[1, \frac{\Lambda^3 N}{V} \exp\{\beta[\mu + E_{N-1} - E_N]\}\right] \tag{2.7}$$

2.4.3 Swap

The swap move allows the movement of molecules between the two simulation boxes in the Gibbs ensemble. It is not used in either the Grand canonical or Canonical ensembles. If the two simulation boxes have a total volume of V and box 1 has a volume of V_1, and there are N molecules in total (N_1 in box 1) then the acceptance rule for the exchange of a molecule from one box to the other is given by,

$$acc(\text{boxSwap}_{1\to 2}) = min\left[1, \frac{n_1(V - V_1)}{(N - n_1 + 1)V_1} \exp\{-\beta[E_{new} - E_{old}]\}\right] \tag{2.8}$$

where E_{old} is the energy of the system with the molecule in box 1 (i.e. at the start of the move) and E_{new} is the energy of the system with the molecule in box 2 (and NOT in box 1), after the swap.

2.4.4 Volume change

The volume change move is an integral part of the Gibbs ensemble. Although the Gibbs ensemble is a constant volume ensemble, the volume of each simulation box can change, so long as the total volume remains constant. The acceptance rule for a change in volume of box 1 from V_1^o to V_1^n is given by,

$$acc(\text{volumechange}) = min\left[1, \frac{(V_1^n)^{n_1}(V - V_1^n)^{N-n_1}}{(V_1^o)^{n_1}(V - V_1^o)^{N-n_1}} \exp\{-\beta[E_{new} - E_{old}]\}\right] \quad (2.9)$$

where V is the total volume of both boxes, N is the total number of molecules and n_1 is the number of molecules in box 1.

2.4.5 Configurational Bias Monte Carlo algorithm

The Configurational Bias Monte Carlo (CBMC) technique [41] was developed to enable the simulation of large chain molecules within microporous materials. The acceptance rate for the random insertion of an entire molecule is vanishingly small for large molecules, because many of the atoms will overlap with the porous structure. However, if the positions of the atoms of the molecule are accepted or rejected at each step of the growth process, by taking into account the interaction with the surroundings (including the zeolite/mesopore structure) then the molecule will be 'grown' avoiding overlap with the zeolite/mesopore. In this way, the completed molecule can be grown in a tight fitting pore avoiding overlap with the pore and thus the acceptance rate is significantly increased compared with conventional growth techniques. However, this method creates a bias in the conformation of the grown molecules (which explains the name of the algorithm) so that they fit within the pores, the removal of the bias will be dealt with in this section.

The method of growing a molecule using the CBMC technique is as follows:

- choose a molecule to (re)grow
- for each pseudoatom in the molecule:
  - choose k trial positions based on the internal constraints (bond angles, torsion angles etc.)
  - select a trial position based on the Boltzmann weight of its external potential (i.e. based on the interaction with the zeolite/mesopore and surrounding molecules),

$$P_{\text{selecting}}(i) = \frac{\exp\left[-\beta U_i^{\text{ext}}\right]}{\sum_{j=1}^{k}\left[-\beta U_j^{\text{ext}}\right]} \tag{2.10}$$

where U_i^{ext} is the external potential of pseudoatom i.

However, the step by step nature of the CBMC growth technique which chooses the position (based on the external potential) of each atom as it is being grown, introduces a bias into the growth which must be removed. This is done by a careful choice of acceptance rules. The acceptance rule for the completed molecule is,

$$acc(\text{CBMC}) = min\left[1, \frac{W_n}{W_o}\right] \tag{2.11}$$

where W_o and W_n represent the Rosenbluth factors for the old and new configuration of the molecule (i.e. before and after the CBMC growth). The Rosenbluth factor is simply the product of all of the Boltzmann factors for each of the trial positions for each atom in the molecule. Thus, if there are k trial positions for each of the N atoms in the molecule then the Rosenbluth weight comprises k^N terms and would be given by,

$$W_n = \prod_{i=1}^{N}\left[\sum_{j=1}^{k}\left[-\beta U_j^{\text{ext}}\right]\right] \tag{2.12}$$

The CBMC technique allows the simulations of large molecules within zeolites that would be impossible to simulate using conventional techniques due to the vanishingly small acceptance rates.

2.5 Ideal Adsorption Solution Theory (IAST)

IAST is a widely used technique developed by Myers and Prausnitz [145] which predicts the adsorption isotherm of mixtures based on the single component adsorption isotherms. The theory is based on Raoult's law for vapour-liquid equilibrium,

$$P_i = x_i P_i^o(\pi) \tag{2.13}$$

where P_i represents the pressure of pure component i in the bulk gas phase, x_i is the mole fraction of component i in the adsorbed phase and $P_i^o(\pi)$ is the pressure of component i at the spreading pressure π. The spreading pressure (π) is found by integrating the single component adsorption isotherm,

$$\frac{\pi A}{RT} = \int_0^{P_i^o} \frac{N_i}{P_i} dP_i \tag{2.14}$$

where A is the surface area of the adsorbent, R is the gas constant, T is the temperature, N_i is the number of molecules adsorbed at pressure P_i and P_i is the pressure of pure component i. Since the term on the left of equation 2.14 does not need to be separated, the surface area is not required. By finding the pressure of the pure components which share the same value for the term on the left of equation 2.14, it is possible (using equation 2.13) to determine the mole fraction of each component in the adsorbed mixture. Combining this with the amount of each pure component which is adsorbed at the pressure which is found from equating the term on the left of equation 2.14 for each component, it is possible to calculate the amount of each species adsorbed in the mixture.

To calculate the spreading pressure for each component, the pure adsorption isotherms must be fitted with a suitable equation. The Langmuir equation (equation 2.2) is used and can be expanded for different isotherm types.

One of the assumptions of IAST is that the adsorbent area available to each adsorbate in the mixture is equal. In the case of mixture adsorption in zeolites this assumption may not be true. For example, if the mixture consists of very large and very small molecules then the large molecule will not have access to the same area as the small molecules which find it easier to navigate through the small channels of a zeolite which may be too tight to admit the bulkier

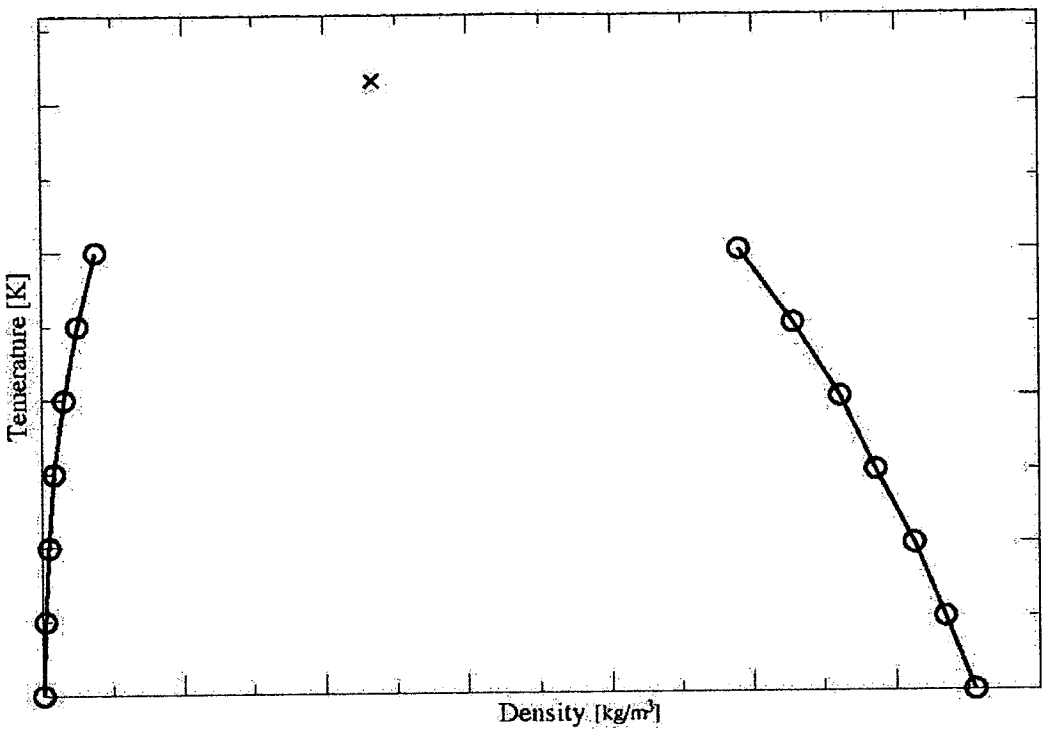

Figure 2.3: A typical Vapour liquid coexistence curve as determined by computer simulation. The cross represents the critical point

molecules. However, despite this restriction, IAST works well in predicting the adsorption isotherms for mixtures in zeolites where the molecules are of a similar size.

2.6 Vapour liquid coexistence

The simulation of the adsorption of a molecule within a zeolite/mesopore makes use of two Lennard-Jones potentials - one for the zeolite/mesopore-adsorbate interaction and one for the (non bonded) adsorbate-adsorbate interaction. (The next Chapter will explain in more detail the potentials and potential parameters used for the simulation.) One way in which the adsorbate-adsorbate potential can be validated is by comparing the results of a vapour-liquid coexistence simulation with the experimental data, [74] and [146]. The Gibbs ensemble is used to simulate the coexistence curves: each of the two simulation boxes are initialised to have an equal density of particles. The particles can swap between boxes and are free to move around within their

simulation box. As the simulation progresses, the system changes from two boxes at equal density to one box with the density of a vapour and one with the density of a liquid. At this point, meaningful statistics can be taken from the system and the vapour-liquid coexistence for that temperature can be found. Figure 2.3 shows a typical vapour liquid coexistence curve as found by Monte Carlo simulations, with the experimental critical point shown. Note that the simulations cannot predict the vapour liquid coexistence close to the critical point since the system does not settle into a stable state. Instead, close to the critical point, the two boxes are constantly changing their identity and so a direct measure of the vapour and liquid densities is not possible. In such situations, it is possible to instead measure the probability of finding a given density in one of the two boxes. Using this probability distribution it is possible to obtain data closer to the critical point. However, at temperatures approaching the critical point, there will exist vapour-liquid interfaces forming within each box which results in the simulations being unable to predict accurately the correct densities. This is discussed in detail in reference [74].

An approximation to the critical properties of the vapour liquid mixture can be made using the simulation data at temperatures below the critical point. Using the density scaling law [147], the critical temperature can be approximated as follows,

$$\rho_L - \rho_V = B(T - T_C)^{\beta} \tag{2.15}$$

where ρ_L and ρ_V are the density of the liquid and vapour phases, B is a constant and β is the critical exponent (set to 0.32 in this study [14]). Using the value obtained for the critical temperature it is possible to then predict the critical density using the law of rectilinear diameters [148],

$$\frac{\rho_L + \rho_V}{2} = \rho_C + A(T - T_C) \tag{2.16}$$

where A is a constant and ρ_C is the critical density. Using equations 2.15 and 2.16 a good approximation to the critical properties can be made with the simulation data below the critical temperature.

2.7 Liquid-liquid mixtures

As will be seen in Chapters 4, 5 and 6 the number of molecules which are able to adsorb within a zeolite is significantly less than the number which adsorb within the pores of the mesopore. Indeed, the phase of the molecules within zeolites is very different to that in mesopores. In the zeolites, the molecules adsorb in small numbers and are relatively well spaced - their density is very low with only around 10 molecules adsorbing within the zeolite porous network. However, in mesopores, many molecules are able to squeeze into the much larger pores and their density is much higher, approximately fluid density (more than 200 molecules within the pore). In Chapter 6 the structure of the adsorbed phase in the mesopore is analysed. It is therefore important to know the structural properties of the molecules outwith the mesopore, so that a comparison between the 'natural' structure and the structure within the pore can be compared - to determine the effect that the pore has on the structure of the adsorbates.

An ideal binary mixture is one in which the two components are fully mixed - the total volume of the resultant mixture is simply the weighted sum of the molar volume of each of the components. This ideality requires that there are no regions in which one component is excluded - even simple molecules that appear macroscopically miscible can exhibit non ideality on a microscopic scale as recent computational and experimental studies have shown [149,150]. Thus, before an analysis of the structure of mixtures within the mesopore can be made, it is vital to know what structure the mixture would have if it were not in the mesopore.

Experimentally, structures of mixtures can be determined by examining the excess volume of the mixture of two species. The excess volume is defined as the difference between the actual molar volume of the mixture and the molar volume that the mixture would have if it were ideally mixed:

$$V^E = V - (x_1 V_1 + x_2 V_2) \tag{2.17}$$

where V^E is the excess molar volume (in cm^3/mol), V is the molar volume of the mixture (in cm^3/mol), x_1 and x_2 are the mole fractions of the two components of the mixture, and V_1 and V_2 are the molar volumes of each component. Figure 2.4 shows the excess volume for a mixture of hexane and cyclohexane, taken from reference [151]. The graph shows that the

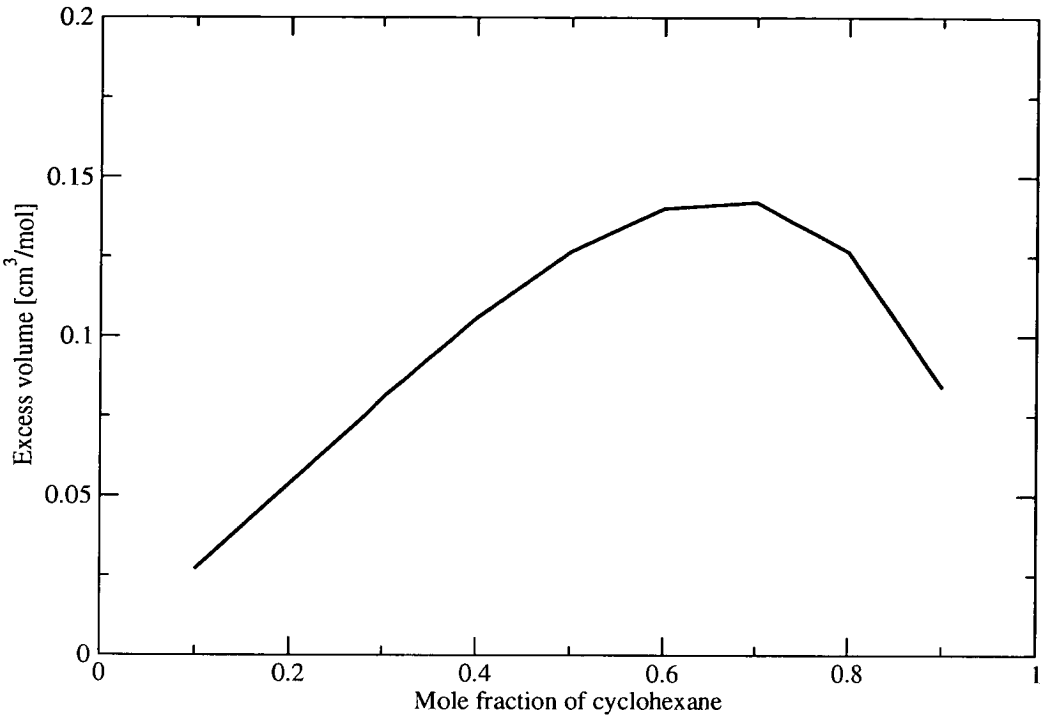

Figure 2.4: A graph of composition (of cyclohexane) against excess volume for a mixture of cyclohexane and hexane at 298.15K. From reference [151].

excess volume for all compositions is very small (less than 0.2% of the total mixture volume) indicating that a mixture of hexane and cyclohexane is approximately ideal at all compositions.

Data for mixtures of hexane and 2-methylpentane or cyclohexane and 2-methylpentane could not be found. However, it is reasonable to expect that 2-methylpentane would have similar mixing properties to those of hexane, since both have similar structures, densities, vapour pressure and boiling points. Thus, when an analysis of the structure of mixtures in the mesopore is made, any arising structure can be attributed to the mesopore and is not a property of the mixture itself.

2.8 Visualisation

The output from most molecular simulations includes details (such as coordinates or centre of mass or orientation) of the molecules at some (and in many cases all) of the time steps. If

the simulation is over many million time steps it is clear that simply looking at the raw output file is not an efficient way to examine the results of the simulation. There exist many tools (for example GOPENMOL [152]) for visualising molecules based on their coordinates but, in general, these are not easily modified to tailor their use to specific tasks. In contrast, OPENDX [153] is a visualisation package with a built-in series of functions that can be assembled to create powerful solutions tailored for specific tasks. For example, if there are several hundred files, each containing snapshots of molecules within a zeolite/mesopore at different pressures, a network can be built up in OPENDX to read in each file and render and image of the molecules within the porous structure and finally create a movie of the adsorption as the pressure changes. Figure 2.5 shows an example network which reads in the adsorbate-zeolite/mesopore energy at each point within the zeolite/mesopore and plots an isosurface of all energies at a specific value. It also draws a slice through the zeolite/mesopore depicting the areas of high and low energy.

Using a combination of GOPENMOL and OPENDX it is possible to build up a detailed picture of the adsorption process deep within the pores of a zeolite/mesopore.

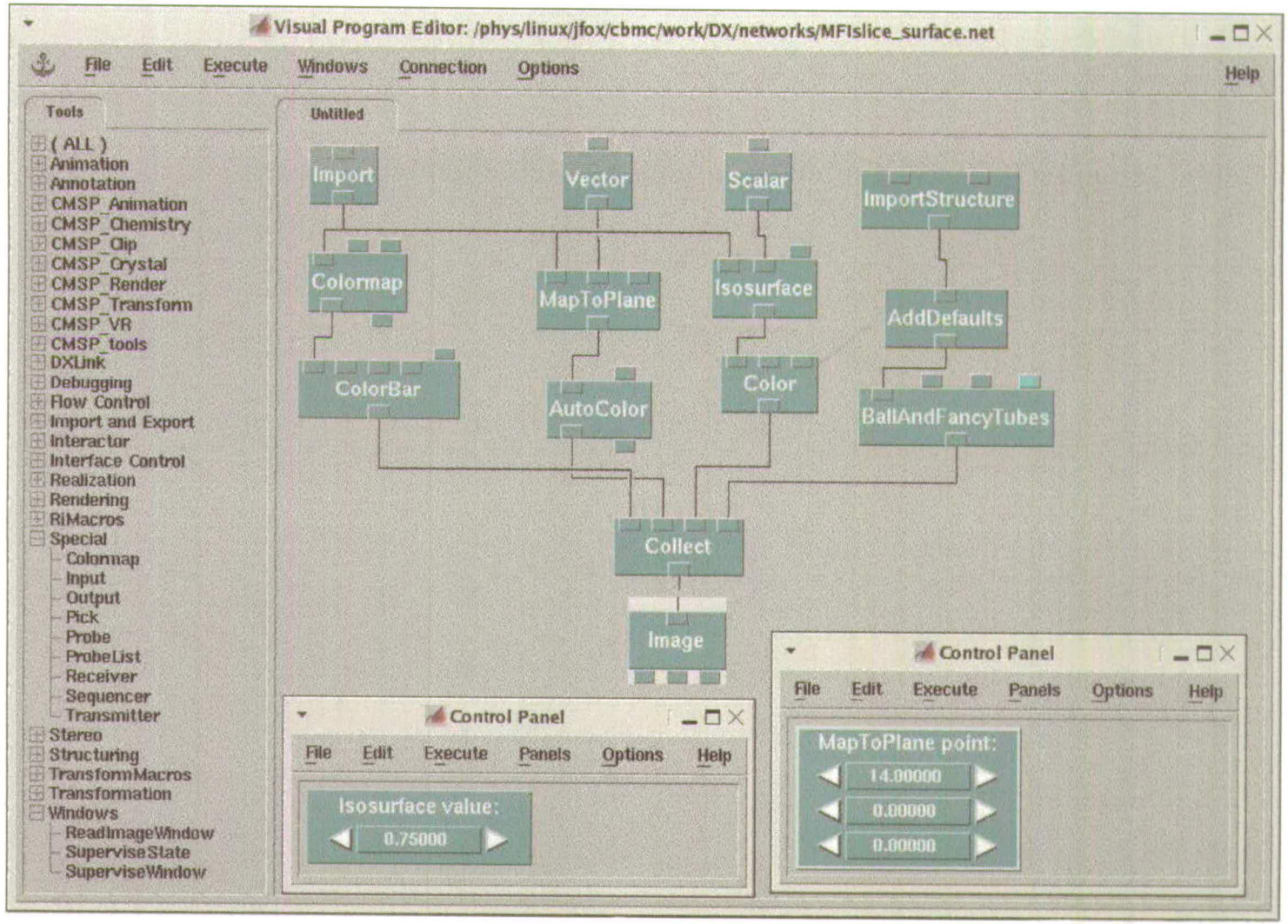

Figure 2.5: A typical network in OPENDX.

Chapter 3

Simulation model

The aim of this chapter is to describe the model used to simulate the adsorption of alkanes in zeolites and mesopores. The potentials which describe the interactions will be explained and any approximations used will be discussed.

3.1 The Lennard-Jones potential

The non-bonded interactions within the simulations are described by a 12-6 Lennard-Jones interaction. This relatively simple potential has two parameters, ϵ and σ and is of the following form:

$$U_{lj}(r) = 4\epsilon \left[\left(\frac{\sigma}{r}\right)^{12} - \left(\frac{\sigma}{r}\right)^{6} \right] \tag{3.1}$$

Figure 3.1 shows a graph of typical Lennard-Jones potential, highlighting the attractive and repulsive parts. The repulsive part, at low separation, arises due to the fact that one atom cannot diffuse through another. The attractive part of the potential is due to the dipole-dipole attraction between two particles.

The Jorgensen mixing rules [26], which are used to determine the Lennard-Jones parameters between different species, are given by:

$$\begin{aligned} \sigma_{ij} &= \sqrt{\sigma_{ii}\sigma_{jj}} \\ \epsilon_{ij} &= \sqrt{\epsilon_{ii}\epsilon_{jj}} \end{aligned} \tag{3.2}$$

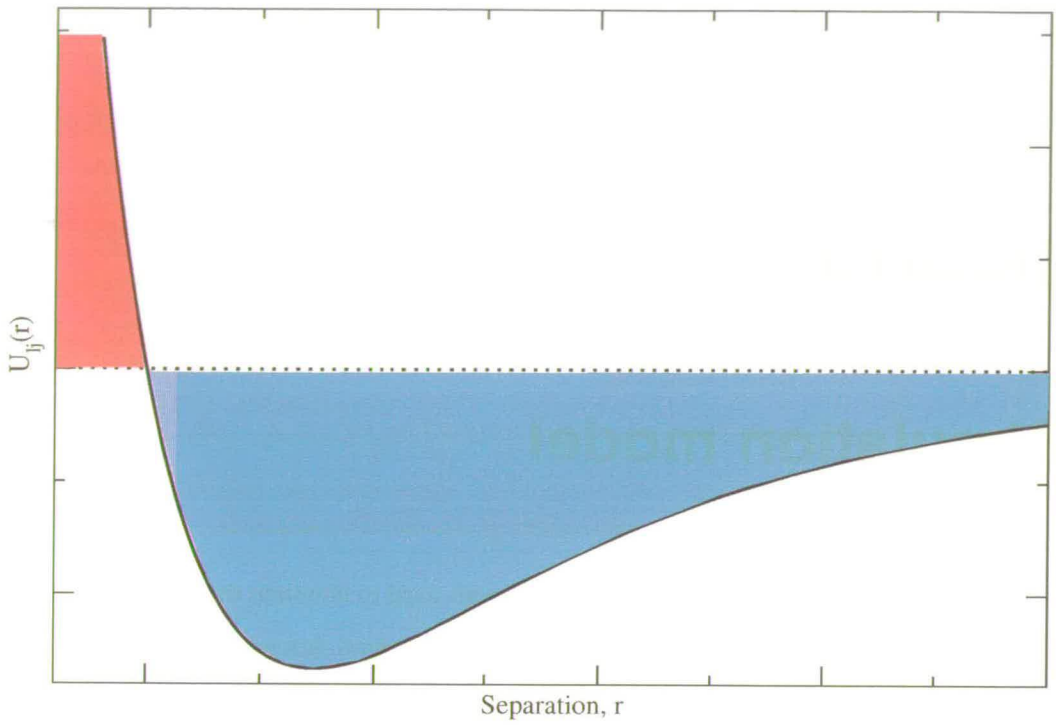

Figure 3.1: A typical 12-6 Lennard-Jones potential. The red region is the repulsive part of the potential and the blue region is the attractive part.

where σ_{ij} and ϵ_{ij} are the different species parameters and σ_{ii} and ϵ_{ii} are the parameters for the interaction between two pseudoatoms of type i.

Other mixing rules exist which combine the values for ϵ and σ for two different species. One such example is the Lorentz-Berthelot rule [154, 155] which differs from the Jorgensen mixing rule in its calculation of σ_{ij}. In the Lorentz-Berthelot mixing rule, σ_{ij} is given by,

$$\sigma_{ij} = \frac{\sigma_i + \sigma_j}{2} \tag{3.3}$$

However, the Jorgensen mixing rules have been shown to work very well for many different molecules [17] whilst the Lorentz-Berthelot mixing rules have been shown [16] to be less applicable for combining groups whose σ values differ greatly.

The simulations employ a cut-off distance, r_{cut}, above which the Lennard-Jones interaction is set to zero. For simulations involving all zeolites and mesopores, $r_{\text{cut}}$is set to 13.8Å.

3.2 United Atom Approximation

The United Atom Approximation [27] treats CH, CH_2, CH_3 and CH_4 groups as single 'pseudo-atoms' which interact via a Lennard-Jones potential. In this way the number of atom-atom interactions is significantly reduced without appreciable change to the behaviour of the alkanes.

This approximation is only made possible due to the fact that the hydrogen atoms do not play a significant role in the interaction between two molecules - and so their contribution can be 'averaged' along with the carbon atom to which it is bonded to create CH_x pseudo atoms (where $_x$ is 0, 1, 2, 3 or 4).

3.3 Inter-atomic potentials

The internal potential for a molecule is made up of contributions from the bond bending and torsion angle potentials,

$$U_{bend}(\theta) = \frac{1}{2} k_\theta \left[\theta - \theta_0\right]^2 \tag{3.4}$$

$$U_{tors}(\phi) = C_0 + C_1 \cos(\phi) + C_2 \cos^2(\phi) + C_3 \cos^3(\phi) + C_4 \cos^4(\phi) + C_5 \cos^5(\phi) \tag{3.5}$$

where k_θ is the bond bending constant, θ_0 is the equilibrium bond angle and $C_0 \ldots C_5$ are the torsion angle constants and ϕ is the torsion angle. As in previous experimental studies [27,41, 86] and in line with experimental data [38,156,157] the bond lengths are kept fixed throughout the simulation. Equations 3.4 and 3.5 are used to determine the possible trial positions for each pseudo-atom when the molecule is being grown.

3.4 Rigid, cyclic molecules

Conventional CBMC techniques are not suited to growing a cyclic molecule since the nature of the growth technique will result in a molecule which is very unlikely to form a cyclic structure. The alternative method of inserting the fully grown molecule into the zeolite/mesopore will

result in a negligible insertion probability since the chance of inserting the large (relative to the pore size) molecule without an overlap with the porous structure will be vanishingly small. To overcome this problem the CBMC growth technique is modified to permit the growth of cyclic molecules.

One approximation that is made in the modified growth technique is that the cyclic molecules are treated as rigid molecules. In the case of cyclohexane, this means that the molecules are assumed to be in their lowest energy and most abundant, *chair* conformation (see Figure 3.2). In its gaseous phase, cyclohexane is comprised of less than 1% molecules in the higher energy conformation, the *boat* conformation (see Figure 3.2).

The CBMC growth technique exploits the flexibility of the molecule that it is growing to avoid overlaps with the framework and thus improve the efficiency of the growth. However, if the molecule is rigid, can the CBMC growth technique be used to improve the chances of inserting it into the zeolite/mesopore? The answer is yes! Despite the molecule being rigid there is some flexibility in the way in which the positions of some of its pseudo-atoms are chosen [37]. The position of the first pseudo-atom is chosen in the same way as the conventional CBMC technique. The next pseudo-atom in cyclohexane can now be placed anywhere on a sphere of radius r centred on the first pseudo-atom. Once the position for the second pseudo-atom is chosen, the third pseudo-atom must be placed. Whereas the position of the second pseudo-atom was chosen according to a prescribed distance, the position of the third pseudo-atom is chosen according to a prescribed angle - so possible positions lie on a circle. Once the third pseudo-atom is in place, the positions of all of the other pseudo-atoms are defined by the (fixed) torsion angles.

By using the CBMC technique to grow the first half of the cyclohexane molecule, the insertion probability rises to a level similar to that of linear or branched molecules, which enables simulations to be carried out with an efficiency comparable to that of the linear and branched alkanes.

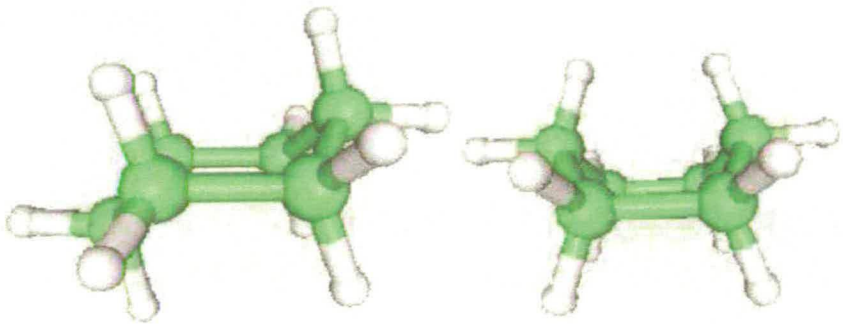

Figure 3.2: The chair (left) and boat (right) conformations of cyclohexane. The green spheres represent carbon and the white spheres represent hydrogen.

3.5 Rigid, flexible molecules : the JIGGLE method

All of the simulations in this work are carried out using a rigid molecule approximation for cyclohexane. The cyclohexane molecules are grown in their lowest energy conformation and remain in this conformation for the duration of the simulation. However, cyclohexane can, by overcoming an energy penalty, change its conformation. In an effort to determine what effect the conformation of the molecules has on their adsorption, the JIGGLE method was developed and is now described.

Conventional CBMC [41] is not suitable for the simulation of cyclic molecules due to the step by step nature of the growth of an alkane - the molecule is unlikely to close to form a cyclic structure. To overcome this problem the JIGGLE method is proposed. This method grows the cyclic molecule using a blueprint (the lowest energy conformation) and then perturbs each pseudo atom to allow the molecule to deviate from its lowest energy state. The blueprint molecule is grown using the CBMC technique for the growth of the first 3 pseudo atoms. The first 3 pseudo atoms completely define the rigid molecule and thus no further techniques are required to complete the growth of the blueprint molecule. Once the molecule has been completely grown, the JIGGLE method is used to allow it to explore any of its other conformations. The JIGGLE method is shown schematically in Figure 3.3.

The black spheres labelled A to F represent the CH_2 pseudo atoms. The JIGGLE method alters the conformation of the molecule by rotating a pseudo atom about a line which joins its two

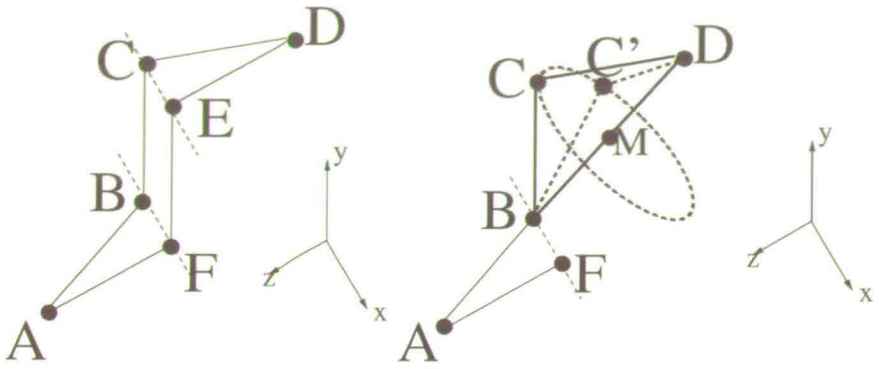

Figure 3.3: Left: The initial conformation of the molecule. Right: The JIGGLE method in action, pseudo atom E has been removed for clarity. See text for details.

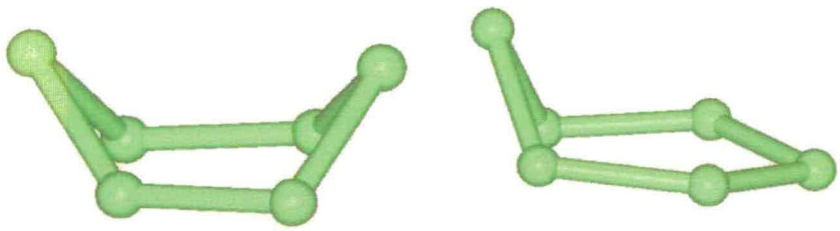

Figure 3.4: The boat (left) and chairboat (right) conformations of cyclohexane found using the JIGGLE method. The green spheres represent a CH_2 pseudo atom and the green tubes represent a CH_2-CH_2 bond.

nearest neighbours. In Figure 3.3 (right), pseudo atom C is being rotated around the line which joins B to D. M denotes the midpoint of the line connecting B to D. The vector from M to C is then rotated about the line BD. In this way, the distance between neighbouring atoms remains unchanged. Care must be taken to ensure that the perturbations are realistic - a rotation of the line MC through a large angle will result in a non-physical molecular structure. Therefore rotation angles are limited to ± 0.3 radians. The JIGGLE method will allow a cyclohexane molecule to visit each of its possible conformations (see Figure 3.4 for two such conformations). The method is not an energy bias method - each molecule is free to take on any of its conformations without penalty. In this way the method is over-complete - a cyclohexane molecule will easily change from one conformation to another whereas in reality there may be an energy penalty associated with a change in conformation. However, whilst the method is not energy biased in its selection of conformations it does allow a study of the effect that molecular conformation has on the adsorption isotherm.

The results from running simulations using the JIGGLE method to describe the cyclohexane molecules did not differ from those found from a simulation using rigid cyclohexane molecules. The vapour-liquid coexistence curve, the Henry coefficient and heat of adsorption, and the adsorption isotherms found using the JIGGLE method were all identical to the corresponding simulations using the rigid model.

3.6 Zeolites/mesopore modelling

Both the zeolites and the mesoporous materials used in this work are modelled as rigid structures whose atomic coordinates do not change throughout the simulation. This approximation is typical in the field of zeolite simulation and is discussed in more detail in reference [158]. This approximation provides a balance of accuracy and efficiency, enabling simulations to be carried out in an order of magnitude shorter time compared with the corresponding flexible framework simulations. However, framework flexibility is known to influence the dynamics of large molecules, whose kinetic diameter is commensurate with or even slightly larger than the size of the pore. This structural flexibility has been reported for 1,3,5-tri-methyl benzene in silicalite-1 [159] and *p*-/*o*-xylene mixtures in silicalite-1 [160]. Framework flexibility will not

be expected to influence the adsorption behaviour of small molecules with low loadings since these molecules will not interact sufficiently with the zeolite/mesopore to cause a substantial distortion. However, for large molecules / high loadings (such as cyclohexane in silicalite-1 at high pressure) the rigid approximation will be less appropriate. It may be expected that the location of the adsorption sites will not be as greatly influenced as the dynamics in using the rigid framework approximation.

Table 3.1: Simulation cell size for silicalite-1, $AlPO_4$-5, ITQ-22 and MCM-41.

	silicalite-1	$AlPO_4$-5	ITQ-22	MCM-41
Cell X (Å)	40.044	47.548	42.134	45.990
Cell Y (Å)	39.798	41.178	38.967	55.305
Cell Z (Å)	53.532	42.420	38.042	31.930
Volume ($Å^3$)	85312	83055	62458	81213
Repeat(x,y,z)	2,2,4	2,3,5	1,3,3	1,1,1

Some semi-flexible zeolite simulations have been carried out [103]. However, the scheme used to model the flexibility used only a nearest neighbour potential and so global structural changes will not be able to be seen using this semi-flexible zeolite model. The semi-flexible simulations carried out by Vlugt and Schenk [103] showed that at low partial pressures the difference between flexible and rigid zeolite simulations was negligible. However, there was a slight difference at higher pressures, for the larger molecules in the study, especially those which exhibit inflection behaviour in their adsorption isotherm.

In the rigid framework approximation only the oxygen atoms are taken into consideration - this approximation is motivated by the fact that the other zeolite/mesopore atoms are outnumbered, recessed, and less polarizable than the oxygen atoms, which dominate the framework-adsorbate interaction.

The three zeolites, silicalite-1, $AlPO_4$-5, and ITQ-22, along with the mesopore, MCM-41, are all modelled as infinite (using periodic boundary conditions) frameworks composed of repeated

Table 3.2: Molecular bond length and bond angle potential parameters

	Bond Length r (Å)	Bond Angle θ_0 (degrees)	Bond Angle Constant k_θ (K rad^{-2})
Hexane	1.530	113.0	85000.0
2-methylpentane	1.530	113.0	65000.0
Cyclohexane	1.535	110.0	——

unit cells. Table 3.1 shows the size of the basic unit cell of each zeolite and the mesopore and the total volume of each simulation box along with the number of unit cells which make up each simulation cell.

3.7 Potential Parameters

This section lists the values for the parameters used in the simulations.

Table 3.2 presents the bond length and bond angle for the three molecules which are the main focus of this work. The bond lengths remain constant throughout the simulation whereas the bond angles for hexane and 2-methylpentane are flexible, governed by equation 3.4 with value of k_θ given in Table 3.2.

The torsion angle parameters shown in Table 3.3 are well established and have been used in various forms (by way of a re-parameterisation to fit different torsion angle equations, similar to equation 3.5) to simulate different properties of both linear and branched molecules.

Table 3.4 lists the Lennard-Jones potential parameters for the interaction between pseudo-atoms. The values have been used in previous work [20,31,32] to investigate the vapour-liquid coexistence curves for various molecules. These established values are used in this work to calculate the interaction between non-bonded pseudo-atoms.

The zeolite/mesopores are modelled as rigid networks of oxygen atoms, ignoring contributions from silicon or aluminium/phosphorous. The parameters for the Lennard-Jones interaction

Table 3.3: Intramolecular torsion angle potential parameters. These value are from the forcefield of reference [119]. The torsion angle for cyclohexane is fixed at ± 60 degrees. 'X' stands for 'any pseudo atom'.

	X-CH-CH_2-X	X-CH_2-CH_2-X
C_0 (K)	1367.086	1204.654
C_1 (K)	4360.147	1947.740
C_2 (K)	416.005	-357.845
C_3 (K)	-6499.427	-1944.666
C_4 (K)	-832.004	715.690
C_5 (K)	1646.129	-1565.572

Table 3.4: Lennard-Jones potential parameters for pseudo-atoms (see references [20, 31, 32]) . CH_{3B} refers to a CH_3 group bonded to a CH group within a branched molecule. CH_{3BL} refers to a CH_3 group connected to a CH_2 group in a branched molecule. CH_{2B} and CH_B refer to CH_2 and CH groups in a branched molecule whilst CH_{2C} is a CH_2 group in a cyclic molecule. To determine the Lennard-Jones parameters for the interaction between two different species, the Jorgensen mixing rules are used (equation 3.2).

	σ (Å)	ϵ (K)
CH_3	3.750	98.0
CH_{3B}	3.930	78.0
CH_{3BL}	3.930	114.0
CH_2	3.950	46.0
CH_{2B}	3.930	47.0
CH_{2C}	3.863	51.3
CH_B	3.850	32.0

Table 3.5: Lennard-Jones potential parameters for the interaction between pseudo-atoms and the zeolite/mesopore oxygen atoms (the silicon atoms do not take part in the interaction.) See reference [119] and [83].

	σ (Å)	ϵ (K)
$CH_{3\mathrm{ALL}}$	3.60	80.0
$CH_{2\mathrm{C}}$	3.30	66.0
$CH_{2\mathrm{NON-C}}$	3.60	58.0
CH	3.60	58.0

between the oxygen atoms and the pseudo-atoms of the adsorbed species is given in Table 3.5. The parameters have been shown [83, 119] to accurately represent the zeolite-adsorbate interaction and thus allow for the simulation of the adsorption process. However, this work is the first time that these potential parameters have been used to investigate adsorption of larger hydrocarbons in mesopores.

3.8 The simulation code

This work makes use of the BIGMAC simulation code [161, 162], developed by the group of Prof. Berend Smit. The original code has been heavily modified to allow for the simulation of rigid and flexible cyclic molecules.

Figure 3.5 shows a flow diagram outlining the main steps of the simulation. Once the input files have been read, a grid of Lennard-Jones potential values for the interaction between the zeolite (or mesopore) and the adsorbates is made. The grid reduces the amount of computational effort required to calculate the adsorbate-zeolite/mesopore potential during the simulation - only a quick interpolation calculation is required to determine the energy. The simulation cell is then filled with adsorbate molecules (at random, energetically feasible positions) up to the number specified in the input files. The simulation can now begin; a suitable Monte Carlo move is chosen (at random) and the molecule to which it will be applied is also chosen (again, at random). The move is carried out and accepted or rejected based on the rules in the previous

chapter. The statistics are then updated if the equilibrium period has finished. Finally, once the simulation has finished, the statistical data is stored in files, along with the position of the adsorbed molecules (if there are any).

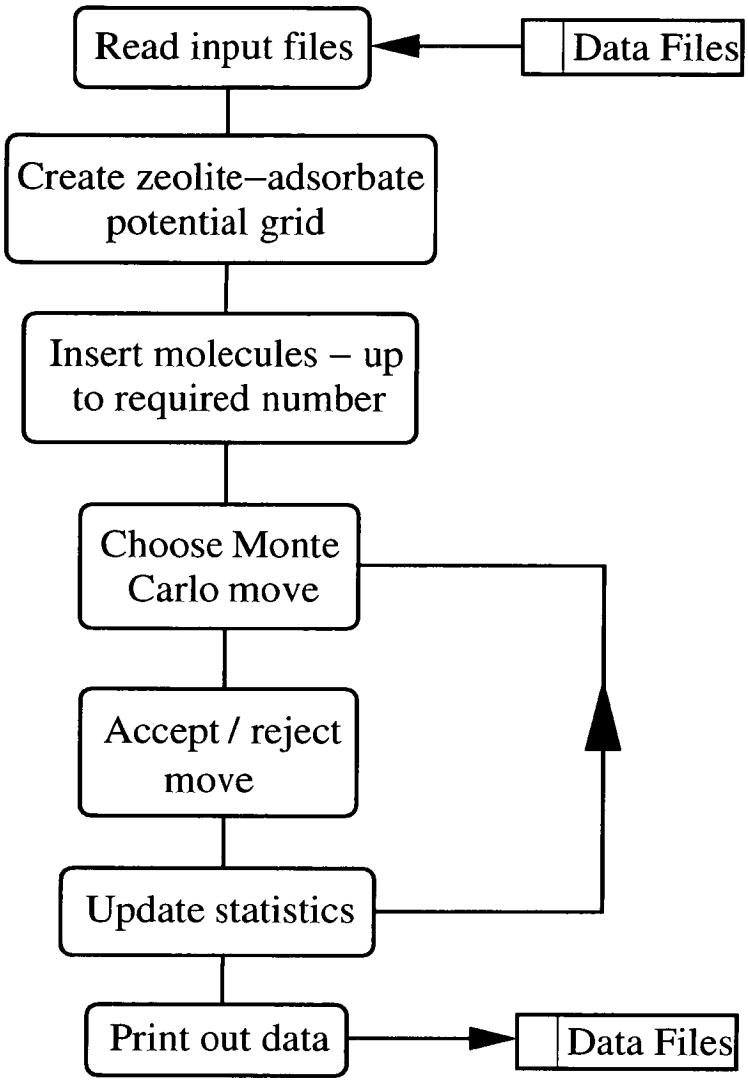

Figure 3.5: Flow diagram for the simulation code. In this figure, 'zeolite' means 'zeolite or mesopore'.

3.9 The zeolites

Since each zeolite used in this study has a different structure, each will be described in this section. The structure of the mesopore is covered in detail in Chapter 6 and so will not be introduced here.

Figure 3.6 shows the three zeolites from different angles. The top row shows silicalite-1, the middle row shows ITQ-22 and the third row contains a single projection of $AlPO_4$-5. The left column is a projection onto the XZ axis, the middle row is on the YZ axis and the right row is onto the XY axis.

The porous structure of silicalite-1 consists of straight channels, seen in the top left image which are connected via sinusoidal (or zig-zag) channels which can be seen in the top middle image. ITQ-22 also consists of straight channels (middle left) connected by zig-zag channels (middle image) whilst $AlPO_4$-5 is a more simple structure which has straight, unconnected channels (lower image).

The size of the channels in each of the zeolites is represented by two numbers, one indicating the shortest diameter and the other indicating the longest diameter. The pore sizes for the three zeolites are as follows: in silicalite-1, the straight channel is 5.1Å by 5.5Å, the zig-zag channel is 5.3Å by 5.6Å. In ITQ-22, the small straight channel is 3.3Å by 4.6Å, the large straight channel is 6.0Å by 6.7Å and the sinusoidal channel is 4.8Å by 5.2Å. In $AlPO_4$-5, the single straight channel is 7.3Å by 7.3Å.

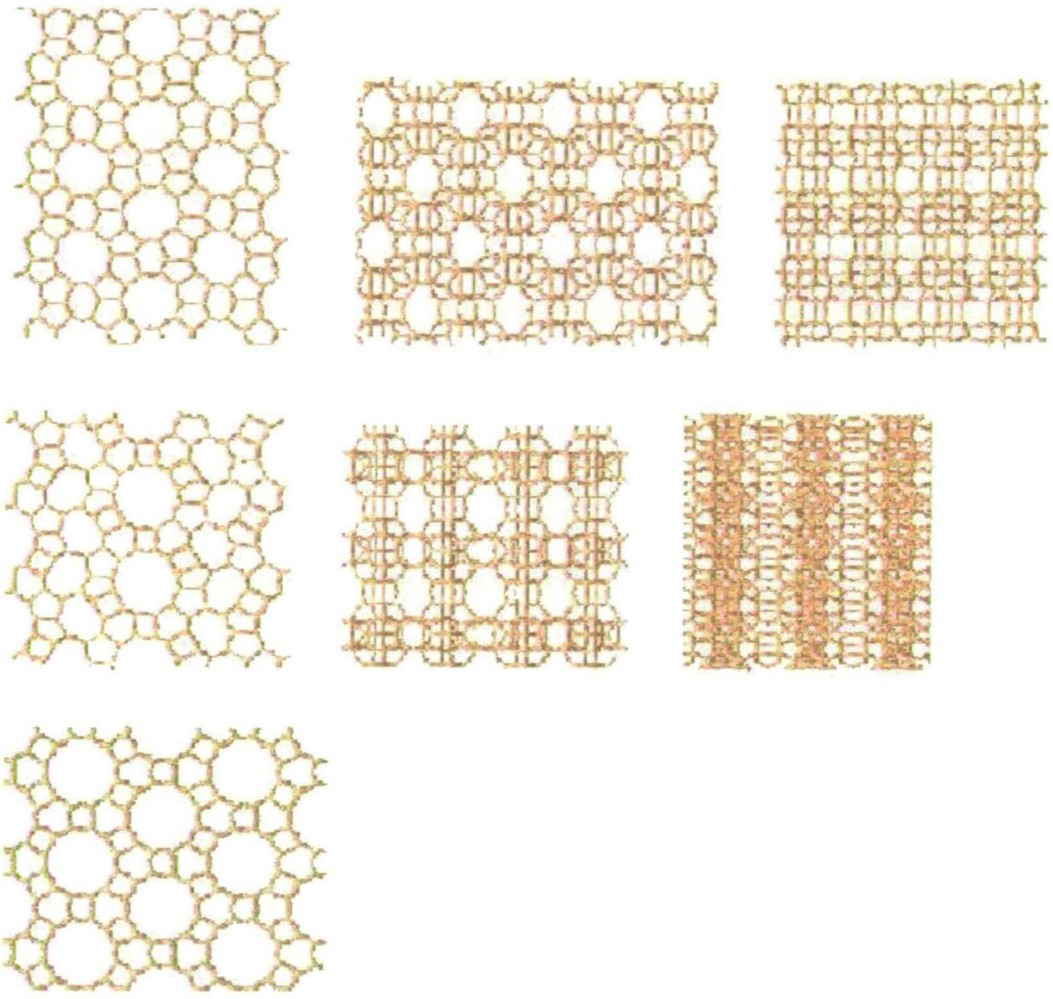

Figure 3.6: The three zeolites from different angles. The top row shows silicalite-1, the middle row shows ITQ-22 and the third row contains a single projection of $AlPO_4$-5. The left column is a projection onto the XZ axis, the middle column is on the YZ axis and the right column is onto the XY axis.

Chapter 4

Single component adsorption in zeolites

The focus of this chapter is to confirm that the various parts of the simulation (the code, the potentials and the potential parameters) combine to form an accurate method for investigating the properties of both hydrocarbons and zeolites. Comparison of the simulated vapour-liquid coexistence curves with the available experimental data will highlight any inaccuracies within the model used to describe the hydrocarbons. Next, the zeolite-adsorbate interaction will be tested by determining the heat of adsorption which can be verified by comparison with experimental data. The adsorption isotherms of various molecules within the zeolites will then be explored and their adsorption locations at various temperatures and pressures discussed.

It is vital that by using this model it is possible to correctly simulate the single component isotherms. Not only will this provide confidence in the model, but it will also allow the single component isotherms to be represented by a Langmuir approximation. This is necessary for the Ideal Adsorption Solution Theory predictions of the adsorption of mixtures in zeolites. This will be covered in Chapter 5.

4.1 Vapour-liquid curves - testing the hydrocarbon potentials

In Chapter 3 the potential parameters for the bonded and non-bonded interactions were presented, along with the equations which describe the interactions. The torsion angle, bond angle, pseudo-atom Lennard-Jones potentials have, individually, been used in previous work. However, since this work uses a combination of these parameters, it is necessary to explore their accuracy. As discussed in Section 2.6 the vapour-liquid coexistence curve provides an excellent test for the potentials used to simulate a molecule.

Figure 4.1 shows the simulated and experimental [33,37,163] vapour-liquid coexistence curves for a hexane, 2-methylpentane and cyclohexane. The agreement is very good with only slight differences at higher temperatures in the case of 2-methylpentane and cyclohexane. The agreement with the experimental data shows that the model is able to accurately simulate the different molecular types (linear, branched and cyclic) over a large temperature range. This confirms that the parameters for the bond angle, torsion angle and pseudo-atom potential combine to give a good model of these hydrocarbons.

In Section 2.6 the failure of the Gibbs ensemble to correctly model the vapour-liquid coexistence curve at high temperature (close to the critical point) was discussed. This failure, which is evident in Figure 4.1 does *not* mean that the simulation of molecules at that temperature is not possible. It simply means that the simulation of molecules at that temperature *in the Gibbs ensemble* does not reach equilibrium - the size and density of the two simulation boxes is constantly fluctuating. Using a different ensemble (such as the Canonical ensemble) to simulate a different aspect of the molecules (such as their heat of adsorption) results in good agreement with experimental data. In short, the failure is a result of the choice of ensemble, not the potential parameters or the potentials themselves.

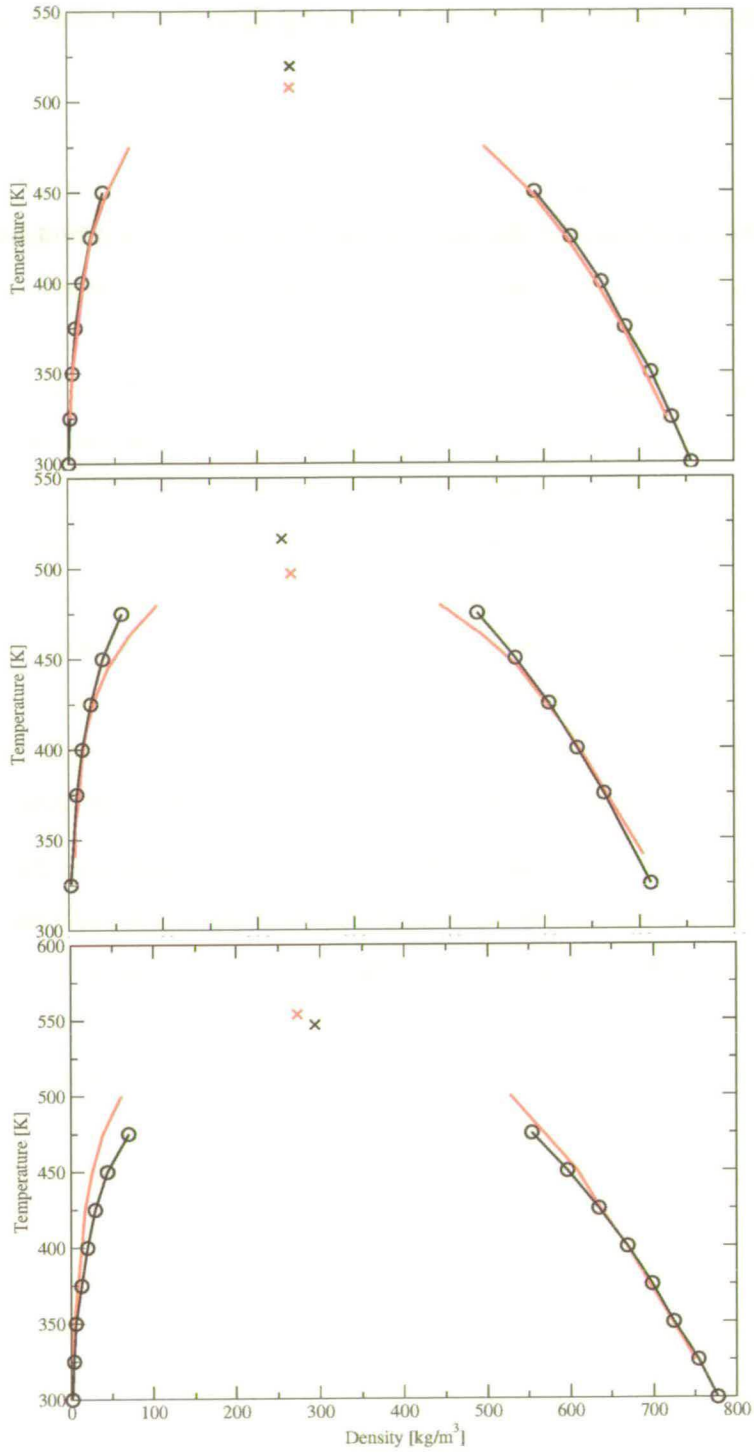

Figure 4.1: The vapour liquid coexistence curves for hexane (top), 2-methylpentane (middle) and cyclohexane (bottom). The red lines are the experimental data and the black lines are the simulation data. The crosses represent the experimental (red) critical point and the extrapolated critical point (black) found from the simulation data using the law of rectilinear diameters, see Section 2.6 for more details.

4.2 Heats of adsorption and Henry Coefficients - testing the zeolite potential

The previous section used the vapour-liquid coexistence curve to compare the potentials used to model the hydrocarbons with the experimental data. Whilst this provides for a check of the molecular potential and its parameters, it does not allow the validation of the zeolite-hydrocarbon potential parameters. To determine the applicability of the zeolite-hydrocarbon potential, the Henry coefficient and heat of adsorption are calculated. The Henry coefficient is found by performing a simulation of a single hydrocarbon within the pores of the zeolite. The results of such a simulation, coupled with a relatively straightforward simulation of a single hydrocarbon in the ideal gas phase, can be used to determine the Henry coefficient of the hydrocarbon in that zeolite. The heat of adsorption is calculated during a simulation in the Grand Canonical Ensemble and is found by evaluating the change in energy when one molecule is adsorbed within the zeolite. The experimental heat of adsorption and (to a lesser extent) the Henry coefficient are experimentally available quantities with which the simulated values can be compared. This comparison is one way of validating the zeolite-hydrocarbon potential.

The Henry coefficient requires analysis of very low pressure simulations. At such low pressures, experiments are more easily influenced by slight changes in pressure and as a result the quoted values for the Henry coefficient can differ between experiments. For example, slight differences in the zeolite samples used in the experimental measurement of the Henry coefficient can, at low pressure, result in a large difference in the uptake of the two zeolites. Since it is the uptake at very low pressures which determines the Henry coefficient, any small sample differences greatly affect the Henry coefficient. This effect is larger for larger molecules which will not adsorb in as great number as small molecules, at low pressure. Thus, the change in Henry coefficient caused by permitting fewer molecules to adsorb within the zeolite is not as large when there are already many molecules adsorbed. Preventing a few molecules adsorbing (by having defects within the zeolite structure) can play a large role when the molecules are large and thus there are only a few molecules adsorbed at low pressure.

Table 4.1 shows the comparison between the simulated and experimental heats of adsorption and Henry coefficients for hexane, 2-methylpentane and cyclohexane. The experimental data

Table 4.1: The heats of adsorption ($-Q_{st}$) and Henry coefficients (K_H) for hexane (N6), 2-methylpentane (2MP), and cyclohexane (C6) in silicalite-1, ITQ-22, and $AlPO_4$-5 at 300K. $-Q_{st}$ is in units of kJ/mol, K_H is in units of mol/kg/Pa.

	silicalite-1				ITQ-22		$AlPO_4$-5			
	K_H	$K_H^{(expt)}$	$-Q_{st}$	$-Q_{st}^{(expt)}$	K_H	$-Q_{st}$	K_H	$K_H^{(expt)}$	$-Q_{st}$	$-Q_{st}^{(expt)}$
N6	2.35	3.05	70.8	71	0.65	61.3	0.38	12.3	53.4	56.5
2MP	3.25	–	71.4	63-89	0.88	63.0	1.06	15.8	57.2	62.2
C6	1.30	–	61.8	63	1.04	58.7	2.52	29.0	55.2	57.2

for silicalite-1 is from references [164–168] and for $AlPO_4$-5 is from reference [169]. There is no experimental data available for either the heat of adsorption or Henry coefficient for ITQ-22 since this zeolite has only recently been synthesised and has yet to be the focus of an experimental adsorption study.

The comparison between the experimental and simulation data in Table 4.1 shows that the potential parameters used to model the adsorbate-zeolite interaction work well for different zeolites and different adsorbate types. Examining the data in more detail reveals that, for silicalite-1, the agreement between the heats of adsorption is excellent, although it should be noted that the range of experimental data is quite large in the case of 2-methylpentane. The Henry coefficients in silicalite-1 determine the low pressure adsorption behaviour and comparison with the available experimental data (for hexane) is reasonable. It should be noted that the simulated Henry coefficient is extremely sensitive to the choice of potential parameters and it is possible for two separate simulations, which predict different Henry coefficients, to produce adsorption isotherms which are very similar. For example, references [83] and [86] report Henry coefficients of 1493 and 3040 mol/m^3/kPa at 423K respectively whilst both producing very similar adsorption isotherms for cyclohexane in silicalite-1. Despite having different Henry coefficients, the heats of adsorption in references [83] and [86] are similar (-61.8 and -57.1 kJ/mol) and thus it would seem that the heat of adsorption is the more important quantity when determining the adsorption isotherm. The trend in the Henry coefficients in silicalite-1

indicate that, at very low pressure (the regime in which the Henry coefficient is applicable) cyclohexane will adsorb in much smaller numbers than either hexane or 2-methylpentane. To get a clearer picture of the adsorption of these alkanes, an analysis of their locations within the zeolite at various temperatures will be presented in the next section.

Both the heats of adsorption and the Henry coefficients in ITQ-22 show that more cyclohexane than hexane or 2-methylpentane will adsorb at low pressures. Again, a detailed discussion of the adsorption locations will be given in the next section which will explain the reversal in the heat of adsorption hierarchy compared with silicalite-1.

The third section of Table 4.1 compares the simulated and experimental adsorption properties in $AlPO_4$-5. The first point to note is that $AlPO_4$-5 contains both Aluminium and Phosphorous - atoms which are not included in the zeolite potential - the zeolite is assumed to be a network of oxygen atoms. This assumption has been tested for siliceous zeolites but not for aluminophosphates such as $AlPO_4$-5. However, the simulated heats of adsorption in $AlPO_4$-5 are in reasonable agreement with the experimental data - indeed the differences are not more than 5 kJ/mol. Furthermore, the hierarchy is maintained - the experiments show that 2-methylpentane has the largest heat of adsorption followed by cyclohexane and then finally hexane - this trend is reproduced in the simulations. Examining the Henry coefficients again shows that the overall trend is the same in both the experiments and the simulations. However, the simulated Henry coefficients are much lower than the experimental equivalents. The next section will explore the full adsorption isotherm for the hexane, 2-methylpentane and cyclohexane in $AlPO_4$-5 and discuss any differences between simulation and experiment.

The simulated heats of adsorption show that the same zeolite-adsorbate potential parameters can be used to accurately describe the interaction between hexane, 2-methylpentane, cyclohexane and two siliceous zeolites and one aluminophosphate.

4.3 Adsorption isotherms in silicalite-1

The previous section focused on the heats of adsorption and Henry coefficients and their comparison with experimental work. Both quantities are important in determining the applicability

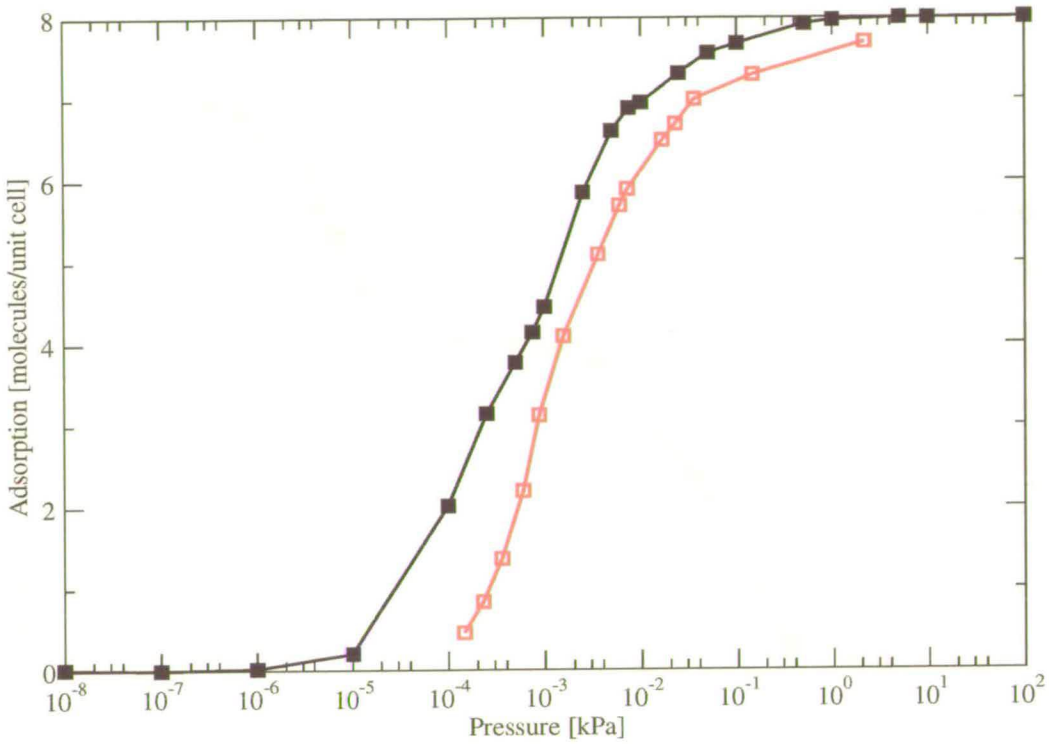

Figure 4.2: The adsorption isotherm of hexane in silicalite-1 at 303K. The red line is the isotherm from the experimental work in reference [164].

of the potential parameters and are the first step in the simulation journey. A further check of the simulation model is to determine the adsorption isotherm of each molecule in each zeolite. In this way a macroscopic quantity - the number of adsorbed molecules - can be compared with experiments over a wide pressure range. If the experimental and simulated isotherms are in agreement then an analysis of the microscopic properties of the adsorbed molecules can be made with confidence. This section presents the adsorption isotherms of linear, branched and cyclic molecules in silicalite-1.

4.3.1 Hexane and heptane

The experimental and simulated adsorption isotherms for hexane in silicalite-1 are shown in Figure 4.2. The agreement between the two isotherms is good at higher pressures but at very low pressure the simulations predict a loading which is much larger than the experimental

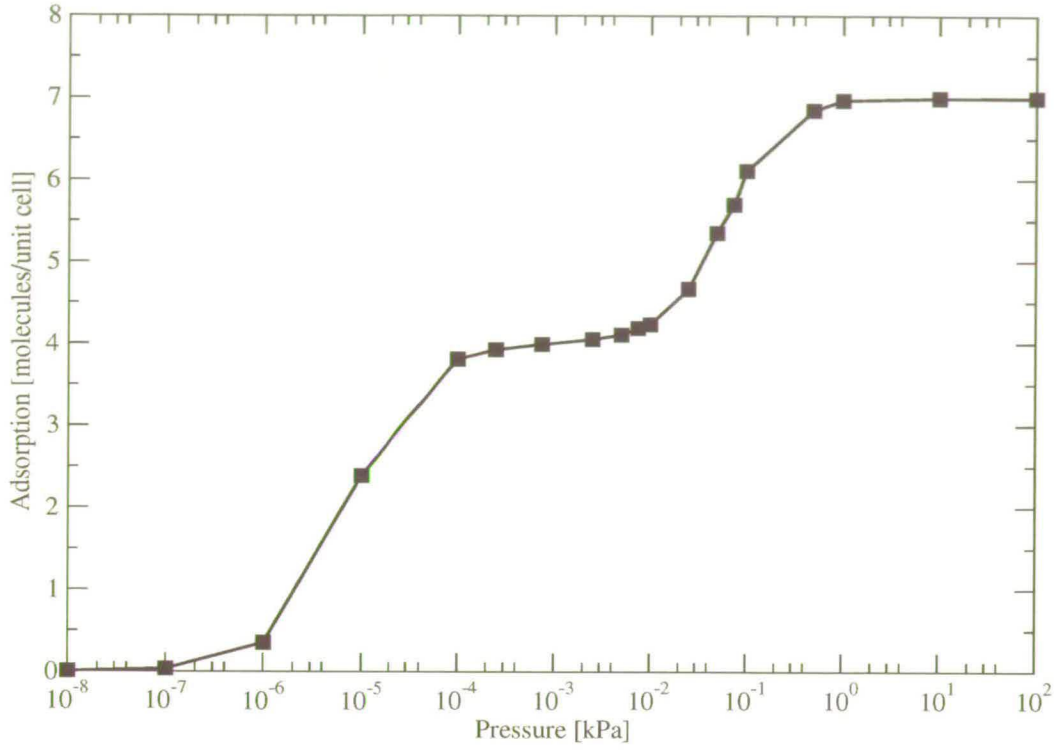

Figure 4.3: The adsorption isotherm of heptane in silicalite-1 at 303K.

findings. The discrepancy at low pressure could be due to the fact that experimentally silicalite-1 may have pore imperfections which create restrictions, preventing the molecules finding their adsorption locations. Such restrictions are not present in the simulation model of silicalite-1. It is interesting to note that there is a kink in the simulated isotherm around 4 molecules per unit cell. This inflection is not very pronounced but it is an important feature of the hexane isotherm. Increasing the length of the alkane to heptane results in the adsorption isotherm shown in Figure 4.3. Now the inflection is very pronounced and exists over a much wider pressure range.

Inflections in the adsorption isotherm of molecules within a zeolite may be attributed to adsorption of molecules *between* the zeolite crystals where capillary condensation may take place. However, the computational model used in determining the simulated adsorption isotherm involves only the bulk zeolite - it is not possible for a molecule to adsorb on the external surface

of the zeolite crystal. There must therefore be a different explanation for the inflection in the simulated isotherms.

In reference [96], Smit and Maesen use Grand Canonical Monte Carlo simulations to investigate the adsorption properties of hexane and heptane (among others) in silicalite-1. They too found evidence of isotherm inflection in hexane and heptane but, significantly, not for linear alkanes of a different length. They proposed a molecular explanation for the step in the isotherms which involved the rearrangement of adsorbed molecules to free up space within the zeolite pores and thus allow further adsorption. The loss of entropy associated with the rearrangement of the adsorbed molecules is offset by the increase in chemical potential which occurs due to the fact that the rearrangement happens as the pressure increases and that no more molecules are adsorbed until the rearrangement is complete. An analysis of the molecular locations of hexane and heptane at various pressures confirms this theory and will now be discussed.

At low pressure (below the inflection) the hexane molecules are distributed equally in the straight channels, zig-zag channels and at the intersections. Indeed, it is the case that a molecule which is adsorbed in the intersection may impinge upon one of the channels (and vice-versa), preventing adsorption of another molecule in that channel. This situation continues until the inflection, when the hexane molecules move in such a way as to fit neatly into the zig-zag channels, without impinging upon the intersections. As the pressure increases, the molecular rearrangement results in the straight channels becoming available to molecules for adsorption and the gradient of the adsorption isotherm increases. The whole rearrangement process occurs over a short pressure range in hexane but in heptane there is a larger range over which the number of adsorbed molecules remains constant. This extra pressure is used to balance the loss of entropy which occurs as the molecules occupy more ordered positions.

The isotherm inflections are not seen for shorter or longer alkanes because hexane and heptane are the only alkanes which have lengths commensurate with the length of the zig-zag channels and thus they are the only alkanes which can be 'frozen' in the zig-zag channels, resulting in the freeing up of the straight channels. Longer molecules will impinge upon the intersections if they reside in the zig-zag channels and shorter molecules will easily fit into the zig-zag

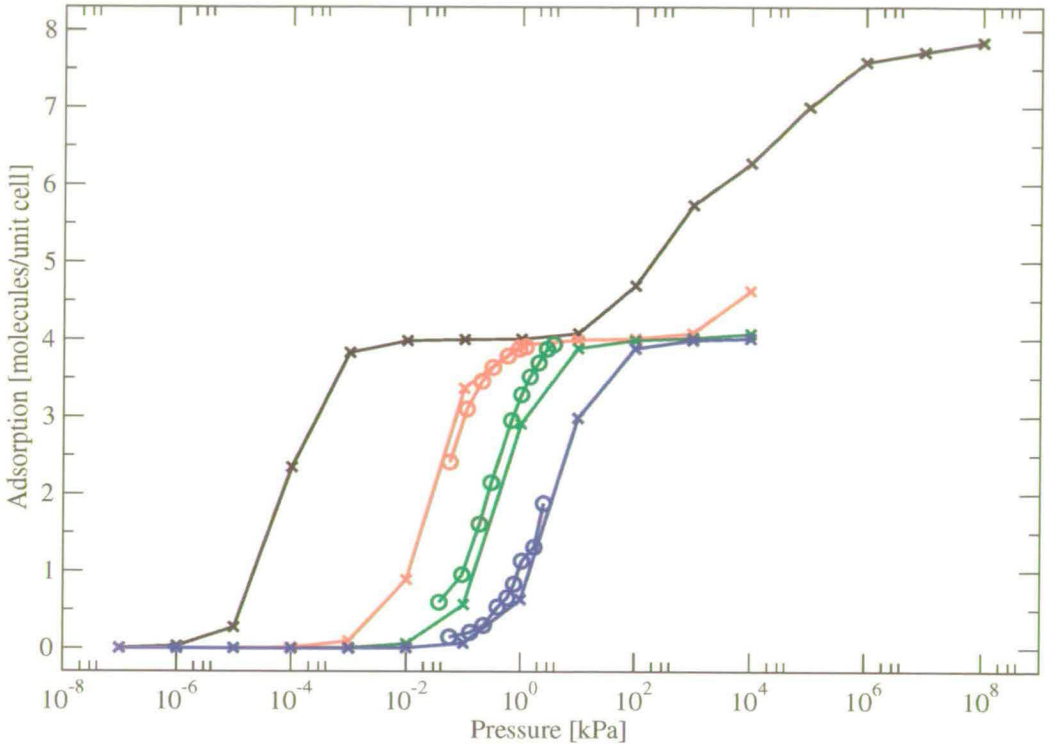

Figure 4.4: The adsorption isotherm of 2-methylpentane in silicalite-1. The black line is at 303K, the red lines are at 373K, the green lines at 423K and the blue lines at 473K. The circles represent the experimental data taken from [170].

channels and so will not benefit from collective rearrangement. The 'commensurate freezing' of hexane and heptane was first explained by Smit and Maesen in reference [96].

4.3.2 2-methylpentane

Figure 4.4 shows the simulation adsorption isotherms for 2-methylpentane in silicalite-1 at 303K, 373K, 423K and 473K together with the available experimental isotherms. The agreement with the experimental isotherms is excellent over a wide temperature and pressure range. A brief glance at the 303K isotherm reveals that the maximum loading is identical to that of hexane at the same temperature but is only achieved at extremely high pressures (above 10^6kPa). The difference between the pressure at which the maximum adsorption level is reached is likely to be due to the extra steric hindrance of the branched 'head' in 2-methylpentane; at 303K hex-

ane will be relatively long and thin compared with 2-methylpentane which, due to the branched head will find it harder to fit into the narrow channels of silicalite-1. The extra restriction imposed on 2-methylpentane by the branched head means that it requires a higher pressure to squeeze it into the channels, whereas hexane is able to fit into the channels more easily and thus achieves its highest loading at a lower pressure.

At all temperatures the isotherms are kinked, with an inflection at 4 molecules per unit cell. As shown in the previous section, inflections are indicative of a molecular rearrangement whereby the molecules which are already adsorbed within the zeolite move in such a way that they free up areas of the zeolite and thus allow further adsorption. In the case of hexane and heptane this rearrangement involved movement of the molecules to specific locations within the pores of the zeolite. Analysis of the locations of the 2-methylpentane molecules at 303K and various pressures reveals that the molecular rearrangement takes on a slightly different form to that observed with hexane or heptane. At low pressures (below 10^{-4}kPa on the 303K isotherm) the 2-methylpentane molecules adsorb only at the intersections (of which there are 4 per unit cell - hence the inflection in the isotherms at 4 molecules per unit cell). The orientation of the molecules is such that the branched heads are in the intersection and the straight tails point, without preference, into either the straight of the zig-zag channels. However, as the pressure is increased (from 10^{-4} to 10^{0}kPa) the orientation of the molecules changes, without increasing the number of molecules that are adsorbed. The branched head is still located in the intersections whilst the tails, which were in either the straight or zig-zag channels now move into the straight channel - leaving the zig-zag channel completely free of any obstruction. Once this reorientation has taken place, more 2-methylpentane molecules can adsorb (shown by the increase in gradient above 10^{1}kPa in the 303K isotherm) in the zig-zag channels.

As was the case with hexane and heptane, the decrease in entropy brought about by the reordering of the adsorbed 2-methylpentane molecules is compensated for by the increase in pressure during the rearranging process.

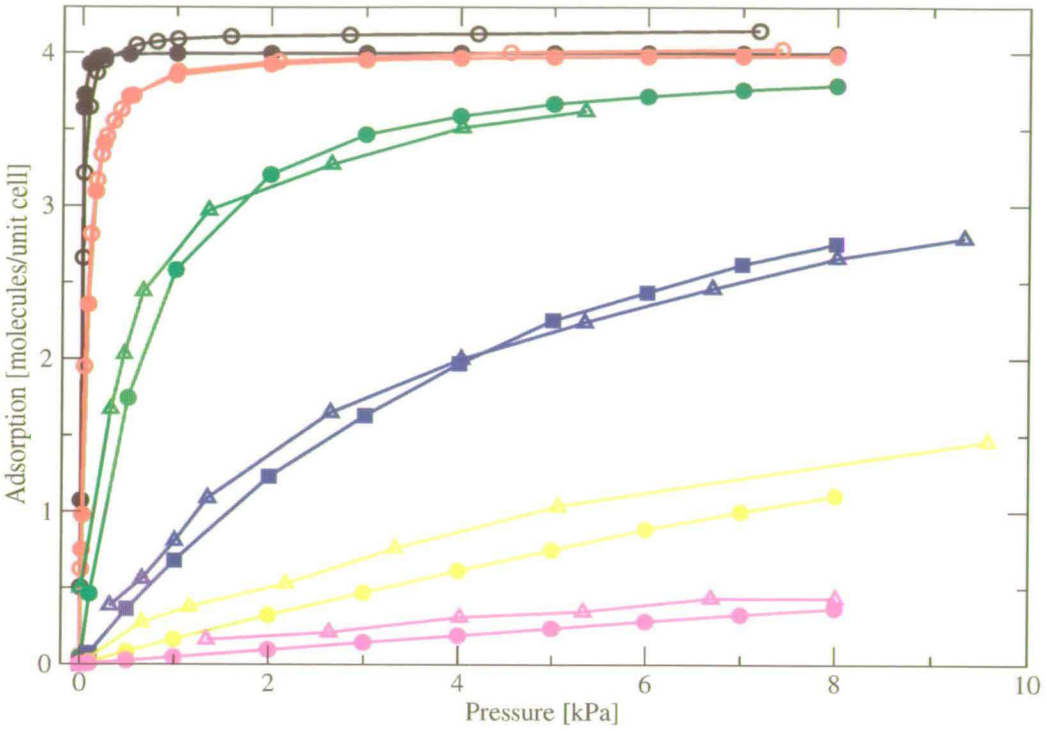

Figure 4.5: The adsorption isotherms of cyclohexane in silicalite-1. The isotherms are as follows: 323K(black), 373K(red), 423K(green), 473K(blue), 523K(yellow), and 573K(purple). The open symbols represent the experimental data from reference [73] (circles) and from reference [170] (triangles).

4.3.3 Cyclohexane

As discussed in the previous sections, both hexane and 2-methylpentane have isotherms which exhibit an inflection that was found to be as a result of rearrangement of the adsorbed molecules to free up space within the pores and permit adsorption of extra molecules. Figure 4.5 shows that there is no such inflection in the adsorption isotherm of cyclohexane in silicalite-1. The agreement between the simulated and experimental isotherms is very good over the entire temperature and pressure range. As the temperature increases, the number of molecules which adsorb at a given pressure decreases. This is due to the increased kinetic energy that the molecules have at higher temperature resulting in them being less likely to 'stick' onto the internal surface of the zeolite.

One particularly interesting feature of Figure 4.5 is the very slight discrepancy between the

323K simulated and experimental isotherms at high pressures. The simulated isotherms show a maximum loading of 4 molecules per unit cell whilst the experimental isotherm has a maximum of slightly more than 4 (around 4.15 molecules per unit cell). An investigation of the adsorbed location of the cyclohexane molecules shows that they adsorb exclusively at the intersections, of which there are 4 per unit cell. Even at high pressure the molecules do not adsorb in any other location and thus the simulated maximum loading is 4 molecules per unit cell. However, experimentally there may be imperfections in the zeolite crystal structure and there may also be gaps between the different zeolite crystals, allowing adsorption on the external surface of the zeolite. These extra adsorption possibilities may account for the enhanced adsorption seen in the experimental 323K isotherm. The simulations make use of a perfect zeolite crystal and so no external surface adsorption is possible.

Another possible explanation for the difference in the high pressure adsorption of the experimental and simulation 323K isotherms is zeolite flexibility. It is well known that zeolite flexibility plays a role in the diffusion of molecules whose size is commensurate with that of the zeolite pores (see references [159] and [160] and Section 3.6). At high pressure the cyclohexane molecules may cause a local distortion of the zeolite structure which may affect the maximum loading. It would be very interesting to perform simulations using a flexible zeolite model to determine if the flexibility does indeed contribute to the overall maximum loading of cyclohexane at high pressure. However, it is questionable whether the zeolite could deform sufficiently to allow another cyclohexane molecule to adsorb or if the deformation would just modify the diffusion properties of cyclohexane in silicalite-1.

The adsorption location of hexane and 2-methylpentane in silicalite-1 are relatively well known [96, 119, 164]. However, the locations of cyclohexane are less well known and contradictory data exists: in reference [171] Ashtekar *et al.* concluded, on the basis of a FT-Raman spectroscopic study, that cyclohexane preferred the straight channels, whilst Rees *et al.* [73], using Frequency Response techniques, conclude that the molecules will adsorb in the intersections. The position of the adsorbed molecules can be determined from the simulation data and confirm the prediction of Rees *et al.* that the intersection is the preferred site. Figure 4.6 shows the averaged centre of mass positions for cyclohexane molecules in silicalite-1 at 323K and 8.0kPa. It is evident that the molecules only adsorb in the intersections - the locations of the

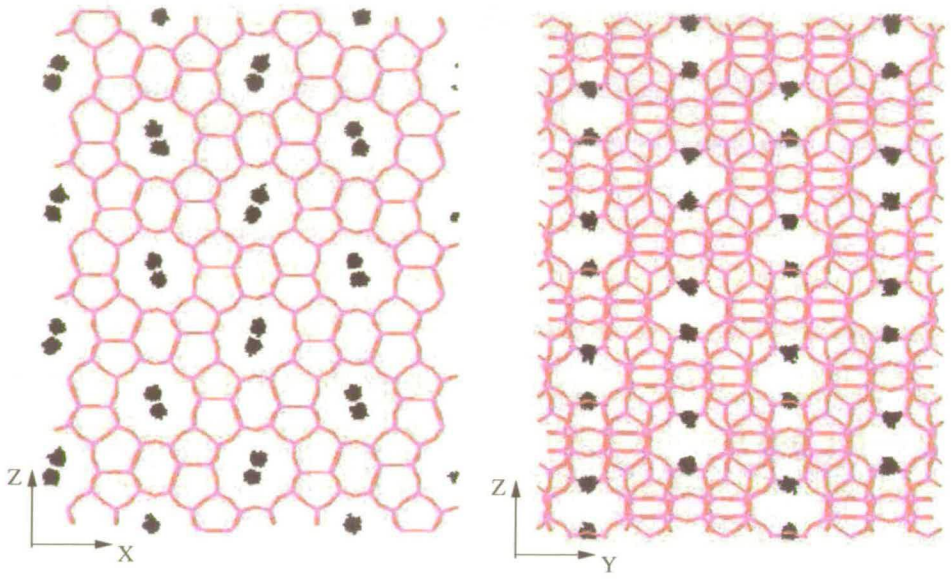

Figure 4.6: The centre of mass of each cyclohexane molecule at each timestep (black dots) at 323K and 8.0kPa. The left hand figure looks down the straight channels. The right hand figure looks along the direction of the sinusoidal channels.

black dots in the figure. The reason for there being two adsorption locations at the intersection is simply due to due to the fact that all of the sites in the Y (or X in the right hand figure) direction are visible - if a slice is taken through the plane of the intersection (as in Figure 4.7) only one of the sites is visible.

A relatively crude map of the likely adsorption locations is also accessible without having to perform a full adsorption simulation. The zeolite can be split up into a grid of small cubes and a pseudo atom with a similar diameter to the critical diameter of cyclohexane is inserted at each cube location and the fictitious insertion energy is recorded. Using this energy, a picture of the accessible volumes and relative strengths of the interaction energy at each point in the zeolite is built up. This array of adsorption strengths can be used to create a qualitative plot of the probability of the cyclohexane molecule adsorbing. Figure 4.7 shows such a plot, depicting the most likely adsorption sites for a single molecule of cyclohexane in silicalite-1. The slices through the zeolite in Figure 4.7 reveal that the most likely adsorption site is at the intersections - this is indeed the case for cyclohexane (as demonstrated in Figure 4.6). The apparent discrepancy between the number of adsorption sites (there appear to be twice as many in Figure 4.6

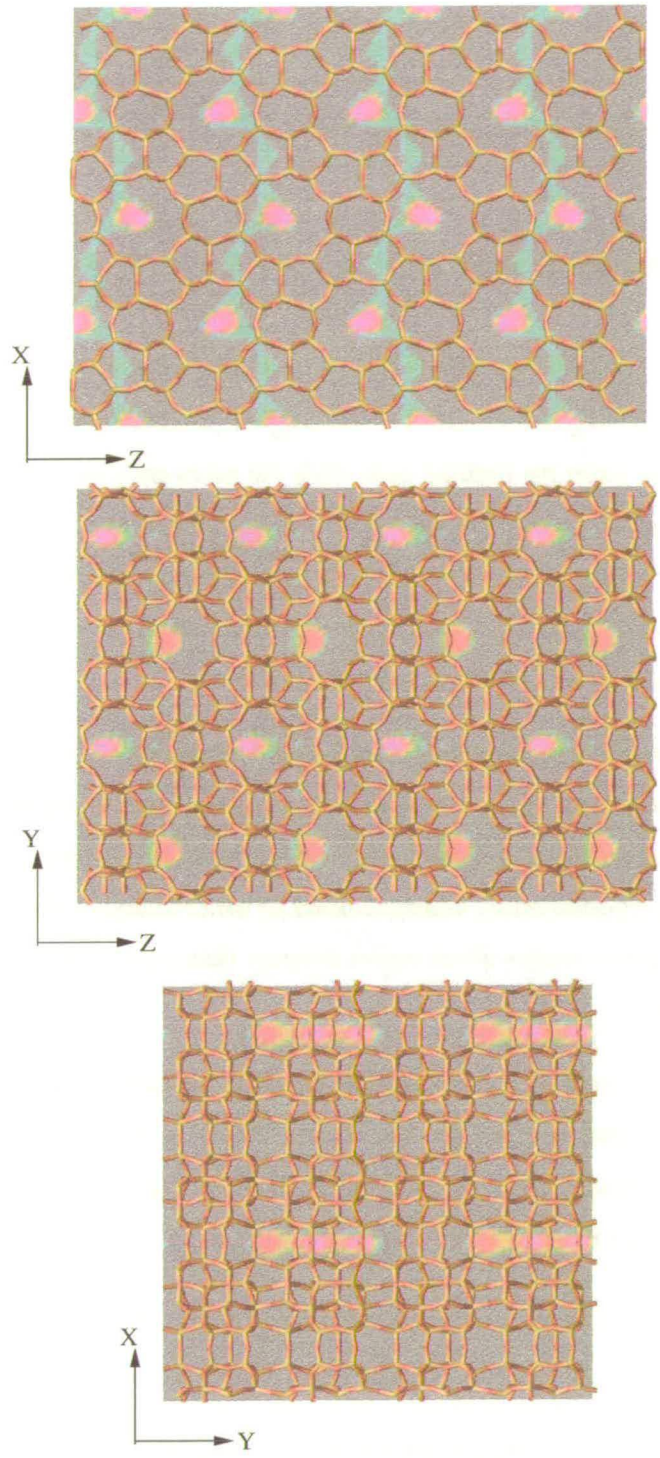

Figure 4.7: Slices through the probability of cyclohexane adsorption isosurface. Red/pink colours indicate regions of favoured adsorption whilst blue/green indicates regions of less favoured adsorption. The grey areas are inaccessible to the cyclohexane molecule. The top figure is a projection on the XZ plane, the middle is onto the YZ plane and the bottom figure is into the XY plane.

as there are in Figure 4.7) is merely due to the fact that in Figure 4.6 it is possible to see down the length of the straight channels whilst in Figure 4.7 the slice is only through one plane in the straight channel - the other planes are not shown.

4.4 Adsorption in $AlPO_4$-5

The previous section showed that in silicalite-1 the narrow pores resulted in cyclohexane only being adsorbed at the large intersections. What happens when the pores of the zeolite are less complicated? What about the limiting case when the pores are simple straight, unconnected channels? Does the same adsorption hierarchy that was seen in silicalite-1 still exist (namely, hexane adsorbing in greater number than 2-methylpentane or cyclohexane)? In an effort to answer these questions, as well as investigating the applicability of the zeolite model to non-siliceous zeolite, a study of $AlPO_4$-5 was undertaken.

$AlPO_4$-5 is an aluminophosphate and is modelled in the same way as silicalite-1, i.e. as a rigid network of oxygen atoms. Table 4.1 in Section 4.2 reveals that this approximation predicts heats of adsorption which are in good agreement with the experimental data. The predicted Henry coefficients are consistently underestimated by the simulations. As discussed in Section 4.2 it is possible for two studies which report different Henry coefficients to predict isotherms which are identical.

Newalkar *et al.* [169] have used gravimetric uptake to investigate the adsorption isotherms for hexane, 2-methylpentane and cyclohexane (among others) in $AlPO_4$-5. They found that the relative adsorption capacities (at maximum loading) of $AlPO_4$-5 for each alkane type (linear, branched, cyclic) fitted the following trend,

$$\text{cyclohexane} > 2-\text{methylpentane} > \text{hexane} \tag{4.1}$$

This trend of decreasing uptake with increasing molecular length is reproduced at all loadings in this work and is shown in Figure 4.8 which shows that despite the fact that the potential parameters for the $AlPO_4$-5-alkane interaction are in fact those optimised for silicalite-1, the overall trend in adsorption capacities is consistent with the experimental findings.

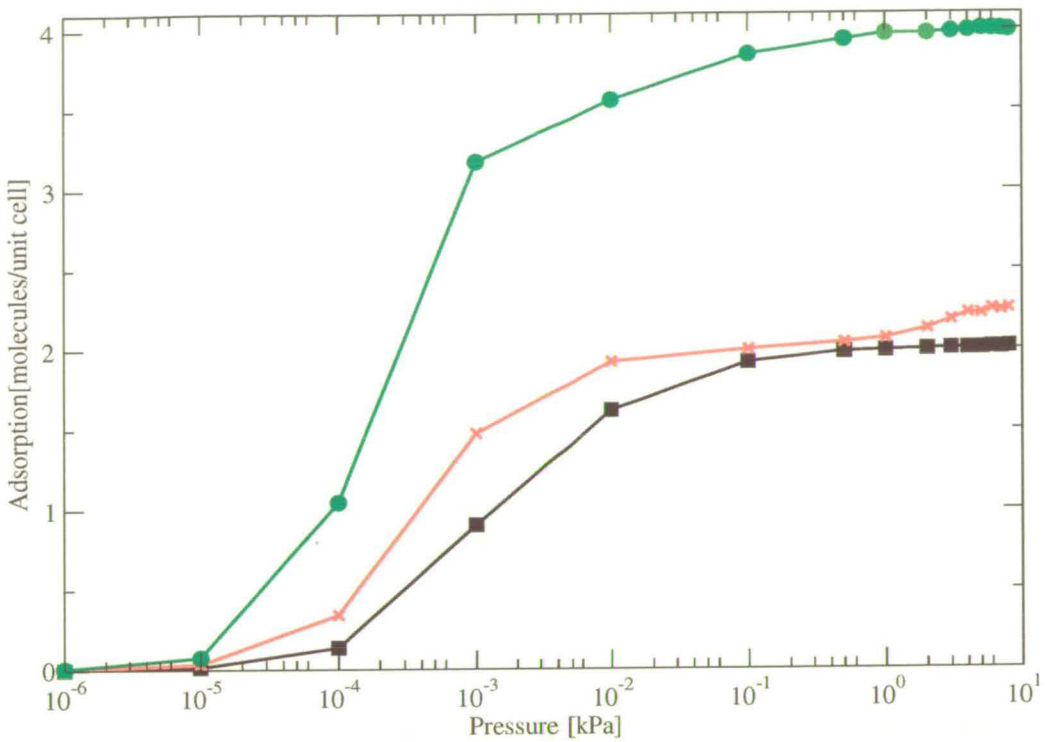

Figure 4.8: Adsorption isotherms for hexane (black), 2-methylpentane (red) and cyclohexane (green) in $AlPO_4$-5 at 303K.

The isotherms in Figure 4.8 do not show the large inflections that were present in the isotherms of 2-methylpentane or hexane in silicalite-1. The molecular explanation for the isotherm inflections in silicalite-1 focused on the movement of the molecules into particular pore locations. Since the pores in $AlPO_4$-5 are unconnected and straight, no such molecular rearrangement can take place and so the isotherms do not show inflections. Despite the lack of inflection it is still interesting to investigate the molecular locations within the long, straight pores of $AlPO_4$-5.

Newalkar *et al.* [169] hypothesised that hexane and 2-methylpentane molecules were not able to pack as efficiently as cyclohexane within the pores of $AlPO_4$-5. Their study focused on the (macroscopic) adsorption isotherms and did not provide any microscopic data (such as position or orientation of the adsorbed molecules) that could be used to verify their predictions. However, using simulations it is possible to analyse the orientation of the molecules within the pores to test the experimental predictions made.

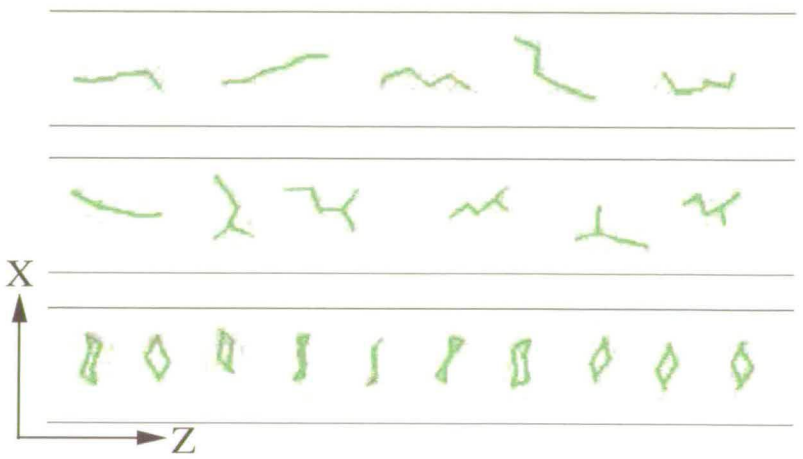

Figure 4.9: The orientation of the hexane (top), 2-methylpentane (middle) and cyclohexane (bottom) molecules in $AlPO_4$-5 at maximum loadings. The zeolite channel walls are shown schematically as the black lines.

Figure 4.9 shows the orientation of the hexane, 2-methylpentane, and cyclohexane molecules in a channel at their respective maximum loadings. It is possible to calculate the average distance between adjacent molecules in the channel, to get some idea of how close together they pack. The average hexane-hexane centre of mass distance is around 4.2Å, for 2-methylpentane it is around 4.3Å, and for cyclohexane around 3.7Å. This shows that the cyclohexane molecules can get closer together than either the hexane or 2-methylpentane. This higher packing density is achieved by the molecules adopting an upright stance within the channels, thus effectively minimising their width and so allowing more molecules to adsorb in the channel. Hexane and 2-methylpentane are unable to stack in this way due to their length which is longer than the diameter of the pore. It is possible for the linear and branched molecules to coil up and therefore occupy approximately the same space as the cyclic molecule, however, the coiled conformation is far from the lowest energy conformation and so it is unlikely that all of the hexane molecules will be coiled and in the correct orientation to occupy the same space as the cyclohexane molecules. It is observed (see Figure 4.9) that the linear and branched molecules tend not to coil and instead lie, with random orientation, along the channel. Newalkar *et al.* [169] proposed this upright stacking in their qualitative predictions and with the aid of computer simulations these predictions have been confirmed.

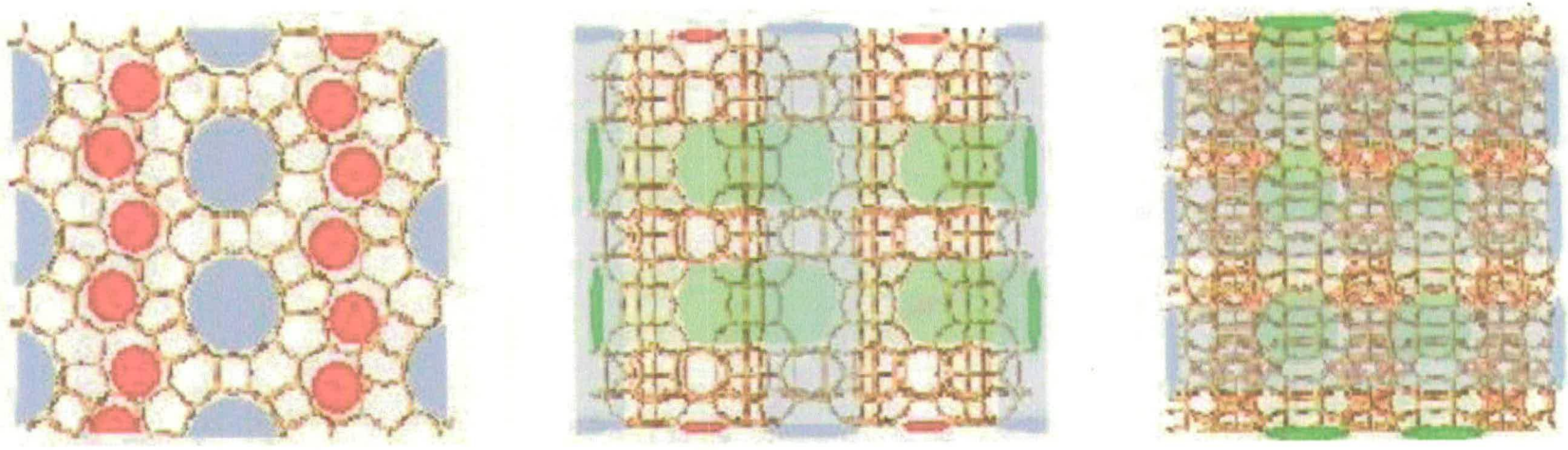

Figure 4.10: The structure of ITQ-22. The left hand image is a projection on the XZ plane, the middle image is on the YZ plane and the right image is on the XY plane. The blue areas represent the 12 membered ring (MR) channels, the green represents the 10MR zig-zag channels and the red areas the 8MR channels.

4.5 Adsorption in ITQ-22

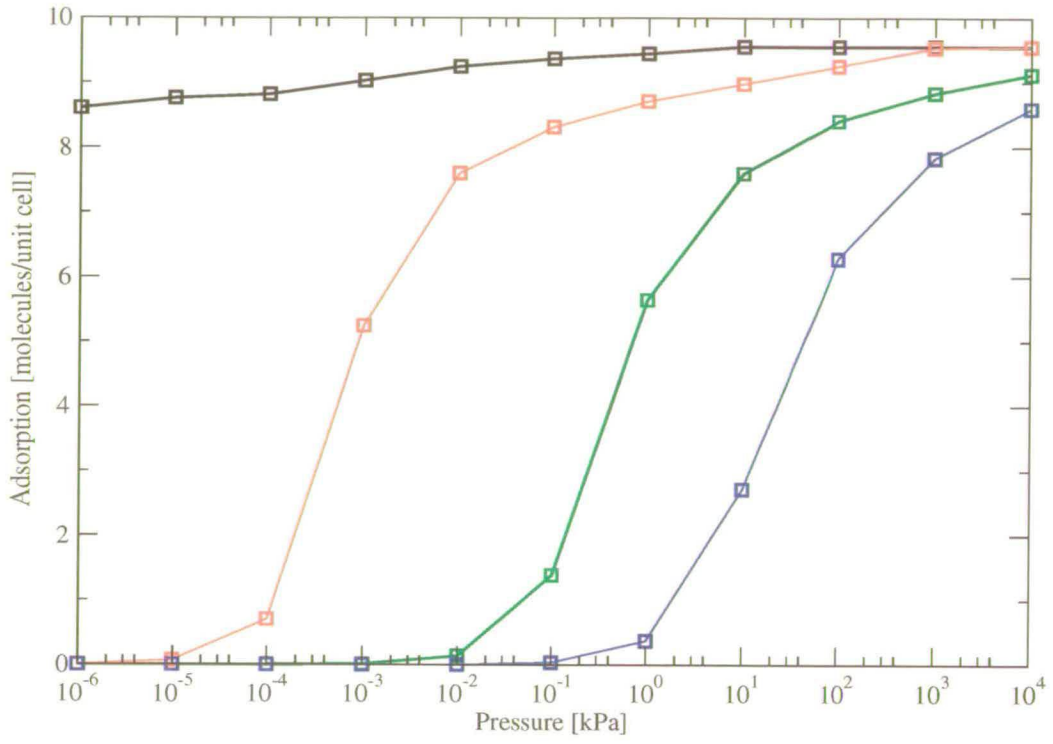

Figure 4.11: The adsorption isotherms of hexane in ITQ-22 at 200K (black), 300K (red), 400K (green) and 500K (blue).

The pore structure of ITQ-22 is shown in Figure 4.10 and consists of 3 interconnected pores: a small 8 membered ring (around 4Å), a 10 MR pore (around 5.5Å) and a large, 12MR pore (around 6.5Å). Figure 4.10 depicts the zeolite as the yellow and red network with the channel structure superimposed as the blue (12MR channel), green (10MR channel) and red (8MR channel). The left image is a projection on the XZ plane, the middle is on the YZ plane and the right is on the XY plane. Whilst the structure of ITQ-22 may look at first sight as a 3-dimensional network, the 8MR channels do not play any part in adsorption of molecules of the size used in this study. Indeed, further simulations revealed that no molecules larger than argon were able to explore the 8MR channel.

Figures 4.11, 4.12 and 4.13 show the adsorption isotherms of hexane, 2-methylpentane and cyclohexane in ITQ-22 at various temperatures. The isotherms do not exhibit any inflections and

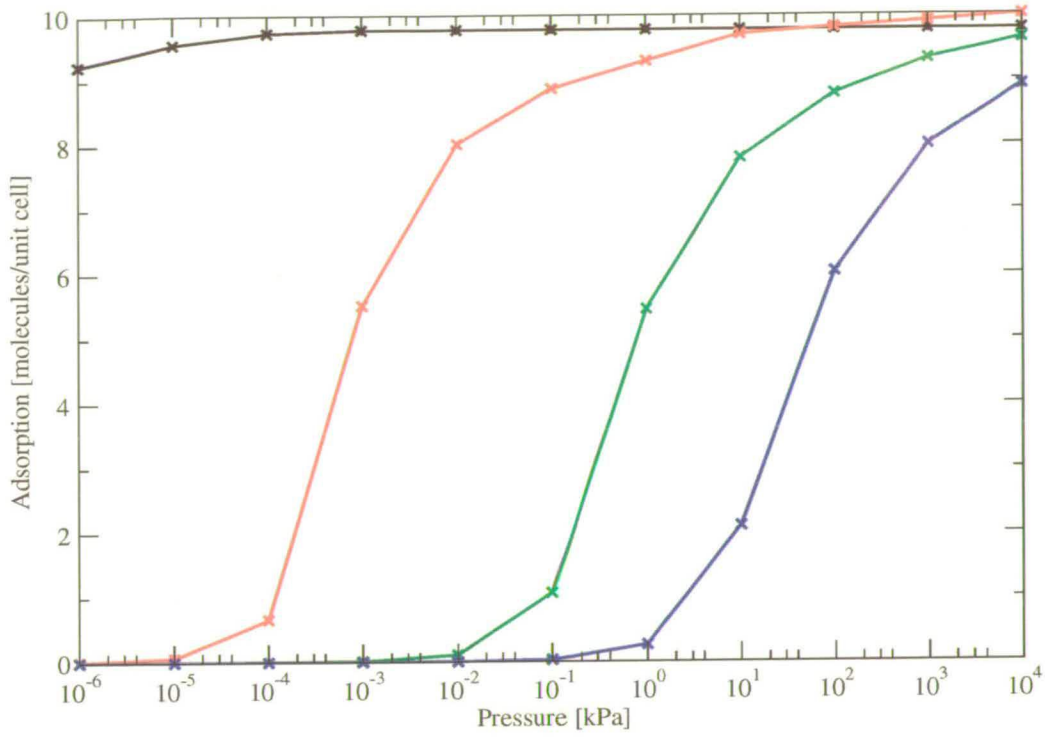

Figure 4.12: The adsorption isotherms of 2-methylpentane in ITQ-22 at 200K, 300K, 400K and 500K. Colours as in Figure 4.11.

simply reflect the tendency that, at a given pressure, fewer molecules adsorb as the temperature is increased. This is consistent with the knowledge that at higher temperature the molecules will have a larger kinetic energy and will therefore find it harder to adsorb.

There are no experimental studies of adsorption in ITQ-22 and therefore the adsorption isotherms cannot be compared with experimental data. However, based on the knowledge that the simulation model is able to predict adsorption properties in both silicalite-1 and $AlPO_4$-5 which agree well with the available experimental data, it is reasonable to expect that the predicted isotherms in ITQ-22 would be consistent with experiments since all three zeolites are modelled as rigid oxygen networks. It is possible to delve a little deeper into the adsorption in ITQ-22 and build up a picture of *where* in the zeolite each molecular type prefers to adsorb. Since ITQ-22 has only recently been synthesised, these results are not yet verifiable with any other studies.

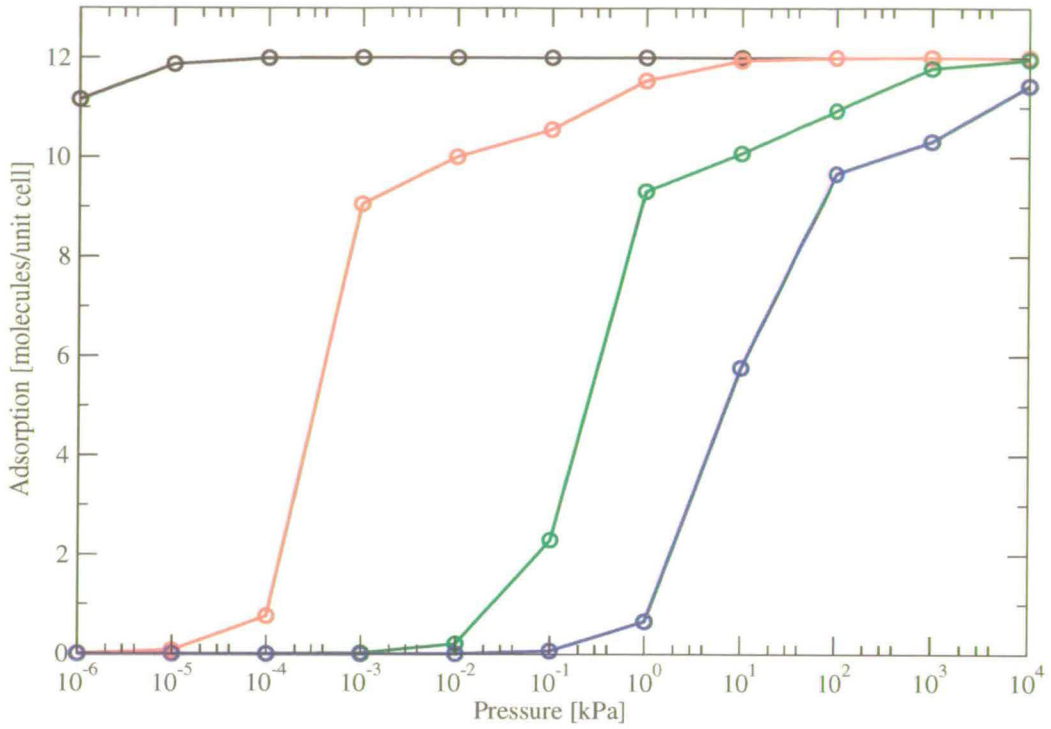

Figure 4.13: The adsorption isotherms of cyclohexane in ITQ-22 at 200K, 300K, 400K and 500K. Colours as in Figure 4.11.

4.5.1 Adsorption in ITQ-22: location of molecules

Hexane

Figure 4.14 summarises the adsorption locations for hexane in ITQ-22 at low, medium and high pressure, at 300K. The top three images are at 0.001kPa, the middle three are at 1.0kPa and the bottom three are at 10000kPa. The left column is the view in the XZ plane, the middle column is in the YZ plane and the final column is in the XY plane. Each blue circle represents the centre of mass of a hexane molecule. The positions of the hexane molecules are sampled throughout the simulation after an equilibration period. From Figure 4.14 it can be seen that, at high pressure, the centre of mass distribution of the adsorbed molecules does not occupy as much of the zeolite pore structure as at low pressure. In all planes, the localisation of the centre of masses is clearly visible as the pressure increases.

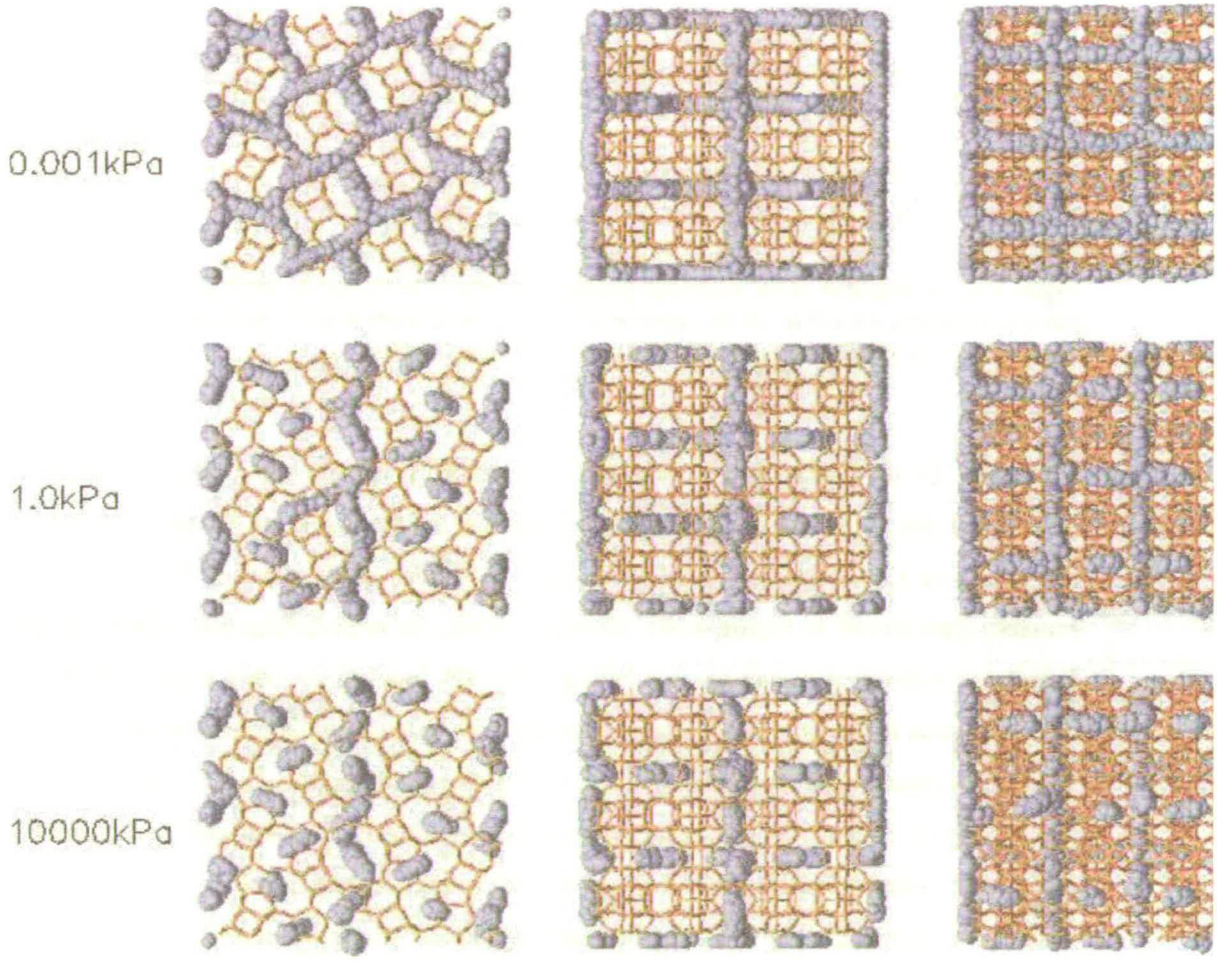

Figure 4.14: The centre of mass of the hexane molecules in ITQ-22 at low, medium and high pressure, at 300K. The left hand column is the projection on the XZ plane, the middle column is on the YZ plane and the right column is on the XY plane. The top row is at 0.001kPa, the middle row is at 1.0kPa and the bottom row data is at 10000kPa. Each blue sphere represent the centre of mass of a hexane molecule. The centre of masses were collected after an initial equilibration period.

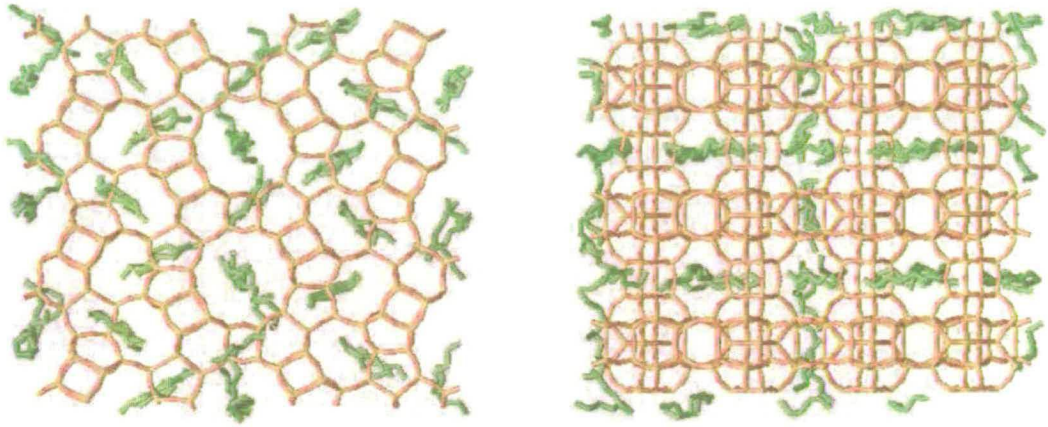

Figure 4.15: A snapshot of the molecular positions of hexane in ITQ-22 at 300K and 10000kPa. The hexane molecules are shown as the green shapes, only the 'pseudo atoms' are shown. The left image is a projection on the XZ plane and the right image is on the YZ plane.

The reason for the localisation of the centre of mass of the hexane molecules as the pressure increases is due to the number of molecules within the zeolite pores. At low pressure (the top row in Figure 4.14) there are only half as many molecules in the pores as there are at high pressure (bottom row in Figure 4.14). At low pressure, these molecules can 'move'[1] around the zeolite without encountering, and having their path blocked by, other molecules - hence the distribution of the centres of mass is relatively even throughout the pores. However, as the pressure increases, there are more molecules within the zeolite and therefore a molecule cannot move along the channels of the zeolite without encountering another molecule - with which it will interact, preventing the molecule from moving freely around the zeolite. In this way, the centre of mass distribution becomes localised around the adsorption sites until, at very high pressure, the loading of molecules reaches a maximum with insufficient space remaining in the zeolite for any more molecules to adsorb.

Whilst Figure 4.14 can be used to quickly determine the general effect of pressure on the distribution of the centre of mass of the molecules within the zeolite, it requires slightly more thought to gain an insight into the locations of the adsorbed molecules. The pore structure of

[1] Of course in Monte Carlo simulations a 'move' is not in real space but in phase space - so the molecule is able to 'jump' around the zeolite without following a physically reasonable path. The quotes around the word 'move' are used to remind the reader that the move is in phase space and not in real space. The blocking argument outlined in the paragraph is valid in both spaces!

ITQ-22 shown in Figure 4.10 will be of use in the understanding of the following discussion of molecular locations.

The left hand column of Figure 4.14 shows the projection on the XZ plane. This is the same orientation as Figure 4.10 (left) and so the 12MR channel runs into and out of the page (at the middle and edges of the image) and the zig-zag, 10MR channel runs across the page. The centre of mass of the hexane molecules at 0.001kPa is evenly distributed within the 12 and 10MR channels, as shown by the continuous network of blue spheres in the top left hand image in Figure 4.14. The top middle image shows the projection in the YZ plane with the 12MR channel running from top to bottom in the middle and at the edges and the zig-zag 10MR channel running from left to right. Both the 12MR and the 10MR channels show an even distribution of hexane molecules. However, the top-middle picture is most useful for determining if any molecules enter into the small 8MR channels which run from top to bottom, mid way between the 12MR channels (which are highlighted by the even distribution of hexane centre of masses). The image clearly shows that no hexane molecules are able to explore the narrow 8MR channels.

As the pressure increases the location of the centre of mass of the molecules becomes more well defined. The molecules in the 10MR zig-zag channels tend to favour the intersection between the 10MR and 8MR channels - this is most clearly seen in the lower middle image. The molecules in the 12MR straight channel are more evenly distributed than those in the 10MR channel, although there is some favouring of the intersection and the middle of the channel - with limited adsorption between these areas (most easily seen in the lower middle image).

Looking at a snapshot of the molecular positions of hexane in ITQ-22 at 300K and 10000kPa (Figure 4.15), reveals that the hexane molecules can fit into the zig-zag channels and are relatively uncoiled. The same is true in the 12MR straight channels whereby the hexane molecules can adsorb in the middle of the channel (again uncoiled) and at the intersection between the straight and zig-zag channels. The combination of the centre of mass images and the snapshots of the molecules provides a detailed picture of the preferred adsorption locations of hexane in ITQ-22.

2-methylpentane

The change of centre of mass distribution with pressure, Figure 4.16, for 2-methylpentane shows a very similar trend to that of hexane. A snapshot of the position of the 2-methylpentane molecules is similar to that of hexane and Figure 4.17 suggests that the ordering of the molecule is almost identical to that of hexane. Looking at the adsorption isotherms of hexane and 2-methylpentane (Figures 4.11 and 4.12) indicates that the maximum loading of 2-methylpentane is slightly greater than that of hexane. This is due to the shorter molecular length of 2-methylpentane, resulting in slightly more molecules fitting within the zeolite pores.

Cyclohexane

The maximum loading of cyclohexane in ITQ-22 at 300K is 20% greater than that of either hexane or 2-methylpentane. It would therefore be reasonable to expect a slightly different centre of mass distribution since cyclohexane finds more adsorption sites in ITQ-22 than hexane or 2-methylpentane. Figure 4.18 presents the centre of mass distribution for cyclohexane at low, medium and high pressures. The first thing to notice is that the centre of mass distribution is more localised at low pressure when compared to hexane or 2-methylpentane. This is simply due to the fact that at low pressures, more cyclohexane molecules have adsorbed compared to hexane or 2-methylpentane and so there are more molecules within the zeolite and so each molecule can explore fewer sites when compared with an empty zeolite. At high pressures, the XZ projection (bottom left image) shows a similar distribution to 2-methylpentane but is slightly more localised. However, the projection on the YZ (bottom middle image) reveals that the distribution in the 12MR channel is different to that of hexane or 2-methylpentane. For hexane and 2-methylpentane, there were 3 adsorption sites associated with the 12MR channel: two at its intersection with the 10MR channel and one in the centre of the 12MR channel - midway between the intersections. Cyclohexane manages to find 4 adsorption sites: two at the intersections and *two* in the channel. This is only made possible by the shape of cyclohexane- which is much more suited to stacking within the channel. This can be seen in Figure 4.19 which shows a snapshot of the molecular locations of cyclohexane in ITQ-22 at 300K and 10000kPa. The molecules are aligned within the 12MR channels and it is possible to fit two

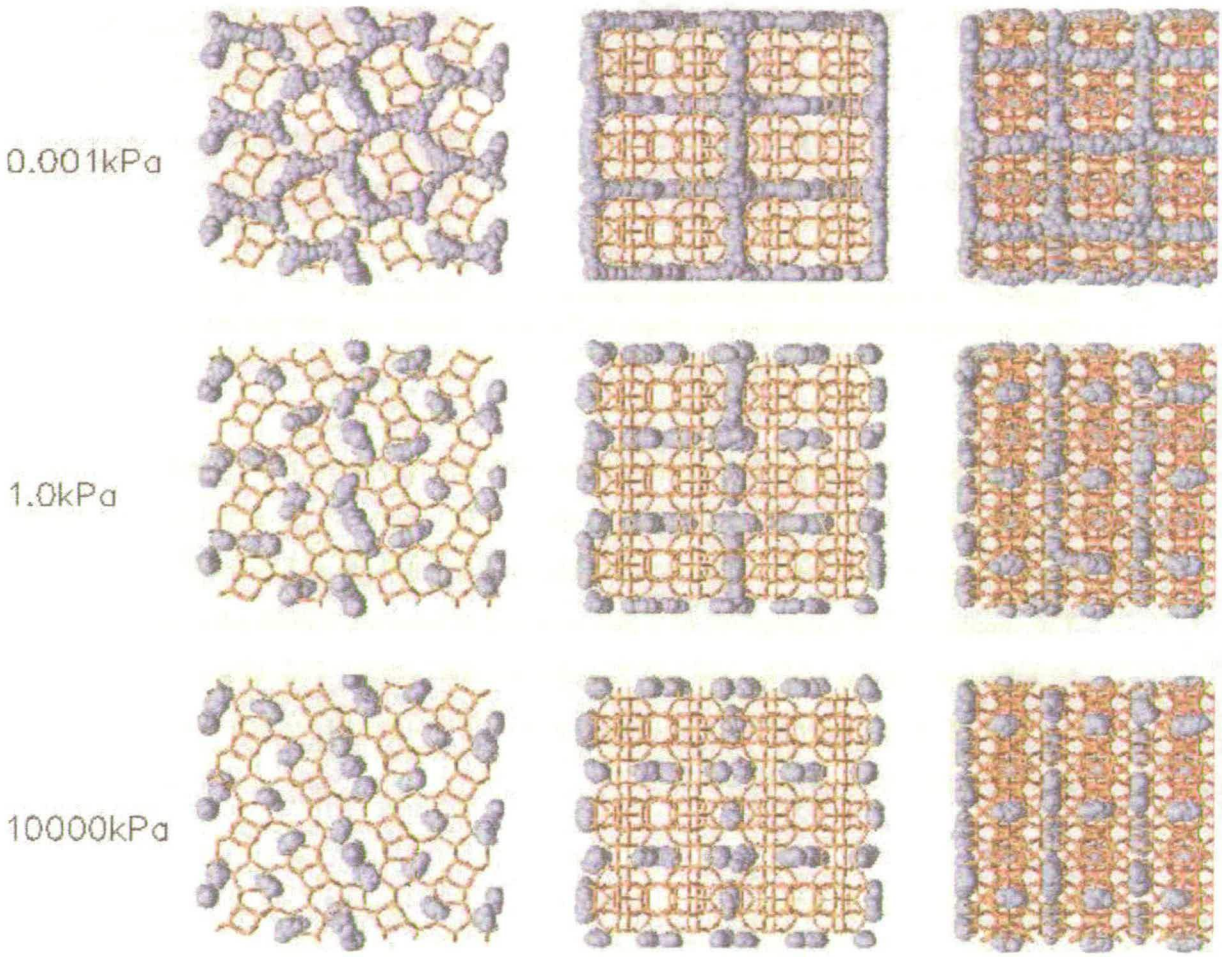

Figure 4.16: The centre of mass of the 2-methylpentane molecules in ITQ-22 at low, medium and high pressure, at 300K. The left hand column is the projection on the XZ plane, the middle column is on the YZ plane and the right column is on the XY plane. The top row is at 0.001kPa, the middle row is at 1.0kPa and the bottom row data is at 10000kPa. Each blue sphere represent the centre of mass of a 2-methylpentane molecule. The centre of masses were collected after an initial equilibration period.

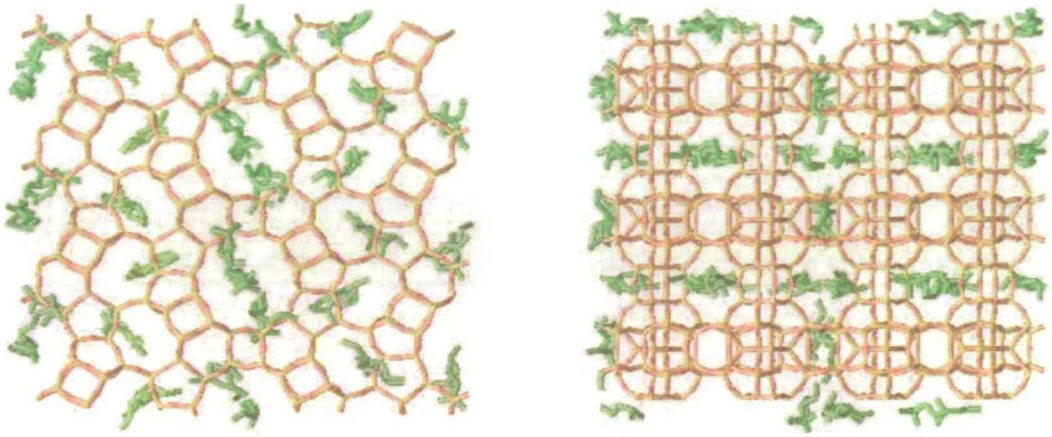

Figure 4.17: A snapshot of the molecular positions of 2-methylpentane in ITQ-22 at 300K and 10000kPa. The 2-methylpentane molecules are shown as the green shapes, only the 'pseudo atoms' are shown. The left image is a projection on the XZ plane and the right image is on the YZ plane.

cyclohexane molecules into the 12MR channel, between the intersections. There are 6 straight channels in the simulation cell of ITQ-22 and this equates to 18 (3 extra sites per channel) extra adsorption sites that cyclohexane has access to and hexane and 2-methylpentane do not. The simulation cell is composed of 9 unit cells and so there are 2 extra sites per unit cell that cyclohexane can use and hexane and 2-methylpentane cannot. This explains the maximum loadings of cyclohexane (12 molecules per unit cell) and hexane and 2-methylpentane (both around 10 molecules per unit cell).

4.6 Conclusions

This chapter has shown that computer simulations can be used to model the adsorption of linear, branched and cyclic alkanes in siliceous zeolites and aluminophosphates, using a single set of potential parameters. The results of the pure alkane simulations to determine the vapour-liquid coexistence curves agreed well with the experimental data, confirming that the alkane is correctly modelled. The heats of adsorption agreed well with the available experimental data (ITQ-22 is a new zeolite and so no experimental data could be found). The Henry coefficients for the various molecules in silicalite-1 were found to agree reasonably well with experiments whilst those for $AlPO_4$-5 were consistently underestimated. Despite this, the ad-

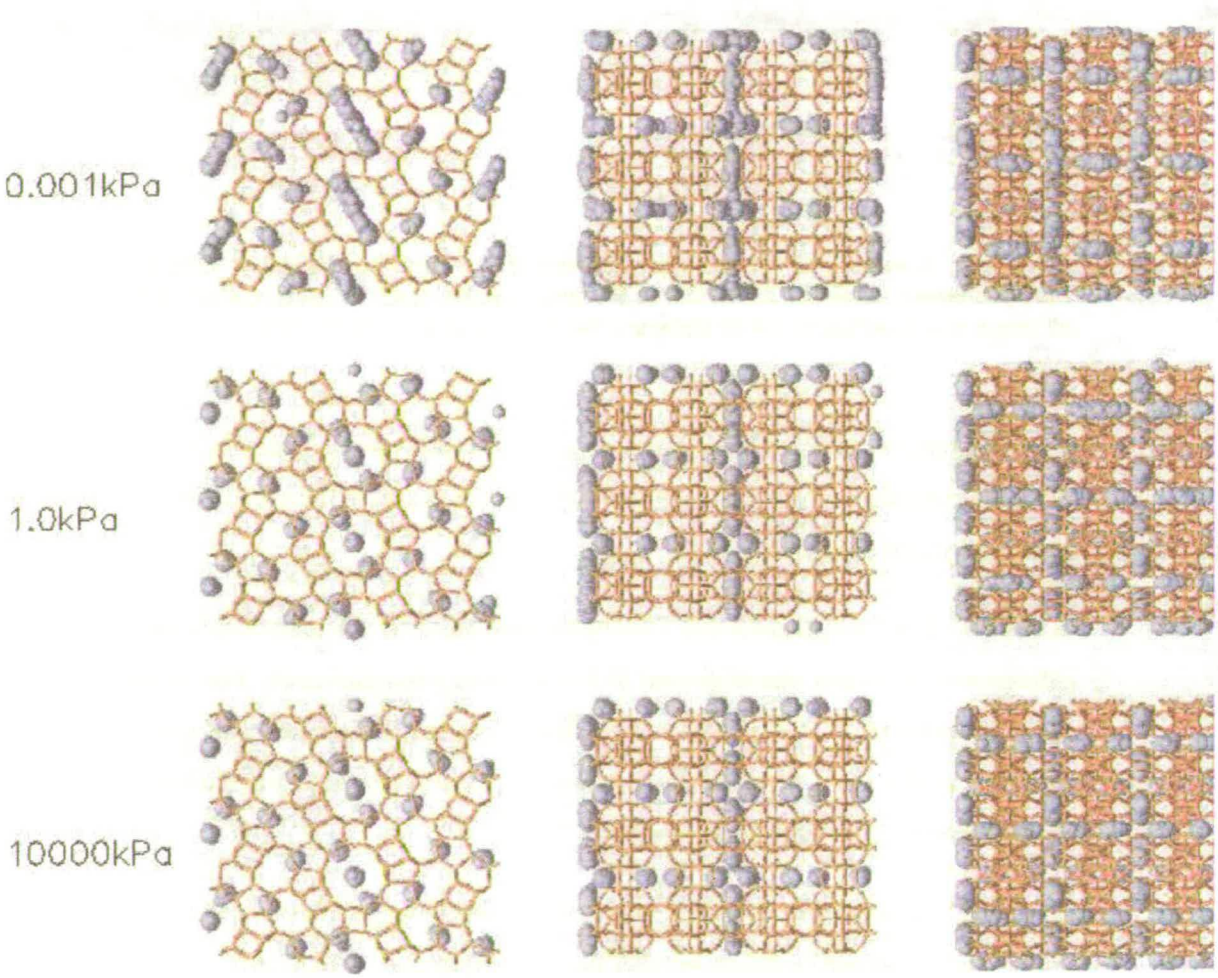

Figure 4.18: The centre of mass of the cyclohexane molecules in ITQ-22 at low, medium and high pressure, at 300K. The left hand column is the projection on the XZ plane, the middle column is on the YZ plane and the right column is on the XY plane. The top row is at 0.001kPa, the middle row is at 1.0kPa and the bottom row data is at 10000kPa. Each blue sphere represent the centre of mass of a cyclohexane molecule. The centre of masses were collected after an initial equilibration period.

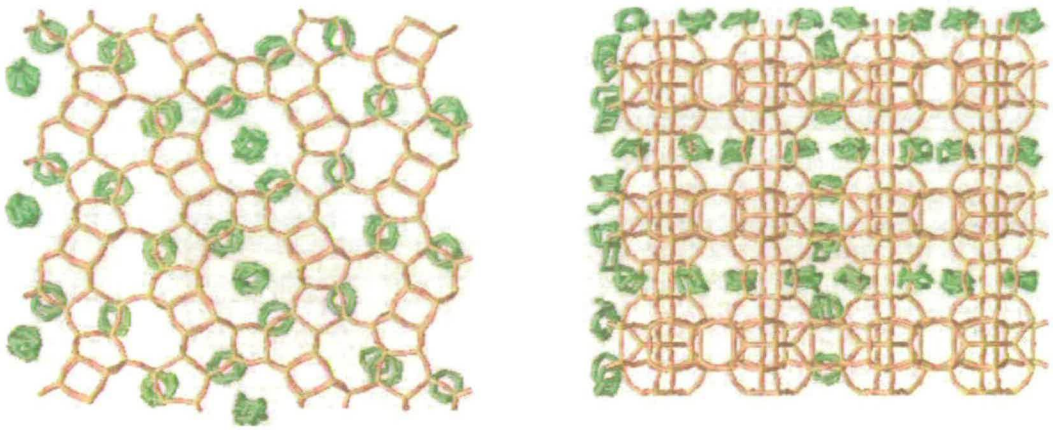

Figure 4.19: A snapshot of the molecular positions of cyclohexane in ITQ-22 at 300K and 10000kPa. The cyclohexane molecules are shown as the green shapes, only the 'pseudo atoms' are shown. The left image is a projection on the XZ plane and the right image is on the YZ plane.

sorption isotherms of linear, branched and cyclic molecules matched the available experimental data and, confident with the simulation model, predictions about the microscopic nature of the adsorption could be made.

In silicalite-1, hexane, heptane and 2-methylpentane all exhibited inflections in their isotherms, indicative of molecular rearrangement to free up extra adsorption sites. The molecular explanation provided by Smit *et al.* [96] was confirmed by analysing the centre of mass distribution within the zeolite pores. Cyclohexane was found to adsorb only at the intersection of silicalite-1 and showed no inflection in its isotherm.

In $AlPO_4$-5, the maximum loadings were reversed when compared to silicalite-1- in $AlPO_4$-5, cyclohexane adsorbed in greater number that 2-methylpentane and hexane. An analysis of the orientation of the molecules was able to confirm the predictions made by Newalkar *et al.* [169] and revealed that cyclohexane molecules are able to stack up at right angles to the direction of the pore whilst hexane and 2-methylpentane were too long and could only lie end to end.

The adsorption in ITQ-22 was studied in detail and it was found that the preferred adsorption sites for hexane and 2-methylpentane was both at the intersections and mid way between the intersections in the large straight channels. The extra adsorption of cyclohexane (maximum loading of 12 molecule per unit cell, compared to 10 molecules per unit cell for hexane and

2-methylpentane) was attributed to it stacking within the straight channels which allowed an extra 2 molecules per unit cell to adsorb.

In summary - the single component adsorption of hexane, 2-methylpentane and cyclohexane in silicalite-1, $AlPO_4$-5 and ITQ-22 is accurately modelled using the model outlined in Chapter 3 and, confident in the model, it is possible to move to the next level of complexity - the adsorption of mixtures of different molecular types in the three zeolites. This is the subject of the next chapter.

Chapter 5

Two and three component mixtures

This chapter concentrates on the adsorption of mixtures - binary and ternary - in the three different zeolites. Both equimolar and different molecular concentrations will be investigated. The effect that temperature has on the selectivity of the zeolites with various mixtures will be discussed and explained. The increase in complexity associated with mixture adsorption is a necessary step in the ongoing challenge of simulating industrial processes involving both zeolites and hydrocarbons, such as oil refining.

The theoretical mixture isotherms will be presented along with any available experimental data so that a comparison can be made with the simulation data.

5.1 Introduction

The previous chapter dealt with the adsorption of single components within the three zeolites. Whilst this is a vital and necessary step in the simulation of adsorption, it does not reflect the complexity of adsorption on the industrial scale where zeolites are used to help separate *mixtures* of different hydrocarbons using their shape selectivity, or molecular sieving, property. Conventional experimental techniques used to study single component adsorption behaviour in zeolites are not easily modified to cope with the increased level of complexity associated

with mixtures, since not only must the uptake be measured but the composition of the adsorbed mixture also determined. In contrast, properties of mixtures within zeolites can be studied efficiently using Monte Carlo simulations, as evidenced by recent simulation studies of the adsorption of binary mixtures of linear and branched alkanes [107, 112, 119]. However, no mixtures involving cyclic molecules have, to the author's knowledge, been investigated. Cyclic molecules play a significant role in many processes such as catalytic cracking, the efficiency of which can decrease dramatically due to the build up of cyclic molecules within the zeolite pores [172–177] and so an understanding of their behaviour is of both fundamental and practical importance.

The simulation of the adsorption of mixtures presents an excellent opportunity to test adsorption theory, which makes predictions about the adsorption of mixtures based upon the single component isotherms. Comparing the theoretical mixture isotherms with the equivalent simulated isotherms allows any discrepancies between the predictions from the two techniques to be highlighted. The theoretical predictions are made at the macroscopic level whilst the simulations permit exploration at the microscopic level, such as the molecular conformation and adsorption location which is of great use in understanding adsorption.

This chapter will present results from simulations of binary and ternary mixtures of hexane, 2-methylpentane and cyclohexane at various temperatures, pressures and concentrations. The comparison with the theoretical (IAST) isotherms will be discussed and the microscopic locations will be used to explain the dependence on temperature of the adsorption selectivity.

5.2 Ideal Adsorption Solution Theory

The Ideal Adsorption Solution Theory [145] uses single component isotherms to predict the adsorption isotherm for a mixture. IAST is discussed in detail in Section 2.5 and so only a brief reminder is given here.

In their original paper, Myers *et al.* formulated the theory based upon several conditions being met. One of these conditions was that each of the adsorbed species (in the mixture) should have an equal area of adsorbent available to it. This means that a mixture of a very small molecule

with a very large (compared to the size of the zeolite pores) molecule adsorbed within a zeolite should *not* be treated with IAST because both molecules will not be able to access all parts of the zeolite. However, IAST *has* been shown to work for mixtures of similar sized molecules in zeolites [178] where the components of the mixture can access the same surface area of the zeolite.

It is important to be able to fit the single component isotherms with a suitable curve so that this curve can be integrated and points on the original isotherm can be found directly. In this work the Dual Site Langmuir fit [141] is used to approximate the single component isotherms. The loading at a given pressure is related to the maximum loading of each adsorption site by the following equation,

$$N(P) = \frac{N_A k_A P}{1 + k_A P} + \frac{N_B k_B P}{1 + k_B P} \tag{5.1}$$

where $N(P)$ is the total loading at pressure P, N_A and N_B represent the maximum loading for site A and B respectively and are estimated from the simulated isotherm - they are not fitted parameters. k_A and k_B are the parameters used to fit the adsorption isotherm, the units of k_A and k_B are kPa^{-1}.

Once two single component adsorption isotherms have been fitted using Equation 5.1, IAST can be used to predict the adsorption of a mixture of the two species. However, it is important to note that the predicted isotherms provide only macroscopic information - they cannot predict the location of the adsorbed molecules, for this it is necessary to use the extra information which is available from the simulations. With this extra knowledge, a deeper analysis of the complex battles for adsorption sites between the mixture components is possible.

5.3 Mixture adsorption in silicalite-1

This section is split into two subsections, the first deals with binary mixtures in silicalite-1 and the second with ternary mixtures. In each section, the comparison with any available macroscopic experimental data, as well as the IAST predicted isotherms will be made. A microscopic description of the adsorption will also be given.

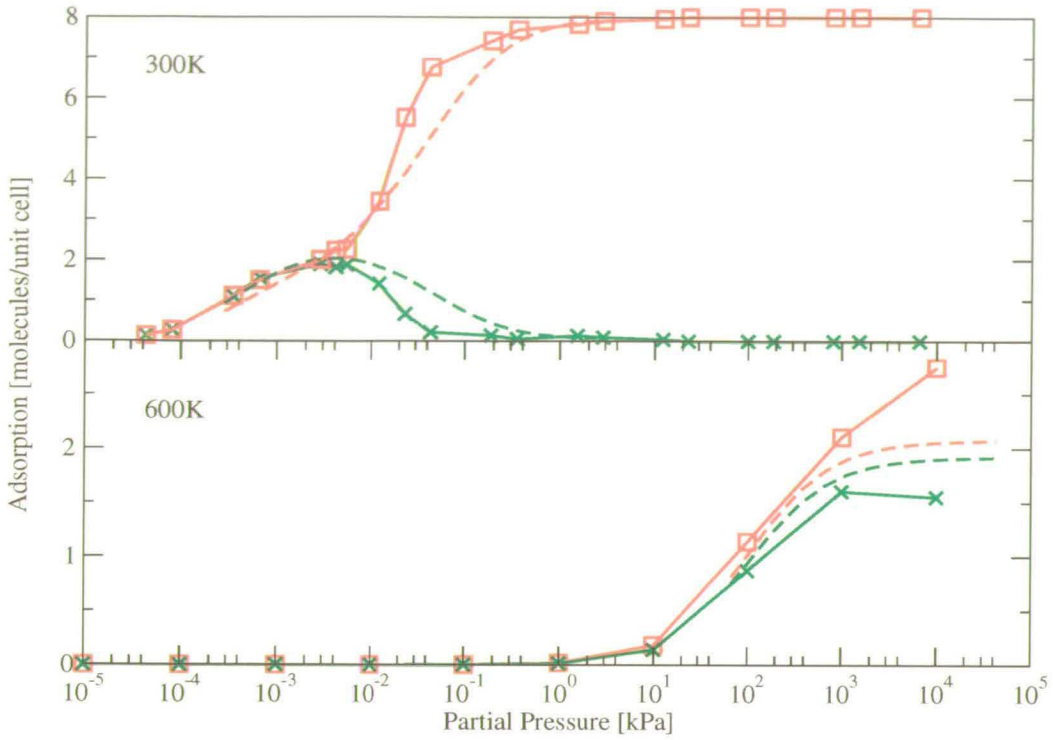

Figure 5.1: The adsorption isotherm for a 50:50 mixture of hexane (red squares) and 2-methylpentane (green crosses) in silicalite-1 at 300K (top) and 600K (bottom). The theoretical isotherms predicted using IAST are indicated by the dashed lines.

5.3.1 Binary mixtures

The adsorption of an equimolar mixture of linear and branched alkanes has already been studied using Monte Carlo simulations [105,109,112,119] and experiments [179–181]. This allows the results of this work to be compared and put into context with previous studies. However, the effect that temperature has on the selectivity is less well understood and will also be discussed in this section.

Hexane and 2-methylpentane

In Chapter 4 the single component adsorption isotherms of hexane and 2-methylpentane in silicalite-1 were presented. The total loading of both species was around 8 molecules per unit cell, although hexane reached this maximum level at a much lower pressure that 2-methylpentane. Figure 5.1 shows the adsorption isotherm of a equimolar mixture of hexane and 2-methylpentane

in silicalite-1 at 300K and 600K. At 300K it is evident that the uptake of 2-methylpentane at all but the very lowest pressures is negligible compared to that of hexane, which appears to be unaffected by the presence of 2-methylpentane in the mixture. Indeed, the total loading (8.0 molecules per unit cell) of hexane is identical to that of the pure adsorption isotherm. The agreement of the theoretical isotherms (indicated by the dashed lines in Figure 5.1) with the simulation isotherms is very good, over a wide pressure range (10^{-5} to 10^{4} kPa). Thus, it is not necessary to perform a simulation (or indeed experiment) to predict the macroscopic adsorption properties of a mixture of hexane and 2-methylpentane- the mixture adsorption isotherms can be predicted using only the pure component isotherms. However, the simulations are vital in order to be able to discuss the microscopic detail of the adsorption - *where* the molecules adsorb.

Examining the locations of the adsorbed mixture molecules within silicalite-1 reveals the following; at low pressures, below 10^{-2}kPa, hexane adsorbs uniformly throughout the zeolite, whilst 2-methylpentane occupies the intersections - both locations are exactly the same as the pure component locations at low pressures. However, as the pressure is increased, the number of adsorbed 2-methylpentane molecules decreases to zero whilst the number of hexane molecule continues to rise. The 2-methylpentane molecules are removed from their intersection locations whilst the hexane molecules continue to adsorb throughout the intersection, straight and zig-zag channels until the number of adsorbed hexane molecules reached 4 molecule per unit cell at which point the molecular reordering which was seen for pure hexane again takes place. The hexane molecules line up so that they fit neatly within the zig-zag channels, freeing up the straight channels which permit extra adsorption (taking the total adsorption to 8 molecules per unit cell). To summarise - the hexane barely notices the effect of the 2-methylpentane in the mixture and the hexane adsorption is almost identical to the pure component adsorption.

It would be reasonable to expect that the removal of the 2-methylpentane molecules from silicalite-1, to replace them with hexane molecules (shown in Figure 5.1 between around 10^{-2} and 10^{0}kPa) would be very time consuming. Experimentally, the 2-methylpentane molecules must diffuse through the network of pores, negotiating any adsorbed molecules, to escape the zeolite. Since diffusion is a slow process, the complete removal of 2-methylpentane in the bi-

nary mixture of hexane and 2-methylpentane in silicalite-1 could take significantly longer to equilibrate than a pure component adsorption. However, the Monte Carlo simulations do not suffer from the problem of diffusion since a (random) non-physical path is followed, allowing the molecules to 'jump' between different sites in the zeolite. Thus, Monte Carlo simulations are able to reach equilibration without having to spend time simulating the diffusion of the molecules.

The lower half of Figure 5.1 shows the adsorption isotherms for the 50:50 mixture of hexane and 2-methylpentane at 600K (note that the vertical scale is different to the 300K isotherms). The first thing to notice is that there is no uptake at low pressures; this is due to the increased energy (since the temperature is higher) of the molecules which are less influenced by the relatively weak interaction with the zeolite compared with the same molecule at low (300K) temperature. Once the molecules do adsorb, above 10^0kPa, the uptake is again dominated by the hexane molecules, with twice as many adsorbing compared to 2-methylpentane, at 10^4kPa. However, the uptake of the 2-methylpentane molecules is closer to that of hexane than it was at 300K. Once again, the theoretical isotherms, indicated by the dashed lines, correctly predict which of the two species is adsorbed in greatest quantity. However, the agreement between the simulation and theoretical isotherms is not as good as in the 300K mixture isotherm, the hexane isotherm is slightly underestimated and the 2-methylpentane is slightly overestimated.

The locations of the adsorbed molecules are similar to the single component isotherms at similar loadings. Hexane adsorbs throughout the zeolite whilst 2-methylpentane is localised to the intersections (with its tail pointing into either the straight or zig-zag channels, without preference).

The adsorption selectivity of a zeolite for an equimolar binary mixture of two molecular species is simply given by the ratio of the amount of each species adsorbed. For the 300K equimolar mixture of hexane and 2-methylpentane the selectivity at room pressure (100kPa) is given by the amount of hexane adsorbed (8.0 molecules per unit cell) divided by the amount of 2-methylpentane adsorbed (0.0 molecule per unit cell). This is undefined but the adsorption of hexane is clearly the favoured species from the mixture. As the temperature increases, the selectivity reduces to 20.68 at 400K and 1.31 at 600K. This dramatic reduction of selectivity

with temperature is also seen in experimental investigations of mixture adsorption. Funke *et al.* [179] performed experiments to determine the adsorption composition of mixtures of various linear, branched and cyclic alkanes at various temperatures in silicalite-1. They found that as the temperature increased, both the total number of molecules adsorbed and the adsorption selectivity for the linear molecule decreased. Whilst they did not perform experiments on a mixture of hexane and 2-methylpentane, they *did* obtain selectivities for mixtures of hexane and 3-methylpentane. They found a dramatic decrease in selectivity with temperature, from a selectivity of 24 at 362K to 1.1 at 443K. The selectivity decrease with increasing temperature seen by Funke *et al.* was reproduced using Configurational Bias Monte Carlo simulations [117].

Hexane and cyclohexane

In the previous section the molecule which dominated the mixture adsorption at low pressure was seen to dominate as the temperature increased, although the domination was less marked at high temperature. In line with experimental work, the selectivity for the dominant species tended to 1 (no selectivity) as the temperature increased. Does the same thing happen for a mixture of linear and cyclic molecules?

Figure 5.2 shows the adsorption isotherms for 50:50 mixture of hexane and cyclohexane in silicalite-1 at 300K (top) and 600K (bottom). As was the case in the mixture of hexane and 2-methylpentane, the low temperature adsorption is dominated by hexane, with little or no cyclohexane adsorbing. In Chapter 4, analysis of the single component adsorption in silicalite-1 revealed the preferred adsorption locations for each molecular species. The adsorption location of the hexane and cyclohexane molecules in the top half of Figure 5.2 is identical to those in the single component isotherms; at low pressures (below 10^{-2}kPa) hexane adsorbs throughout the channels and intersections whilst any cyclohexane that adsorbs does so exclusively at the intersections. At higher pressures, the hexane molecules rearrange to permit extra adsorption in the straight channels. The theoretical isotherms are in agreement with the simulated isotherms and predict that hexane dominates the adsorption.

Increasing the temperature to 600K (the lower half of Figure 5.2 - once again, note that the ver-

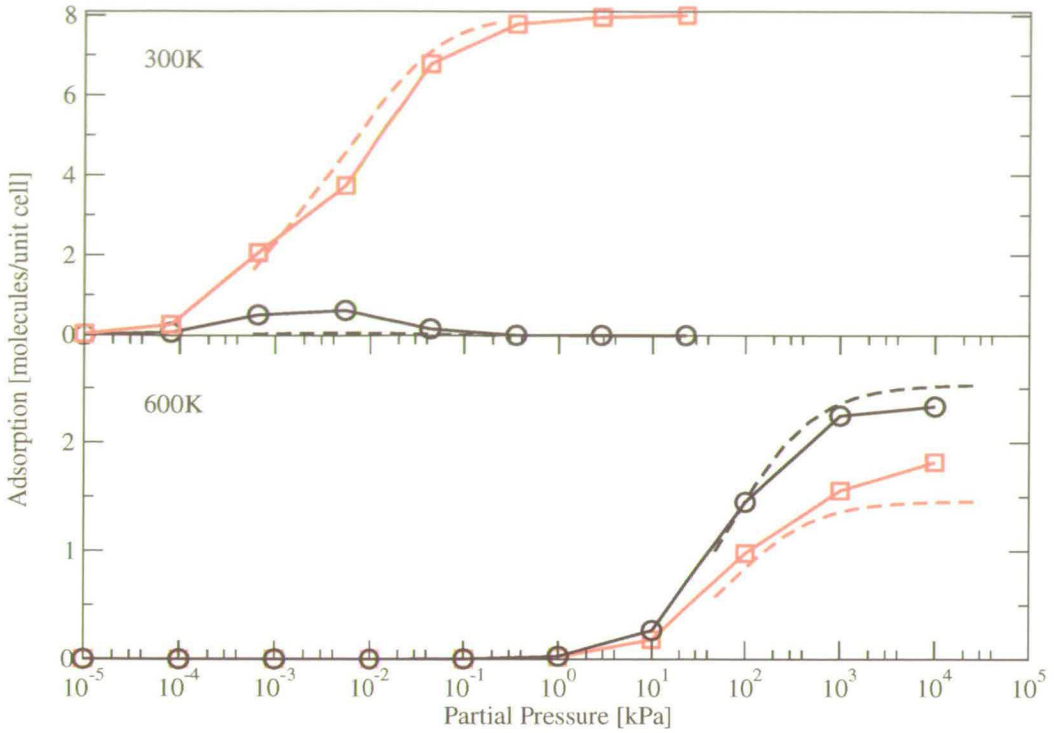

Figure 5.2: The adsorption isotherm for a 50:50 mixture of hexane (red squares) and cyclohexane (black circles) in silicalite-1 at 300K (top) and 600K (bottom). The theoretical isotherms predicted using IAST are indicated by the dashed lines.

tical scale is not the same as the 300K vertical scale) has the immediate effect of limiting the adsorption at low pressures, as explained in the previous section. At higher pressures, above 10^0kPa when the molecules start to adsorb, the selectivity is completely reversed compared to the 300K selectivity. Instead of hexane being the most favourably adsorbed species, cyclohexane is now adsorbed in greater number than hexane. The IAST predicted isotherms also shows this reversal of selectivity at high temperature, and the theoretical isotherms are in good agreement with the simulation isotherms. The selectivity decreases with temperature, from 23.14 at 400K to 0.98 at 500K and 0.67 at 600K. The experimental work of Funke *et al.* [179] predicted the selectivity for a mixture of hexane and cyclohexane at temperatures between 369K and 443K. They found that the selectivity reduced from 55 at 369K to 1.2 at 443K. These values are consistent with the simulation data but do not show a complete reversal in selectivity because the temperatures at which the experiments were conducted did not reach 500K - the temperature at which the simulations predict that a reversal in selectivity occurs. It would be

extremely interesting to carry out experiments at this higher temperature to see if a reversal in selectivity could be seen to confirm the predictions made from the simulations.

The position of the adsorbed molecules is the same as the single component adsorption positions at the same loading. Cyclohexane adsorbs only at the intersections whilst hexane adsorbs at the intersections (but not those which contain a cyclohexane molecule), straight and zig-zag channels.

One possible explanation for the reversal in selectivity at high temperatures comes from examining the range of conformations accessible to the different molecular types at different temperatures. At low temperatures, cyclohexane will be in its lowest energy conformation (the 'chair' conformation), the hexane molecule is most likely to have at maximum one *gauche* [182] bond (the others being *trans*) and similarly for 2-methylpentane in which the all *trans* or one *gauche* conformers will dominate [183]. However, as the temperature increases, the molecules are able to explore their higher energy conformations. In the case of cyclohexane, this means flexing between chair and boat conformations. The change between chair and boat does not significantly alter the shape of the molecule which still maintains its ring-like structure. In contrast, the shape of the linear and branched molecules can change more dramatically as more than one *gauche* bond is accommodated. At higher temperatures, the fraction of hexane and 2-methylpentane molecules with one of more *gauche* bonds will increase. A hexane molecule with all *trans* bonds will find it much easier to fit into the channels of a zeolite compared to a hexane molecule with a *gauche* bond. The same is true of 2-methylpentane which has even more difficulty in fitting into pores when not in its all *trans* form since it has a branched head which creates further restrictions on fitting into a zeolite pore.

An analysis of the end to end length of hexane and 2-methylpentane molecules at high and low temperatures shows that there is a decrease in length of around 10% (from around 6Å to 5.5Å[1]) from the long molecules at low temperature (300K) to shorter fatter, molecules at high temperature (600K). The same analysis of cyclohexane shows that there is no appreciable difference in molecular size at low and high temperatures.

All of the molecules find it harder to adsorb as the temperature is increased due to their in-

[1]To put the value into context, the channels in silicalite-1 have a diameter of just over 5Å.

creased kinetic energy. However, the decrease in uptake of both hexane and 2-methylpentane is greater than that of cyclohexane since both hexane and 2-methylpentane must overcome their configurational barrier - both molecules find it harder to fit into the channels at higher temperatures. The shape of cyclohexane at both high and low temperature is the same and so there is no extra configurational barrier for cyclohexane to overcome at higher temperatures.

2-methylpentane and cyclohexane

The explanation given for the change in selectivity with temperature predicts that linear and branched molecules find it harder to adsorb at higher temperatures whilst the cyclic molecule is able to adsorb on its favoured site since the molecular shape does not change appreciably at high temperature. Thus it would be reasonable to expect that the adsorption of a mixture of 2-methylpentane and cyclohexane would be affected by temperature - the amount of 2-methylpentane adsorbed would decrease faster than the amount of cyclohexane adsorbed, as the temperature increases.[2] Figure 5.3 shows the low and high temperature adsorption isotherms for an equimolar mixture of 2-methylpentane and cyclohexane in silicalite-1. The low temperature mixture adsorption isotherms reveal that 2-methylpentane is adsorbed in greater number than cyclohexane which continues to adsorb even at high pressures - this was not the case for mixtures of hexane and 2-methylpentane and hexane and cyclohexane in which the least favourably adsorbed species eventually became excluded from the zeolite. The fact that the cyclohexane molecules continue to adsorb at all pressures results in a change in the loading at which the 2-methylpentane isotherm exhibits an inflection.

In the pure 2-methylpentane isotherm, the inflection was at 4 molecules per unit cell since there are four intersection sites per unit cell and only when these sites are full does the molecular rearrangement (signified on the isotherm by an inflection) take place. However, in the 50:50 mixture of 2-methylpentane and cyclohexane, the cyclohexane molecules occupy some of the intersections (they can only adsorb at the intersections) and so the 2-methylpentane isotherm exhibits an inflection at around 3.5 molecules per unit cell - with the other 0.5 molecules per

[2]remember that the total amount of adsorbed molecules will decrease with temperature but the *rate* at which each species decreases is the important quantity - if the rate of decrease in uptake of 2-methylpentane is faster than the rate of decrease in uptake of cyclohexane then it may be possible for the selectivity to reverse at high temperature.

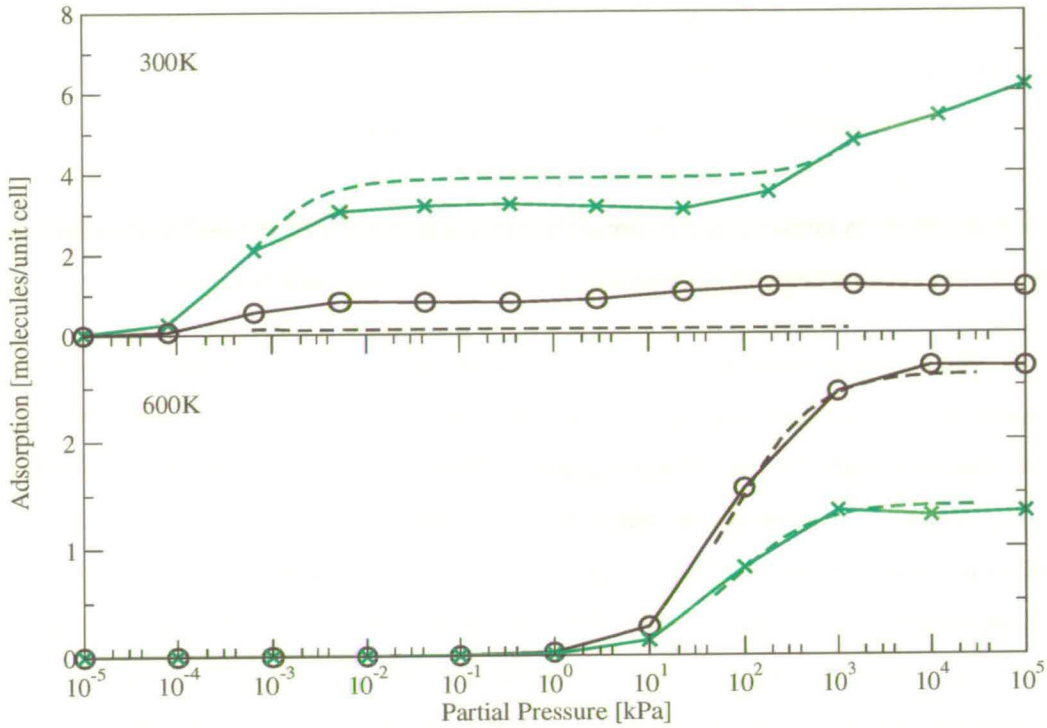

Figure 5.3: The adsorption isotherm for a 50:50 mixture of 2-methylpentane (green crosses) and cyclohexane (black circles) in silicalite-1 at 300K (top) and 600K (bottom). The theoretical isotherms predicted using IAST are indicated by the dashed lines.

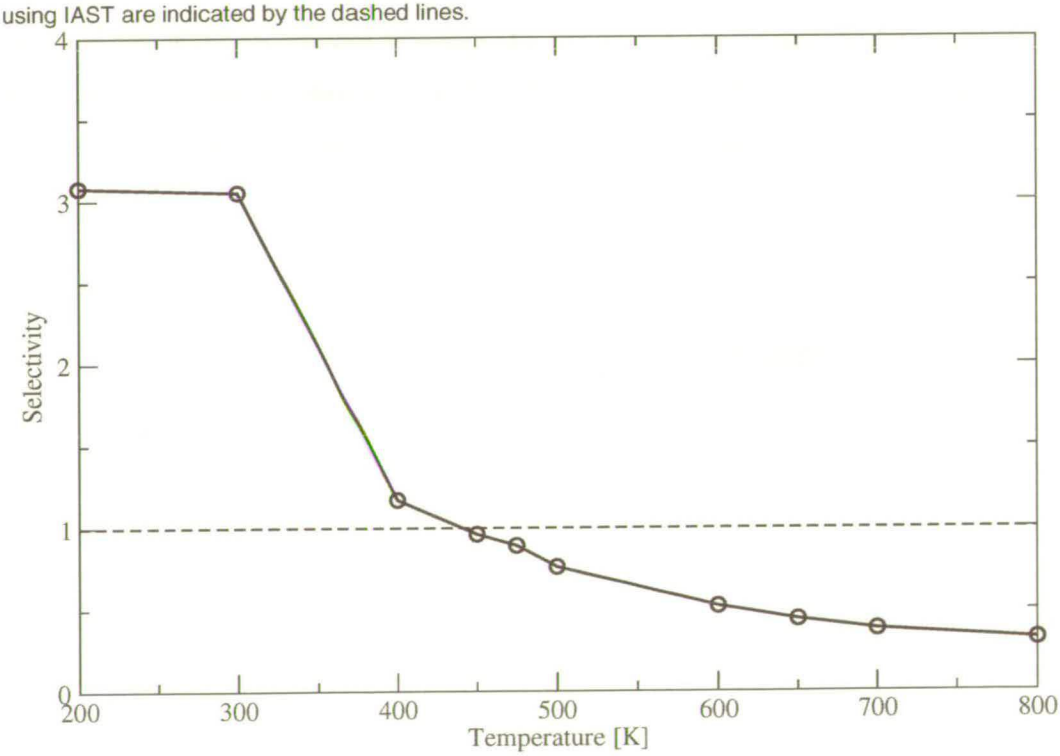

Figure 5.4: The selectivity of a 50:50 mixture of 2-methylpentane and cyclohexane at 100kPa and various temperatures. The selectivity is defined as the ratio of the number of adsorbed 2-methylpentane molecules to the number of adsorbed cyclohexane molecules.

unit cell being occupied by cyclohexane. Once the pressure reaches 10^2kPa (the end of the plateau) the 2-methylpentane molecules can occupy the zig-zag channels and so the number of adsorbed 2-methylpentane molecules increases. Cyclohexane can only occupy the intersections and so the cyclohexane loading remains approximately constant. At 300K, the theoretical isotherms correctly predict which molecule dominates the adsorption but slightly underestimate the cyclohexane loadings whilst overestimating the 2-methylpentane loading.

Figure 5.4 shows the selectivity for a 50:50 mixture of 2-methylpentane and cyclohexane at 100kPa and temperatures ranging from 200K to 800K. At low temperatures (below 450K) 2-methylpentane is adsorbed in the largest quantity. However, above 450K the selectivity reverses so that cyclohexane dominates the adsorption. The adsorption isotherms for the adsorption at 600K can be seen on the lower half of Figure 5.3 (again, note scale on vertical axis), along with the theoretically predicted isotherms, which are in excellent agreement with the simulation isotherms. At 600K, twice as much cyclohexane adsorbs as 2-methylpentane, both of which occupy the intersections. Both species adsorb at the intersections for the entire pressure range of Figure 5.3 (bottom).

Whilst experimental data is available for the adsorption of mixtures of linear and branched and linear and cyclic molecules [179, 180, 184, 185], no data could be found for mixtures of branched and cyclic molecules which could be compared to the simulation data and so the predictions made in this section await experimental verification.

5.3.2 Non-equimolar binary mixtures

The discussion of equimolar binary mixtures in silicalite-1 highlighted that, for each mixture at 300K, there was a clear 'winner' in the adsorption battle - the uptake of one molecular type was much greater than the other. What happens when the mixture is no longer composed of equal quantities of both molecules - does the same species still dominate or does the molecule which makes up the largest part of the mixture now adsorb in greatest number? The effect that mixture composition has on the mixture adsorption will now be investigated.

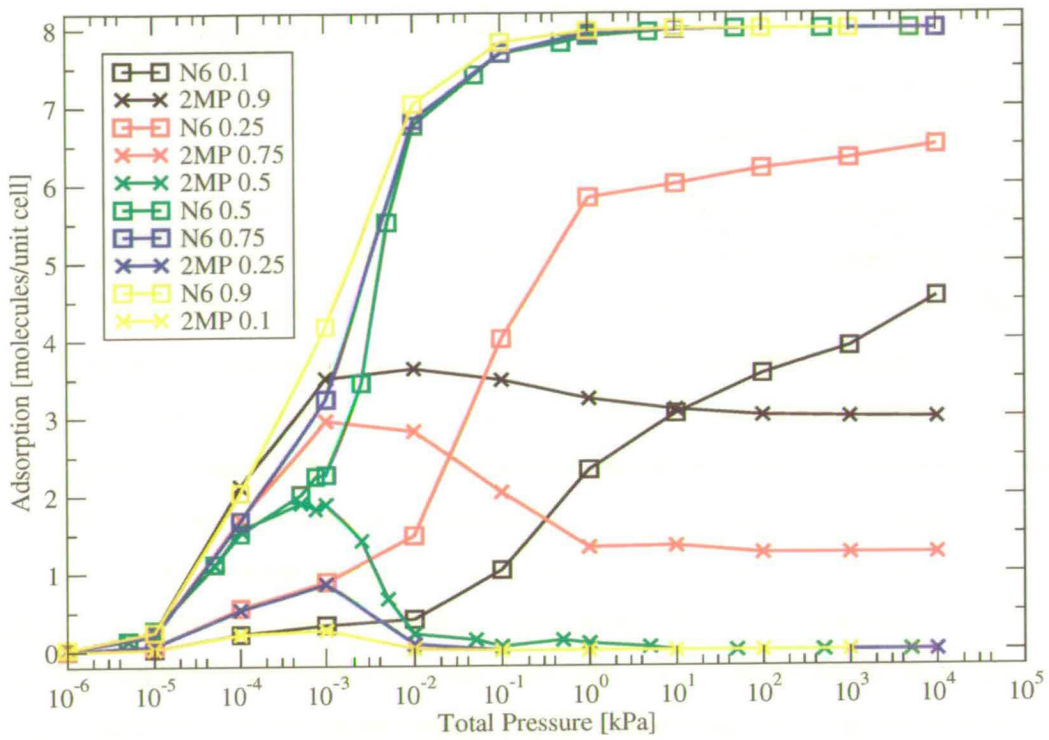

Figure 5.5: The adsorption isotherms for binary mixtures of 2-methylpentane and hexane in silicalite-1 at 300K and various different component loadings. See the legend for details (molecule name followed by its fraction, N6 stands for hexane and 2MP for 2-methylpentane) of each line. Note that the horizontal axis label is now '*Total* pressure' and not '*Partial* pressure' as in the previous adsorption isotherm figures. Using Total pressure allows for the comparison of each mixture composition.

Hexane and 2-methylpentane

Figure 5.5 presents adsorption isotherms for the components of a mixture of 2-methylpentane and hexane at various different compositions. The adsorption of the three mixtures with 50% or more hexane are dominated by the hexane molecule. This is not surprising since the adsorption of the equimolar mixture of hexane and 2-methylpentane was shown, in Figure 5.1, to consist of no 2-methylpentane molecules except at very low pressures. Increasing the fraction of hexane molecule in the mixture would only increase the hexane supremacy.

Examining the adsorption isotherms of mixtures with more 2-methylpentane than hexane (the black and red isotherms) shows that, at pressures below 10^{1}kPa for the black (90% 2-methylpentane) isotherms and 10^{-2}kPa for the red (75% 2-methylpentane) isotherms, more 2-methylpentane molecules than hexane adsorb. However, as the pressure increases beyond these values, the

adsorption of hexane overtakes that of 2-methylpentane so that, despite accounting for only a small fraction of the mixture, the hexane molecules are adsorbed in greater number than those of the more abundant molecule in the mixture, 2-methylpentane.

The single component isotherm for 2-methylpentane exhibits an inflection at 4 molecules per unit cell (see Section 4.3.2, on page 58). This inflection indicated a rearrangement of the 2-methylpentane molecules so that the branched 'heads' were in the intersections and the straight 'tails' pointed into the straight channels - freeing up the zig-zag channels. In Figure 5.5, the black 2-methylpentane adsorption isotherm reaches a peak at around 3.5 molecules per unit cell - there are also 0.5 hexane molecules adsorbed per unit cell. The presence of these hexane molecules prevents further adsorption of 2-methylpentane at any remaining free intersections because the hexane molecules do not only adsorb in the channels but also at the intersections and may prevent adsorption at the intersection if a hexane molecule adsorbed in a channel overlaps with the intersection. From analysis of the *pure* 2-methylpentane adsorption, it is known that once all of the intersections are full, further adsorption of 2-methylpentane can only take place in the channels once the reorientation has taken place. Thus, in the case of the 90% 2-methylpentane, 10% hexane mixture, at 10^{-2}kPa, it is not possible for any more 2-methylpentane molecules to adsorb, without the rearrangement of the molecules which have already adsorbed. However, because hexane *can* adsorb in the channels, it *is* possible for more hexane molecule to adsorb, as shown by the increase in hexane adsorption in Figure 5.5 as the pressure increases past 10^{-2}kPa. At the highest pressure, the 2-methylpentane molecules adsorb only at the intersection whilst the hexane molecules are distributed among the straight and zig-zag channels.

Hexane and cyclohexane

Figure 5.6 reveals that for different compositions of mixtures of hexane and cyclohexane, hexane is able to absorb in greater quantities than cyclohexane at all pressures for all but the lowest composition of hexane (only 10% hexane). Indeed, at room pressure (100kPa), any mixture composition results in significant uptake of hexane with only minimal uptake of cyclohexane. The presence of the cyclohexane molecules do not appear to affect the adsorption of the other

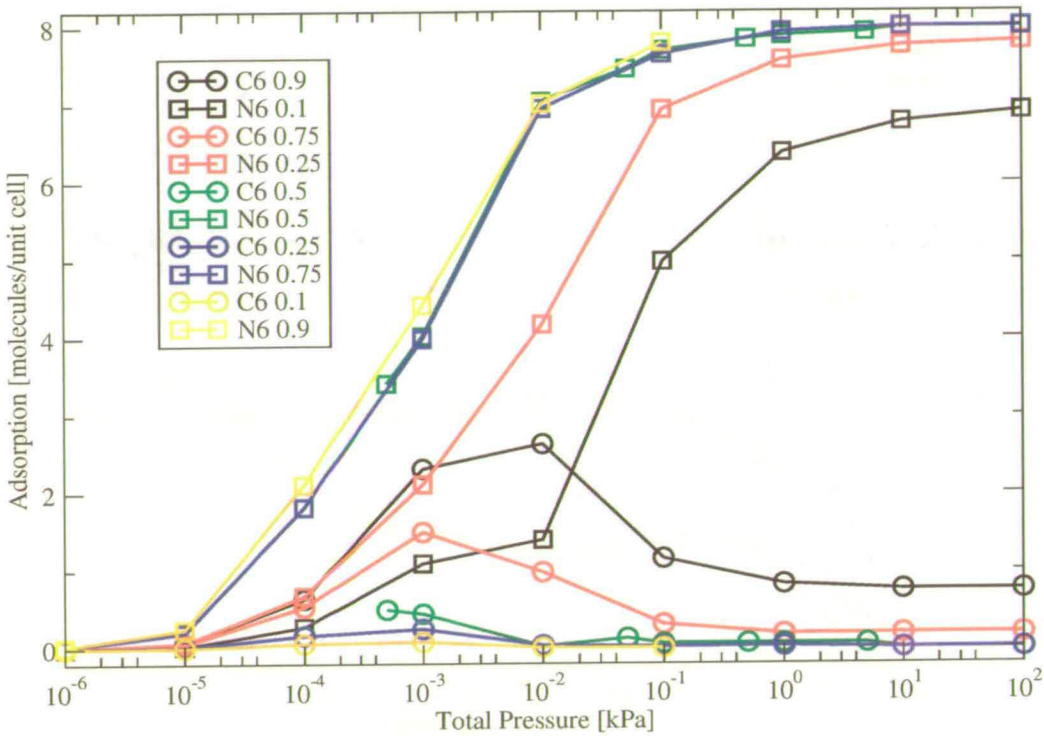

Figure 5.6: The adsorption isotherms for binary mixtures of cyclohexane and hexane in silicalite-1 at 300K and various different component loadings. See the legend for details (molecule name followed by its fraction, N6 stands for hexane and C6 for cyclohexane) of each line.

mixture component, the hexane, until the fraction of the mixture that is cyclohexane reaches 0.75. At lower concentration of cyclohexane, the deviation from the pure hexane adsorption isotherm is minimal and hexane does not appear to be affected by the cyclohexane. When the composition of the mixture is 75% cyclohexane and 25% hexane, the uptake of cyclohexane is limited to less than 2 molecules per unit cell and quickly reduces to almost zero at higher pressures.

When the mixture comprises 90% cyclohexane and only 10% hexane, the initial adsorption (at low pressure, below 10^{-2}kPa) consists of approximately twice as many cyclohexane molecules as hexane molecules. The cyclohexane molecules adsorb only at the intersection whilst the hexane molecules are distributed equally at the intersections (but only those which are unoccupied by the cyclohexane molecules) and both the straight and zig-zag channels. As the pressure increases above 10^{-2}kPa, the hexane molecules adsorb in increasing number, rearranging to free

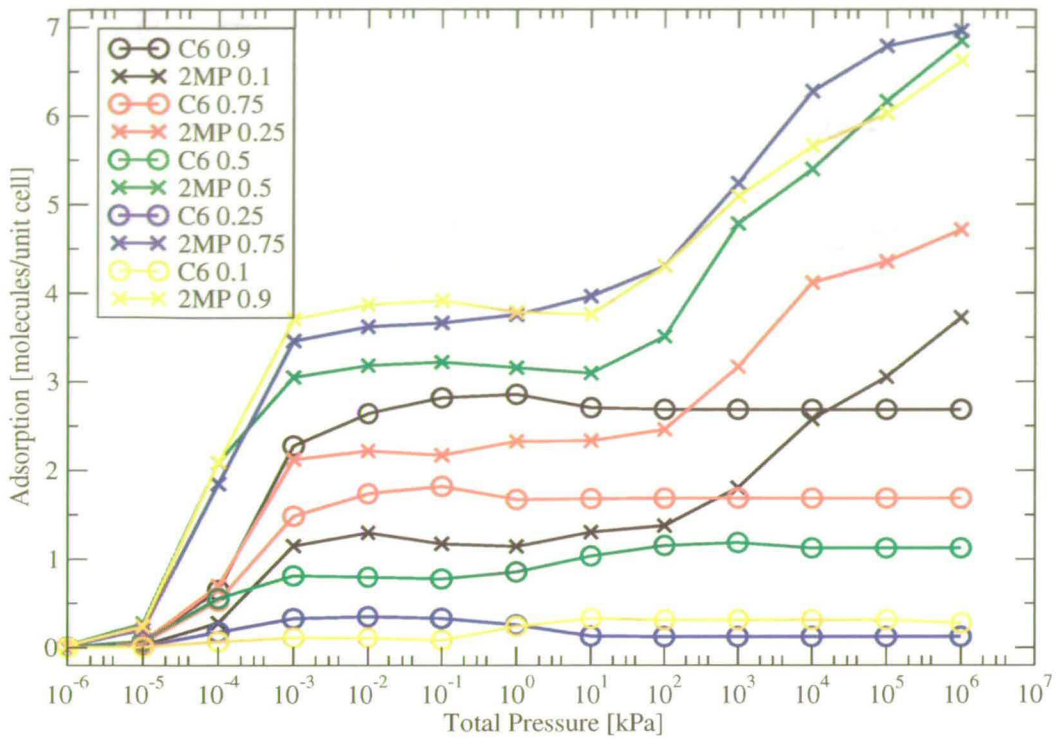

Figure 5.7: The adsorption isotherms for binary mixtures of 2-methylpentane and cyclohexane in silicalite-1 at 300K and various different component loadings. See the legend for details (molecule name followed by its fraction, 2MP stands for 2-methylpentane and C6 for cyclohexane) of each line.

up space and allow extra adsorption in the straight channels. One cyclohexane molecule, adsorbed at the intersection, can prevent the adsorption of a hexane molecule in both the straight and the zig-zag channels which it connects. Slowly, the cyclohexane molecules are removed from the intersections, allowing two hexane molecules to adsorb in the space which becomes available. This process continues throughout the high pressure region (above 10^{-2}kPa).

Cyclohexane and 2-methylpentane

The different composition mixture isotherms for mixtures of hexane and cyclohexane and hexane and 2-methylpentane were both dominated by hexane for all but the lowest hexane mixture fraction or the lowest pressures. Figure 5.7 shows that for a mixture of 2-methylpentane and cyclohexane, at 300K, the battle between the mixture components is more even. It is true that 2-methylpentane does adsorb in greater number than the cyclohexane molecules; however, the

cyclohexane molecules continue to adsorb at high pressures (note the scale on the horizontal axis). This is in contrast to the hexane and 2-methylpentane and hexane and cyclohexane mixtures in which the uptake of 2-methylpentane or cyclohexane molecules tended to reduce with pressure, but in the case of the 2-methylpentane and cyclohexane mixture, the uptake of cyclohexane does not decrease with increasing pressure - even when the pressures were raised to 10^6kPa.

One consistent feature of Figure 5.7 is the position of the plateau on the 2-methylpentane adsorption isotherms. Whilst the plateaus do occur at different 2-methylpentane loadings, the *total* loading of both 2-methylpentane and cyclohexane is identical for all of the plateaus at all mixture compositions. The total loading is 4 molecules per unit cell - this is the sum of the 2-methylpentane loading and the cyclohexane loading. The value of 4 molecules per unit cell is important - it signifies that there is a molecule (cyclohexane or 2-methylpentane) at each intersection in the zeolite. The analysis of the pure 2-methylpentane isotherm locations revealed that 2-methylpentane only rearranges when all of the intersections are full. This is exactly what is happening in the 2-methylpentane and cyclohexane mixtures - only when all of the intersections are full (with either molecular type) do the 2-methylpentane molecules begin to rearrange - signified by the plateau.

There is only one mixture composition which results in more adsorption of cyclohexane than 2-methylpentane. Only when the mixture comprises 90% cyclohexane and 10% 2-methylpentane and then only for pressures below 10^4kPa does the zeolite selectively adsorb cyclohexane. Figure 5.7 shows that even for mixtures which consist of more cyclohexane than 2-methylpentane, it is the 2-methylpentane molecules which are preferentially adsorbed in silicalite-1.

It is possible to speculate what the high temperature, non-equimolar mixture selectivities might be. The mixture of hexane and 2-methylpentane at various compositions was dominated by hexane, except for the mixture comprising 90% 2-methylpentane and only 10% hexane. Thus, it would be reasonable to expect that as the temperature increased to 600K, only the 90% 2-methylpentane, 10% hexane mixture would permit more adsorption of 2-methylpentane than hexane. This prediction is based on the fact that the equimolar mixture of hexane and 2-methylpentane is dominated by hexane at both low and high temperatures and so it is reasonable

to predict that any mixture of hexane and 2-methylpentane that is dominated by hexane at low temperature (for example, all but the 90% 2-methylpentane, 10% hexane mixture) will also be dominated by hexane at high temperature.

The equimolar mixtures of cyclohexane with either hexane or 2-methylpentane were dominated by the non-cyclic molecule at low temperatures but exhibit selectivity reversal as the temperature increased. Thus, it may be the case that a non-equimolar mixture of cyclohexane and either hexane or 2-methylpentane could be dominated by cyclohexane at high temperatures. In the non-equimolar mixture of hexane (or 2-methylpentane) and cyclohexane, it is likely that all of the mixtures which comprise more cyclohexane than hexane (or 2-methylpentane) will be dominated by cyclohexane at high temperatures. However, the mixtures which comprise less than 50% cyclohexane may not be dominated by cyclohexane at high temperatures. On one hand the increase in temperature will decrease the ease with which the hexane (or 2-methylpentane) molecule adsorbs and so based on this it would be expected that cyclohexane would dominate at high temperature, even though it makes up less than 50% of the mixture. On the other hand, there are fewer cyclohexane molecules than there are hexane (or 2-methylpentane) molecules and so perhaps the abundance of these molecules would result in cyclohexane failing to dominate the adsorption at high temperature. The subtle balance between these two factors would be an interesting topic for further study.

5.3.3 Equimolar ternary mixtures

The analysis of the adsorption of binary mixtures of hexane, 2-methylpentane and cyclohexane revealed that, at 300K, silicalite-1 preferentially adsorbed hexane when it was in a 50:50 mixture with either 2-methylpentane or cyclohexane. For the mixture of 2-methylpentane and cyclohexane, the branched molecule was adsorbed in greater quantity than the cyclic molecule. However, when the temperature was increased to 600K, the selectivity of the mixtures involving cyclohexane was reversed; at 600K, cyclohexane adsorbed in greater number than hexane or 2-methylpentane when in a 50:50 mixture. However, the mixture of hexane and 2-methylpentane did not exhibit any high temperature selectivity reversal. Do these trends occur in a ternary mixture consisting of equal parts of each of the three molecular species? This question is

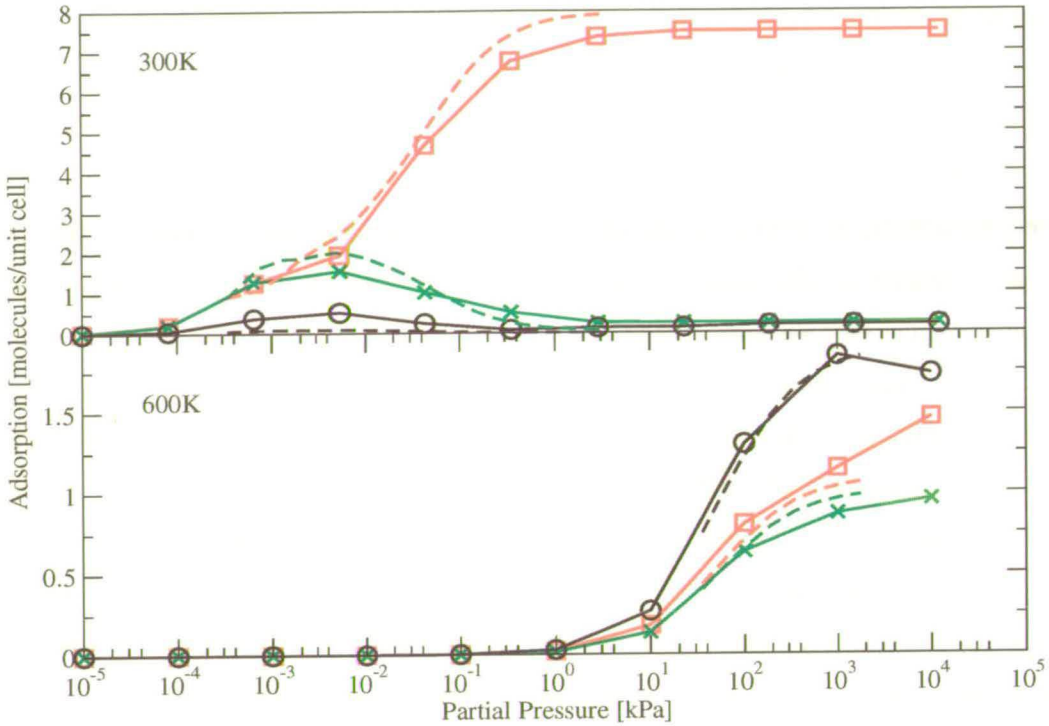

Figure 5.8: The adsorption isotherms for an equimolar ternary mixture of hexane, 2-methylpentane and cyclohexane in silicalite-1 at 300K (top) and 600K (bottom). The red squares represent the hexane data, the green crosses are the 2-methylpentane data and the black circles are the cyclohexane data. The dashed lines represent the theoretical isotherms.

discussed in this section.

Figure 5.8 shows the simulated adsorption isotherms for an equimolar ternary mixture of hexane, 2-methylpentane and cyclohexane in silicalite-1 at 300K and 600K together with the IAST isotherms. As predicted on the basis of the findings from binary mixture adsorption, at low temperature the linear alkane dominates the adsorption, with only a tiny fraction of the adsorbed mixture being made up of branched or cyclic molecules. Indeed, the presence of the branched and cyclic molecules does not seem to significantly alter the maximum loading of hexane, whose isotherm is close to that of the pure component. The theoretical (IAST) isotherms are in good agreement with the simulated isotherms and correctly predict both the selectivity and the amount of each component which is adsorbed. A microscopic analysis of the molecular locations shows that at high pressures the hexane molecules adsorb in the straight and zig-zag channels, but not at the intersections. 2-methylpentane molecules adsorb with their branched

'heads' in the intersection and their 'tails' in the straight or zig-zag channels. Cyclohexane preferentially adsorbs at the intersections in silicalite-1 and yet there is almost no uptake of cyclohexane molecules in the ternary mixture. This is because the hexane molecules (which dominate the adsorption) do not fit perfectly into the channels and thus they may impinge upon the intersections, preventing cyclohexane from having sufficient space to adsorb. Figure 5.9 shows a qualitative representation of a hexane molecule impinging upon an intersection, preventing cyclohexane adsorption. The hexane molecule (just right of centre, shown in green) reduces the chance of a cyclohexane molecule adsorbing in either of the intersections which are close to the hexane molecule - this can be seen by comparing the size of the coloured areas in the intersections, they are much smaller next to the hexane molecule. Each coloured area represents a region of a high probability of cyclohexane adsorption - note that all of the coloured areas appear at the intersections, this has been established as the preferred adsorption location for cyclohexane in silicalite-1. Whilst this figure is only qualitative, it highlights the effect that an adsorbed molecule can have on the possible adsorption sites for other molecules.

The influence of temperature on the adsorption selectivity of binary mixtures was explored in the previous section. The adsorption of cyclohexane was found to increase with temperature whilst that of hexane and, to a greater extent 2-methylpentane, were found to decrease with temperature. Using these findings to predict the ternary adsorption in silicalite-1 at 600K suggests that the amount of cyclohexane adsorbed should increase whilst the amount of hexane adsorbed should be more than that of 2-methylpentane. Figure 5.8 (bottom) shows that indeed the amount of cyclohexane adsorbed has increased, at the expense of hexane which is now the second most favourably adsorbed species, ahead of 2-methylpentane. An analysis of the siting of the three molecular species shows that, at 10^3kPa, cyclohexane and 2-methylpentane both adsorb at the intersections whilst hexane is equally distributed between the straight and zig-zag channels. Once again, the IAST predicted isotherms for the ternary mixture in silicalite-1 (shown in Figure 5.8) correctly determines the adsorption hierarchy at both low and high temperatures.

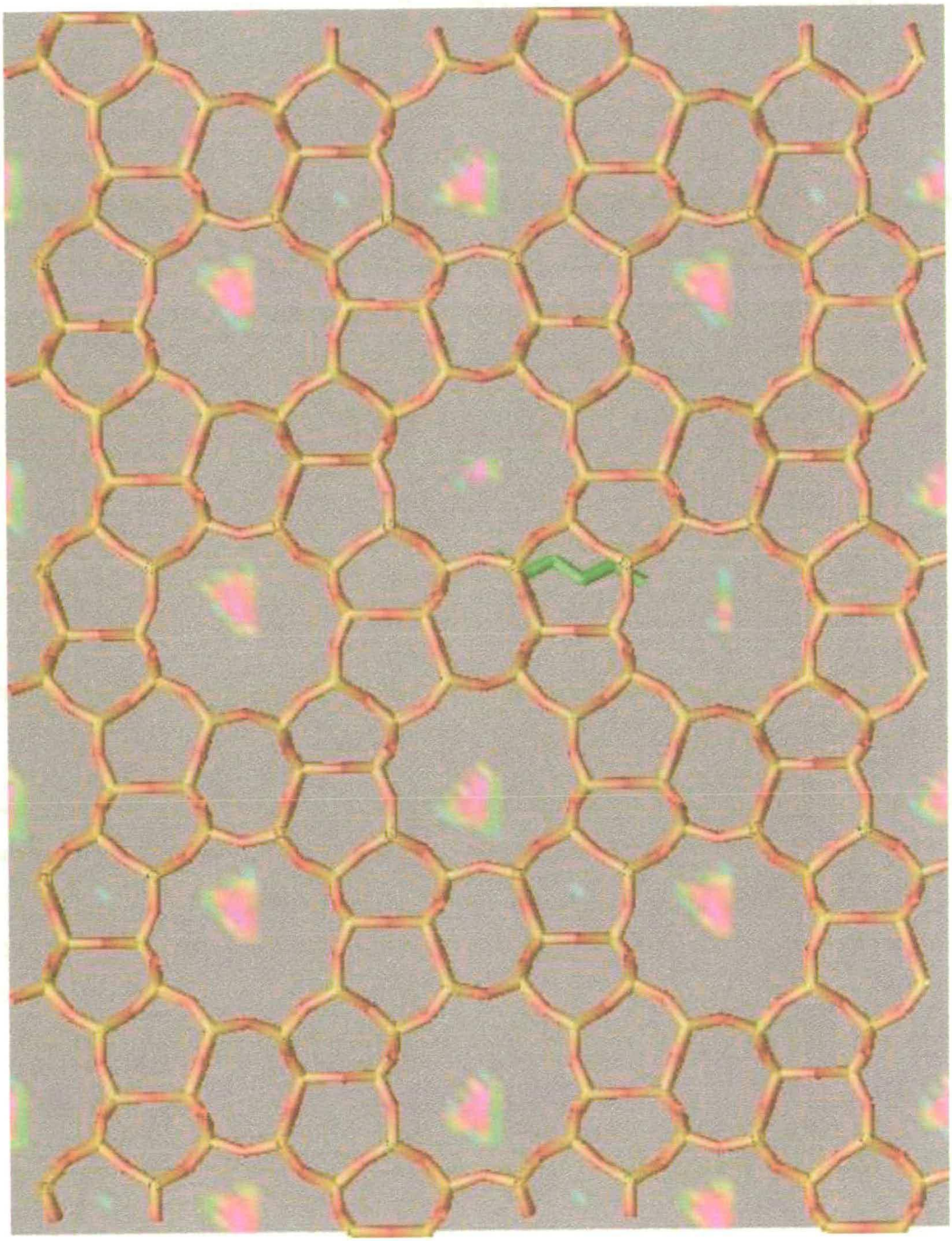

Figure 5.9: A slice in the x-z plane, through the probability of cyclohexane adsorption isosurface with an adsorbed hexane molecule in the zig-zag channel (just right of centre, shown in green). The pink areas represent regions of high probability whilst the green and blue areas are low probability of adsorption. The grey areas are inaccessible to the cyclohexane molecule. The zeolite is shown as the red and yellow network.

5.4 Mixture adsorption in $AlPO_4$-5

In Section 4.4 on page 64, the pure adsorption isotherms of hexane, 2-methylpentane and cyclohexane in $AlPO_4$-5 were presented. The adsorption hierarchy was shown to be the opposite to that of silicalite-1, with the maximum loading of cyclohexane being larger than both 2-methylpentane and hexane.

This hierarchy is repeated in the binary mixture which, at all temperatures, sees one of the mixture components dominating. In the hexane and cyclohexane mixture (see Figure 5.10), almost no hexane adsorbs, at any temperature. The same is true of 2-methylpentane in the cyclohexane and 2-methylpentane binary mixture (See Figure 5.11), regardless of temperature, almost no 2-methylpentane adsorbs. In a mixture of hexane and 2-methylpentane (Figure 5.12) it is the branched molecule which, at all temperatures, adsorbs in greater number than hexane. However, in this mixture, the temperature does play a role, with the number of adsorbed molecules of each species becoming closer as the temperature increases. Figure 5.13 shows the selectivity (defined at the number of adsorbed molecules of 2-methylpentane divided by the number of adsorbed molecules of hexane) of $AlPO_4$-5 at 200K to 600K.

No experimental data could be found to compare with the results of the binary mixture simulations but the single component hierarchy is in good agreement with the available experimental data. The ternary mixture isotherm, Figure 5.14, reveals that the same hierarchy is followed for a ternary mixture, at both 300K and 600K. The cyclohexane molecules dominate the adsorption with only very small quantities of 2-methylpentane or hexane adsorbing within the pores of $AlPO_4$-5. The theoretical isotherms are in good agreement with the simulation isotherms.

5.5 Mixture adsorption in ITQ-22

Chapter 4 introduced the single component isotherms in ITQ-22 and discussed the adsorption locations of the three molecules in the porous network of ITQ-22. The large, interconnected pores lend themselves easily to the adsorption of all three species, with cyclohexane being the most abundantly adsorbed molecule. What will happen when a mixture of different species

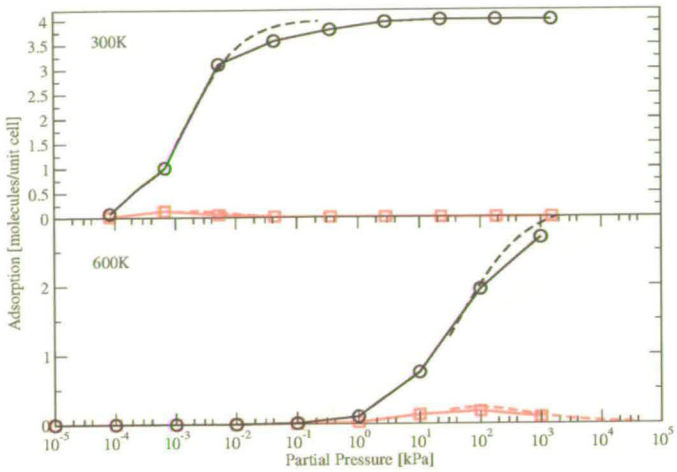

Figure 5.10: The adsorption isotherms for an equimolar mixture of hexane, cyclohexane in $AlPO_4$-5 at 300K (top) and 600K (bottom). The red squares represent the hexane data and the black circles are the cyclohexane data. The dashed lines represent the theoretical isotherms

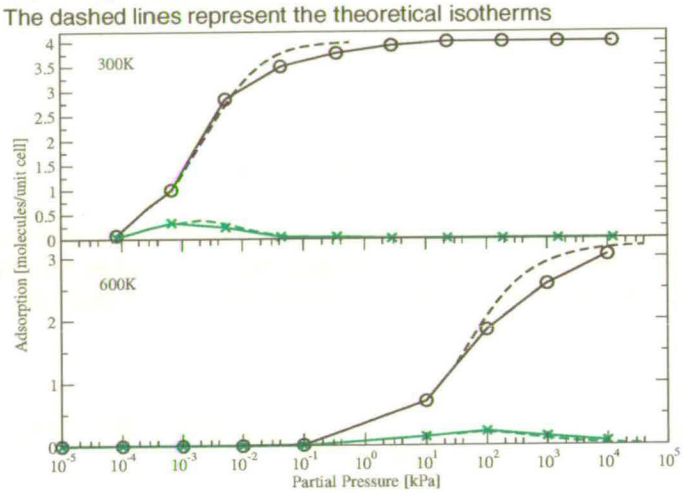

Figure 5.11: The adsorption isotherms for an equimolar mixture of cyclohexane and 2-methylpentane in $AlPO_4$-5 at 300K (top) and 600K (bottom). The green crosses are the 2-methylpentane data and the black circles are the cyclohexane data. The dashed lines represent the theoretical isotherms

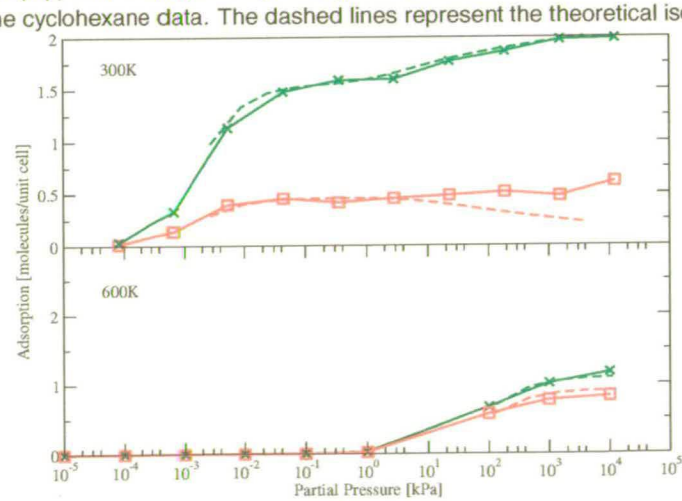

Figure 5.12: The adsorption isotherms for an equimolar mixture of hexane and 2-methylpentane in $AlPO_4$-5 at 300K (top) and 600K (bottom). The red squares represent the hexane data and the green crosses are the 2-methylpentane data. The dashed lines represent the theoretical isotherms

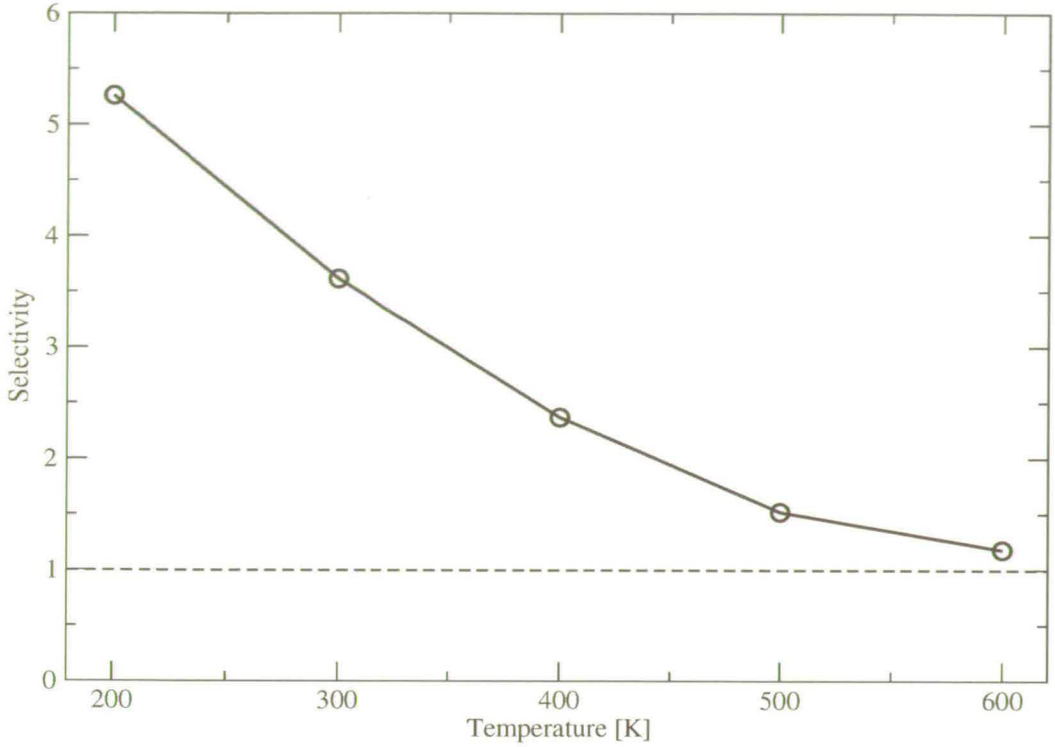

Figure 5.13: The selectivity of $AlPO_4$-5 for 2-methylpentane in a mixture of 2-methylpentane and hexane at 100kPa and various different temperatures. The selectivity is defined as the ratio of the number of adsorbed 2-methylpentane molecules to the number of adsorbed hexane molecules.

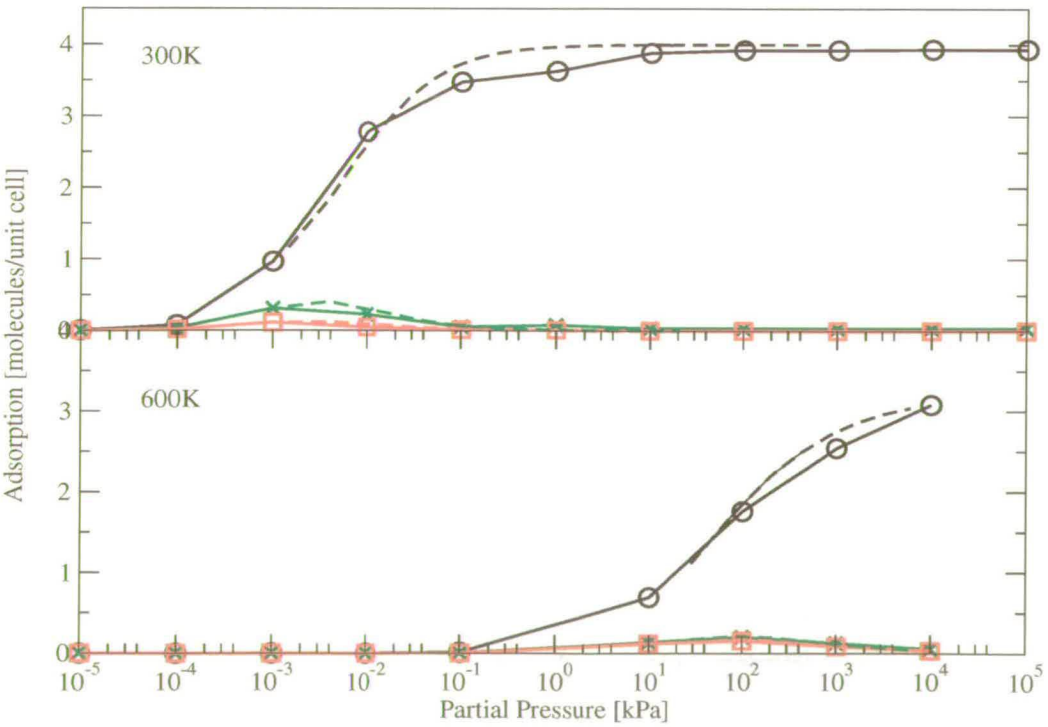

Figure 5.14: The adsorption isotherms for a ternary mixture of hexane, 2-methylpentane and cyclohexane in $AlPO_4$-5 at 300K (top) and 600K (bottom). The red squares represent the hexane data, the green crosses are the 2-methylpentane data and the black circles are the cyclohexane data. The dashed lines represent the theoretical isotherms.

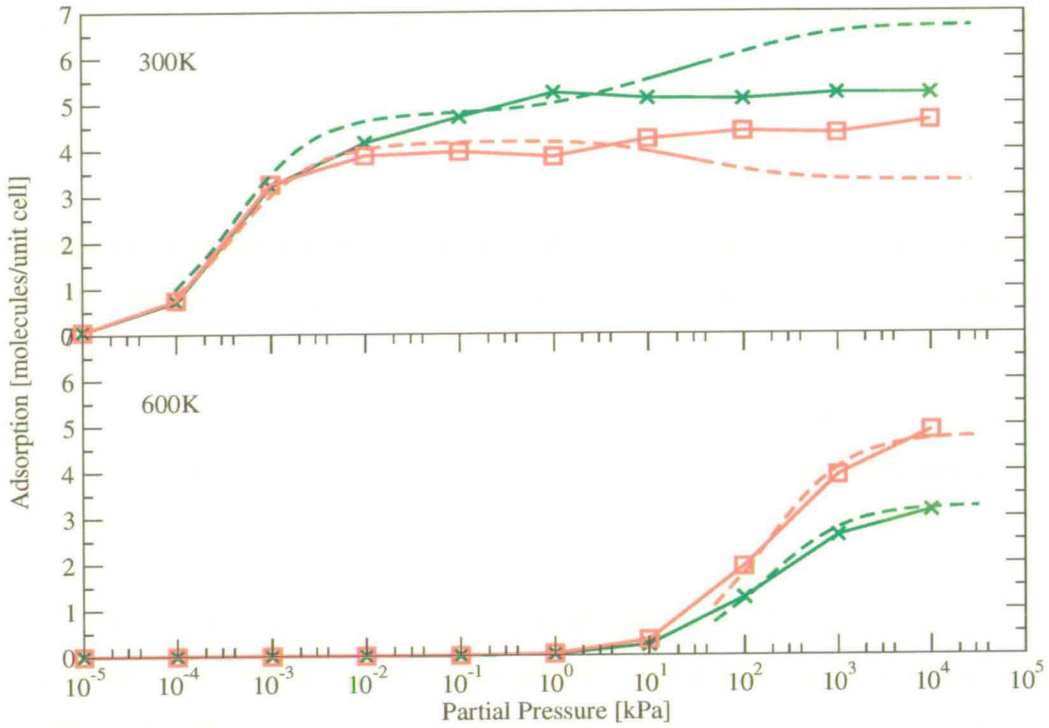

Figure 5.15: The adsorption isotherms for an equimolar mixture of hexane and 2-methylpentane in ITQ-22 at 300K (top) and 600K (bottom). The green crosses represent the 2-methylpentane and the red squares represent the hexane. The theoretical isotherms are shown by the dashed lines.

adsorbs within ITQ-22? Will there be any reversal in selectivity with temperature? These questions will be answered in the following sections.

5.5.1 Binary mixtures

Hexane and 2-methylpentane

The adsorption isotherms of a 50:50 mixture of hexane and 2-methylpentane at 300K and 600K, along with the IAST predicted isotherms are shown in Figure 5.15. The figure shows that the adsorption of a 50:50 mixture of hexane and 2-methylpentane at 300K results in slightly more 2-methylpentane adsorbing than hexane. The preferred locations of the two species are the same - both molecules adsorb in the 10MR channels, at the intersection with the 8MR channel and in the 12MR channels, at both the intersection with the 10MR channels and mid-way

between the intersections, in the 12MR channel. The theoretical isotherms correctly predict the relative adsorption of the two species, although the fit is not perfect.

The direct competition for adsorption locations between hexane and 2-methylpentane continues at high temperatures. At 600K, both species still adsorb in the same locations as the low temperature adsorption. However, as Figure 5.15 shows, at high temperature the selectivity is reversed, hexane is now adsorbed in greater quantities than 2-methylpentane. The IAST predicted isotherms are in good agreement with the simulation data.

Following on from the explanation given in Section 5.3.1 (page 89) for the reversal in selectivity with temperature for a mixture of hexane and cyclohexane or 2-methylpentane and cyclohexane, a conformational explanation can be used to describe the dependence on temperature of the selectivity for a mixture of hexane and 2-methylpentane in ITQ-22. As the temperature increases, the number of *gauche* [182] bonds in both hexane and 2-methylpentane also increases [183]. This means that as the temperature increases, both hexane and 2-methylpentane become less straight and more coiled. Fitting into the channels within the zeolite becomes harder as the molecules become more bulky since they will be less likely to fit into the channels without touching the walls of the channel. This does not explain why hexane appears to be less effected by temperature than 2-methylpentane (since it is hexane which 'overtakes' 2-methylpentane in the adsorption battle at high temperature in ITQ-22). The reason for this is that 2-methylpentane has an extra hindrance which makes it slightly more likely for it to be unable to fit into the channel - it has a branched head group which creates an extra steric hindrance. Thus, as the temperature increases, both molecules find it harder to negotiate the channels in ITQ-22, but 2-methylpentane finds it slightly more difficult that hexane due to the branched head group.

Hexane and cyclohexane; 2-methylpentane and cyclohexane

Both of the binary mixtures involving cyclohexane are grouped together in this section. The reason for this is that the adsorption of both mixtures is dominated by cyclohexane at both low and high temperature and so one discussion will suffice for both mixtures.

Figures 5.16 and 5.17 show the adsorption isotherms for low and high temperature mixtures of

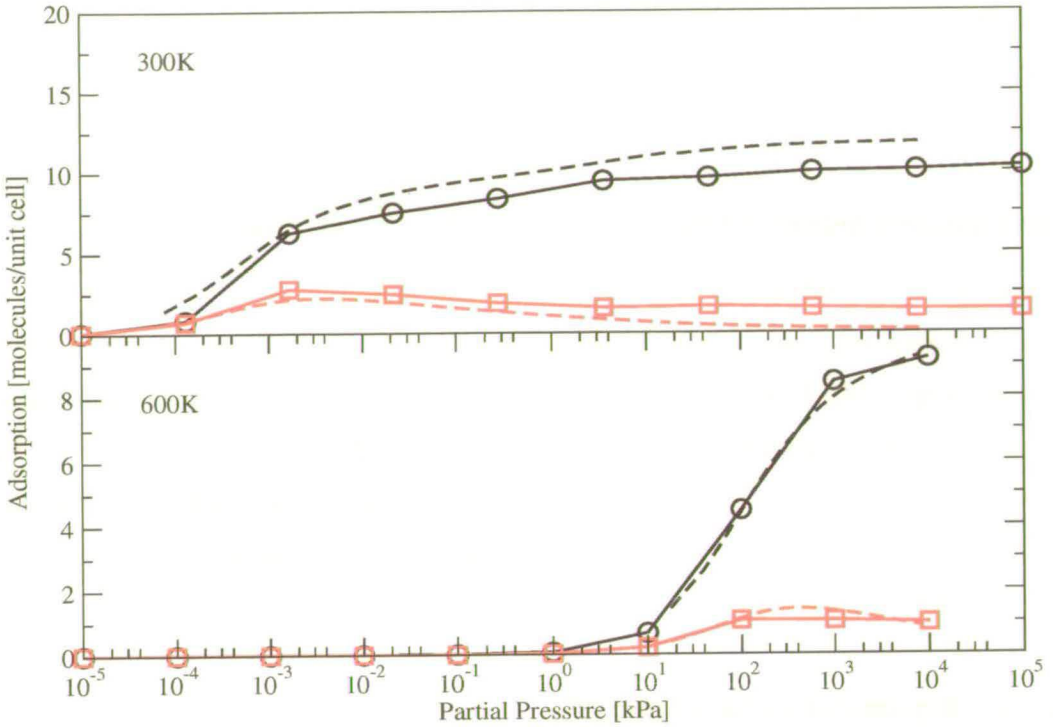

Figure 5.16: The adsorption isotherms for an equimolar mixture of hexane and cyclohexane in ITQ-22 at 300K (top) and 600K (bottom). The red squares represent the hexane and the black circles represent the cyclohexane. The theoretical isotherms are shown by the dashed lines.

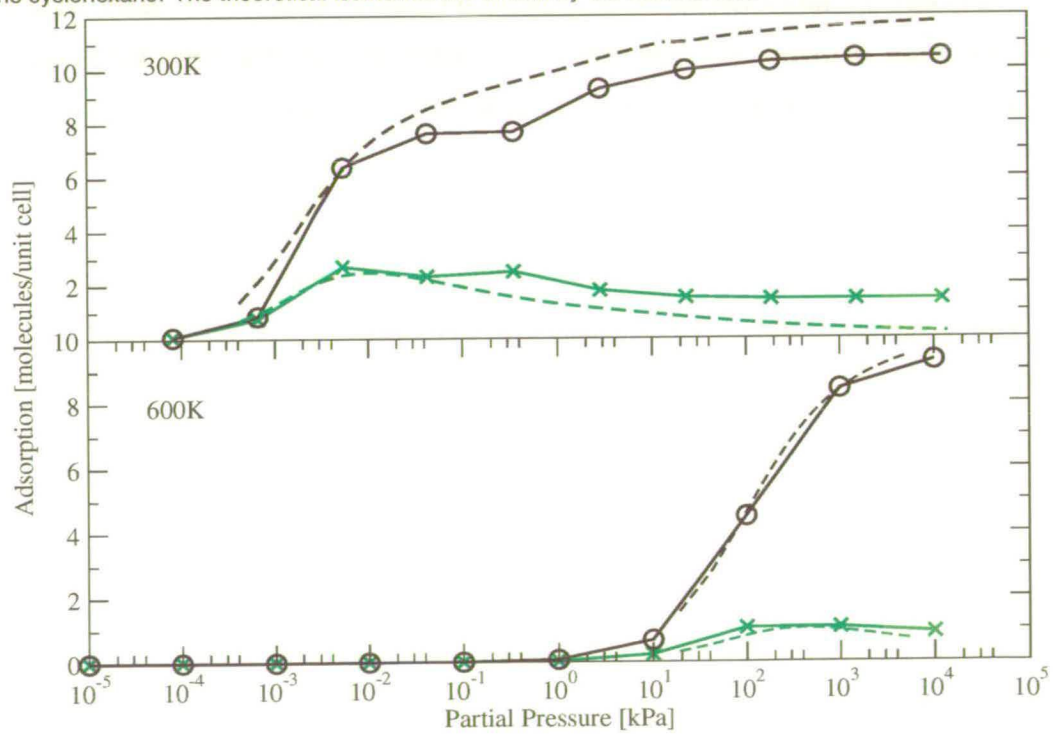

Figure 5.17: The adsorption isotherms for an equimolar mixture of cyclohexane and 2-methylpentane in ITQ-22 at 300K (top) and 600K (bottom). The green crosses represent the 2-methylpentane and the black circles represent the cyclohexane. The theoretical isotherms are shown by the dashed lines.

cyclohexane with hexane and 2-methylpentane respectively. Both figures highlight the dominance of cyclohexane at high and low temperatures, with hexane or 2-methylpentane adsorbing in only very small quantities. Cyclohexane is the clear 'winner' at low temperatures in both mixtures, as predicted by the IAST theoretical isotherms. The position of the adsorbed molecules are in keeping with the pure component adsorption locations.

According to the conformational information given in Section 5.3.1, a rise in temperature results in hexane and 2-methylpentane finding it much harder to adsorb (since they do not fit as easily into the channels) whilst cyclohexane does not change in shape significantly and thus the adsorption is less effected by temperature. This means that if cyclohexane dominates the low temperature adsorption then it will dominate the high temperature adsorption since the other component in the mixture will find it harder to adsorb at higher temperatures. This is clearly seen in Figures 5.16 and 5.17.

5.5.2 Equimolar ternary mixtures

Cyclohexane dominates the binary mixtures in ITQ-22 at both low and high temperature. The story is no different for the ternary mixture, shown in Figure 5.18 where cyclohexane adsorbed in much greater quantities than either hexane or 2-methylpentane. The theoretical isotherms agree well with the simulation adsorption isotherms at both temperatures. There is a reversal in the order of hexane and 2-methylpentane as the temperature increases - this is similar to the binary mixture reversal in selectivity for the hexane and 2-methylpentane mixture.

The siting of the three species is similar to that of the pure components. There does not appear to be any pattern to the location of the hexane or 2-methylpentane molecules - at pressures that permit adsorption of these two species, the molecules adsorb at any of their pure component locations.

5.6 Conclusions

This chapter presented results of the simulations used to investigate the behaviour of binary and ternary mixtures of hexane, 2-methylpentane and cyclohexane in silicalite-1, $AlPO_4$-5 and

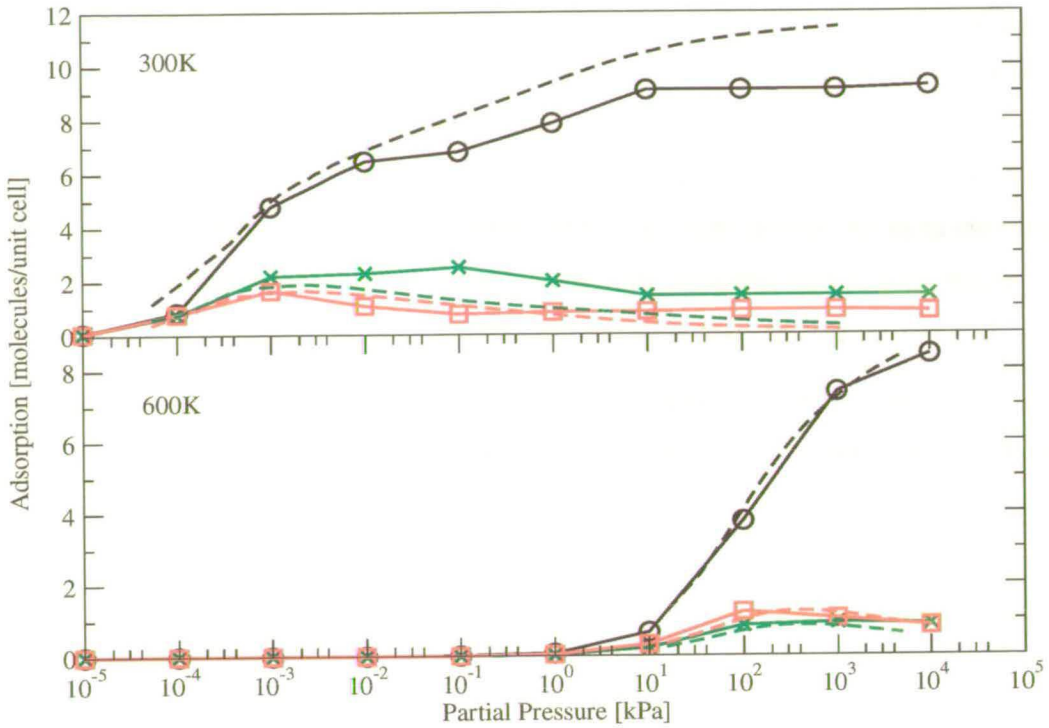

Figure 5.18: The adsorption isotherms for a ternary mixture of hexane, 2-methylpentane and cyclohexane in ITQ-22 at 300K (top) and 600K (bottom). The red squares represent the hexane data, the green crosses are the 2-methylpentane data and the black circles are the cyclohexane data. The dashed lines represent the theoretical isotherms.

ITQ-22. A summary of the key features of the adsorption will be given for each zeolite.

Silicalite-1

The adsorption of both the 300K and 600K equimolar binary mixtures of hexane and 2-methylpentane were dominated by hexane. At 300K, silicalite-1 selectively adsorbed hexane from a 50:50 mixture of hexane and cyclohexane. However, at high temperature (600K) it was the cyclohexane which adsorbed in greater number. The story was similar for an equimolar mixture of 2-methylpentane and cyclohexane; at 300K, 2-methylpentane adsorbed in greater quantities than cyclohexane whilst the selectivity was reversed at 600K when cyclohexane dominated the adsorption.

Non-equimolar mixtures involving hexane resulted in adsorption of more hexane than either

2-methylpentane or cyclohexane, for all but the very lowest concentrations of hexane. Indeed, it was only at very low pressure and very low concentration that hexane was unable to adsorb in greater number when in mixture with either 2-methylpentane or cyclohexane. In the non-equimolar mixture of 2-methylpentane and cyclohexane, it was the branched molecule which adsorbed in greater number than cyclohexane, although there was sustained adsorption of cyclohexane, even at high pressures. At high concentrations of cyclohexane, more cyclohexane than 2-methylpentane adsorbed.

Selectivity reversal was noted for the ternary mixture when the temperature was increased from 300K to 600K. At 300K the adsorption hierarchy was

$$\text{hexane} > 2-\text{methylpentane} > \text{cyclohexane}$$

whilst at 600K it changed to

$$\text{cyclohexane} > \text{hexane} > 2-\text{methylpentane}$$

The reversal in selectivity was attributed to the molecular conformation change with temperature of the three species. Both hexane and 2-methylpentane became shorter and fatter as the temperature increased since they were able to explore more of their higher energy conformations which involve an increase in the number of *gauche* bonds. The high temperature conformations found it more difficult to negotiate the narrow pores and so the number of hexane and 2-methylpentane molecules that adsorbed decreased with temperature. The shape of cyclohexane does not change with temperature and so it did not suffer in the same way as the temperature increased.

$AlPO_4$-5

Unlike the mixture adsorption in silicalite-1, adsorption in $AlPO_4$-5 did not exhibit any selectivity reversal and one species of the mixture dominated at both low and high temperatures. The adsorption hierarchy in $AlPO_4$-5 was found to be

$$\text{cyclohexane} > \text{hexane} > 2-\text{methylpentane}$$

under all conditions. $AlPO_4$-5 has a simple pore structure with no intersections or bends, it consists of straight, unconnected channels. Cyclohexane is found to adsorb with the highest density (the lowest adsorbate centre of mass separation) with hexane and 2-methylpentane taking up more room in the channels and thus adsorbing in smaller quantities than cyclohexane.

ITQ-22

Both the 300K and 600K binary mixtures involving cyclohexane resulted in the uptake of large quantities of cyclohexane and very little of the other mixture species. The binary mixture of 2-methylpentane and hexane exhibited a selectivity reversal as the temperature increased; at low temperature (300K), 2-methylpentane was the most adsorbed species whilst at 600K the situation was reversed with hexane adsorbing in larger quantities. The selectivity reversal was attributed to the extra steric hindrance imposed by the branched head group in 2-methylpentane; both molecules find it harder to fit into the zeolite channels as the temperature increases, due to the increase in the number of *gauche* bonds. However, 2-methylpentane is further restricted by the branched head group which results in it being less easily accommodated in the channels than hexane which does not have a branched section.

The adsorption of a ternary mixture in ITQ-22 was dominated by cyclohexane. At low temperature the adsorption hierarchy was:

$$\text{cyclohexane} > 2-\text{methylpentane} > \text{hexane}$$

whilst at high temperature it changed to:

$$\text{cyclohexane} > \text{hexane} > 2-\text{methylpentane}$$

with the swap between hexane and 2-methylpentane due to the conformational changes, described above.

In all three zeolites, the predicted mixture adsorption isotherms agreed well with the simulated isotherms and were able to correctly predict the selectivity at both low and high temperatures. Indeed, since it is possible to predict the mixture adsorption using only the single component isotherms it is reasonable to ask if there is any point in performing the simulation of the mixtures. However, the simulations provide an extra layer of detail which is not known by using

only the single component isotherms to investigate the mixture adsorption. Whilst the IAST predicted isotherms *do* provide the correct selectivity, they say nothing of the microscopic details of the adsorption, such as *where* the molecules adsorb. This information is available from the simulations and allows an interpretation of the mixture adsorption on the microscopic level. With this extra detail, it is possible to analyse the mixture adsorption on the molecular level and to explain the complex battle between the mixture components as they strive to adsorb within the complex zeolite pore network.

Using computer simulations to explore the adsorption of mixtures in zeolite is an efficient process, allowing mixture adsorption to be analysed in a much shorter time than the corresponding experiments. It is also possible to investigate new zeolites (such as was done in this chapter with ITQ-22) whose adsorption properties are not fully known. In this way, new zeolites can be 'tested' for particular adsorption properties using computer simulations which provide a microscopic level of detail in a relatively short time.

This chapter has shown that by using computer simulations it is possible to predict the behaviour of two and three component mixtures of linear, branched and cyclic alkanes in silicalite-1, $AlPO_4$-5 and ITQ-22 and to analyse the adsorption locations and the conformation of the adsorbed molecules to explain the macroscopic change in selectivity at the temperature increases.

Chapter 6

Simulations of adsorption in the mesopore MCM-41

The aim of this chapter is to introduce the model used to simulate MCM-41, to motivate the study of this mesoporous material and to present results of simulations using the model. Both single component and mixture isotherms of the adsorption of hexane, 2-methylpentane and cyclohexane will be presented along with a discussion of the structure of the adsorbed molecules. Where available, comparison with experiments will be made. Possible refinements to the model will be introduced and their applicability discussed.

6.1 Introduction

MCM-41 is a silica-based mesoporous material consisting of a hexagonal array of uniform pores, whose diameters can be tailored to be between 16Å and 100Å. Despite only being first synthesised [2] in the early 1990s, there have already been many uses proposed for MCM-41, ranging from drug delivery [5] to the removal of sulphur from heavy oils [133]. There have been numerous experimental [5, 6, 123–126, 130, 132–136] and computational [122–126] studies of MCM-41, focusing on both the structural and adsorption properties. Computer simulations are a valuable tool in the study of adsorption properties of both microporous and

mesoporous materials, providing data on the microscopic level which compliments the available (often macroscopic) experimental data, building a more complete understanding of the molecular behaviour within the pores.

In contrast with the study of zeolites, there have been relatively few experimental studies of the adsorption of larger hydrocarbons in MCM-41. Previous simulation studies of MCM-41 have focused on either single component adsorption [122, 126] or adsorption of mixtures of small molecules [123–125]. Mixtures of large molecules have not, to the author's knowledge, been studied. This work uses Configurational Bias Monte Carlo [41] methods to simulate the adsorption properties of single components and mixtures of large molecules (hexane, 2-methylpentane and cyclohexane) within the pores of MCM-41. The pores of MCM-41 are an order of magnitude larger than those of the zeolites studied in the previous chapters and many more molecules are able to squeeze in to the pores. This means that the adsorbate-adsorbate interaction will play an important role - this was not the case in adsorption is zeolites since the molecules were, in general, fewer in number and more disperse.

In this chapter the adsorption of both single components and mixtures of hexane, 2-methylpentane and cyclohexane will be studied. The effect that surface roughness of MCM-41 has on the adsorption of the three molecules will be analysed and the agreement with experimental adsorption isotherms (where available) will be discussed. The structure of the molecules within the pores will be analysed and the adsorption hierarchy of mixtures will be compared to that in zeolites. Refinements to the model of MCM-41 will be proposed and their possible effect on the adsorption properties will be discussed.

6.2 The model

The exact structure of MCM-41 is not known and cannot be determined experimentally due to its amorphous nature. Even the shape of the pores is not precisely known and computational studies of MCM-41 have used pores which vary widely in shape. The shapes of the cross section of the pores range from perfectly circular [120,123,126,128], through roughened circles [121, 122, 124], to hexagonal [122] and ellipses [122] and even constricted pores [122]. Each

of these different simulation studies proposed a model and then investigated its properties to determine the validity of the model for a specific feature, such as the adsorption of certain molecules, by comparison with experimental data. In this way, each model of MCM-41 is very specific and, in some cases, is tailored to provide accurate data for only a small set of molecules.

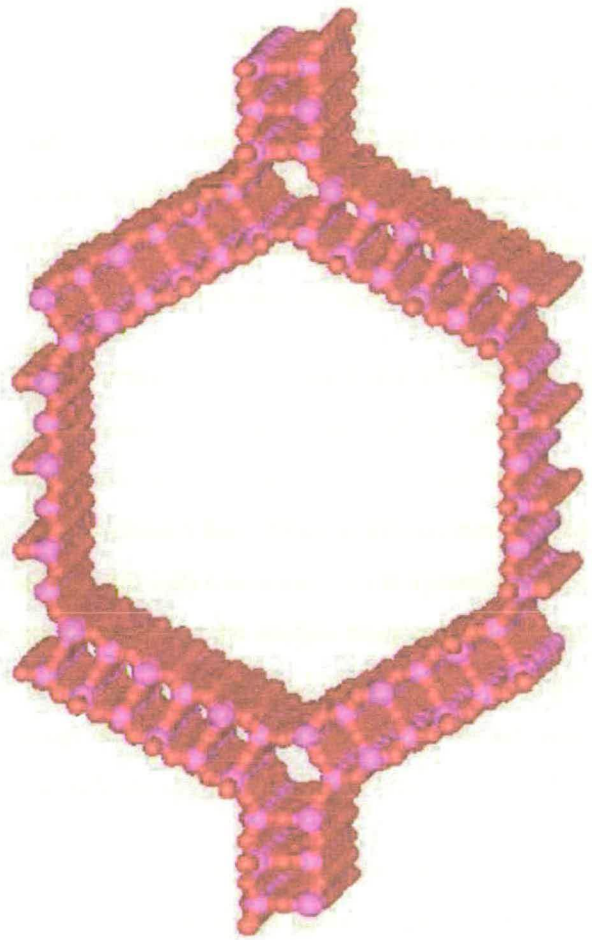

Figure 6.1: The computational model of MCM-41. The oxygen atoms are shown in red and the silicon in purple. The width of the pore is 27.6Å and the height is 31.9Å. The pore cross sectional area is equivalent to a circular cross section of diameter 29Å.

The structure of MCM-41 used in this study is shown in Figure 6.1 and is loosely based upon that of Gusev [186] in which the pore is hexagonal. The structure is modified to make it periodic and so that it contains the correct oxygen/silicon ratio. Whilst this model provides a concise description of MCM-41, it does not include any hydrogen atoms, which exist both in

the body of the mesopore and on the pore surface. It also depicts the mesopore as a perfect periodic crystal - even though MCM-41 is known to have an *amorphous* structure. It is possible to perform simulations using a non-crystalline model of MCM-41- see Section 6.6 for details of such simulations.

The model proposed in this study is a balance between accuracy and computational efficiency. The model is intended to capture the general features of MCM-41: it has a regular array of pores surrounded by a structure composed of silicon and oxygen atoms. Since neither the exact pore shape nor atomic positions of MCM-41 are known experimentally, this model represents a reasonable starting point and will allow the investigation of not only the macroscopic adsorption characteristics (such as the mass of molecules which adsorb in MCM-41) but also the microscopic details such as the structure of the adsorbed molecules.

The potential used to calculate the adsorbate-mesopore interaction is outlined in Chapter 3 and is identical to that used for the study of adsorption in zeolites; the mesopore is modelled as a rigid network of oxygen atoms which interact, via a Lennard-Jones potential, with the guest molecules, which are represented as connected pseudo-atoms. Figure 6.2 depicts the adsorbate-mesopore potential energy at each point on a slice through the mesopore. This image highlights the areas close to the mesopore surface where the adsorbate molecules are repelled by the oxygen atoms (due to the short range Lennard-Jones repulsion) whilst further from the surface lie regions where the adsorbate-mesopore interaction is favourable - areas where the adsorbed molecules find it energetically favourable to position themselves.

Data from several different experimental studies is used in this chapter to compare with the simulated data. However, not all experimental studies are undertaken with mesopores of the same diameter, indeed the diameters vary from 29.5Å up to 40Å. However, even if two experimental studies present data on pores which are not *exactly* the same diameter, it is still useful to compare their results, so long as care is taken to remember that the pores are not identical. The pore diameters of the experimental studies of hexane, 2-methylpentane or cyclohexane adsorption referred to in this chapter are shown in Table 6.1. The experimental pore size is determined using the Barrett-Joyner-Halenda [187] method which relates the size of the pore to the amount of nitrogen adsorbed within the pore.

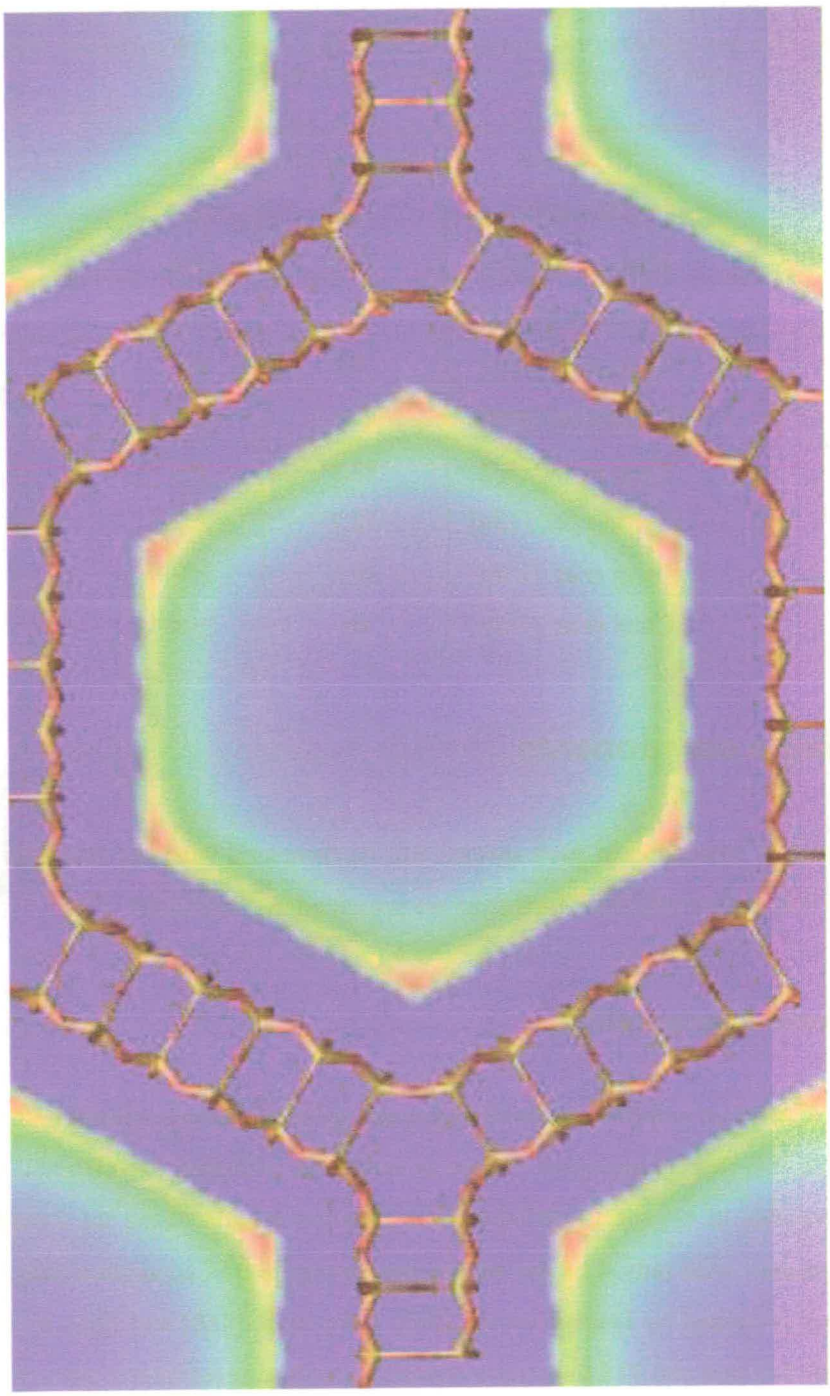

Figure 6.2: A slice through the adsorbate-mesopore potential energy isosurface. Red areas indicate regions of strongest adsorbate-mesopore attraction, through orange, yellow, green and light blue which indicates regions of weakest attraction. Dark blue areas indicate adsorbate-mesopore repulsion.

Table 6.1: The pore diameter of MCM-41 used in experimental studies. Where one reference presents data for more than one diameter, the diameter closest to that used in the simulation model is chosen. The temperature at which each study was undertaken is also shown.

Reference	Diameter (Å)	Temp (K)
This study	29	300
Zhao *et al.* [135]	29.5	296
Jänchen *et al.* [130]	30	303
Qiao *et al.* [132]	30	303
Trens *et al.* [188]	31	303
Zhao *et al.* [133]	32.3	295
Carrott *et al.* [134]	32.7	298
Long *et al.* [136]	39.2	298
Chen *et al.* [189]	40	298

6.3 Single components

First, the heat of adsorption of each species will be compared with any available simulation data before the single component isotherms are presented and discussed.

6.3.1 Heats of adsorption

The heat of adsorption is defined as the change in energy as a molecule adsorbs onto the internal surface of (in this case) a mesopore. There is very little published experimental data on the heat of adsorption of hexane in MCM-41 (the situation is even worse for 2-methylpentane and cyclohexane), with only 4 of the studies presenting heat of adsorption data. The heats of adsorption presented by Jänchen *et al.* [130], Trens *et al.* [188] and Zhao *et al.* [135] are 39kJ/mol, 38.1 kJ/mol and 37 kJ/mol respectively. This close agreement is not echoed by Qiao *et al.* [132] who report a heat of adsorption of 64kJ/mol. The simulated heat of adsorption for hexane in MCM-41, at 300K, is 40.2kJ/mol which is in excellent agreement with the three concurring experimental studies.

Table 6.2: The adsorption capacities of MCM-41 for hexane at a relative pressure of 0.5 (i.e. $P/P_0 = 0.5$) for each of the experimental works and this simulation study. The pore size is included for comparison between each experimental study. Note that there is no data for Chen *et al.* [189] since this work deals only with cyclohexane. The data from Trens *et al.* [188] has also been omitted - see text for details.

Reference	Capacity (mmol/g)	Pore diameter (Å)
This study	4.68	29
Zhao *et al.* [135]	4.7	29.5
Jänchen *et al.* [130]	5.7	30
Qiao *et al.* [132]	4.0	30
Zhao *et al.* [133]	6.5	32.3
Carrott *et al.* [134]	3.3	32.7
Long *et al.* [136]	2.8	39.2
Average of expts	4.5	31.9

No experimental heats of adsorption for 2-methylpentane in MCM-41 could be found to compare with the simulated value of 32.4kJ/mol. The story is the same for cyclohexane where neither of the two experimental studies present heats of adsorption for cyclohexane in MCM-41 to compare with the simulated value of 21.5kJ/mol.

6.3.2 Single component adsorption isotherms

There are seven experimental studies which present data on the adsorption of hexane in MCM-41. In this section, the focus will be on the work of Zhao *et al.* [135] whose pore diameter (29.5Å) is closest to that of the simulation model (29Å). The adsorption capacity in their work is representative of the other experimental studies as can be seen from Table 6.2.

Note that this table does not contain the data from the study of Trens *et al.* [188] since they report a loading which is two orders of magnitude larger than any of the other studies. Indeed, they report an adsorbed volume of hexane which is larger than their reported pore volume.

The adsorption capacities shown in Table 6.2 at P/P_0=0.5 give a quick estimate of the agreement between the simulations and the experiments. However, it is the full adsorption isotherms

which will allow a complete comparison between the two techniques. Figure 6.3 shows the experimental [135] and simulated adsorption isotherms for hexane in MCM-41. The agreement between the two is excellent, over the entire pressure range. The isotherm shape can be explained as follows: at low relative pressure ($P/P_0 < 0.15$) the adsorbed molecules form a mono-layer on the surface of the pore - the adsorption is only one molecule deep and each molecule can find an adsorption site on the pore surface. Between P/P_0 values of 0.15 and 0.25 there is a steep increase in loading during which the adsorbed molecules fill much of the remaining space in the pore, creating multilayer adsorption. Above P/P_0 values of 0.25 there is a levelling off in adsorption as the volume of hexane molecules nears the maximum pore volume. These stages in the adsorption of hexane can be seen in Figure 6.4 which shows a snapshot of the adsorbed molecules at different pressures. The figure shows that at low pressure the molecules can easily get close to, and adsorb onto the pore wall whilst at higher pressures the pore fills with molecules, creating multilayer adsorption.

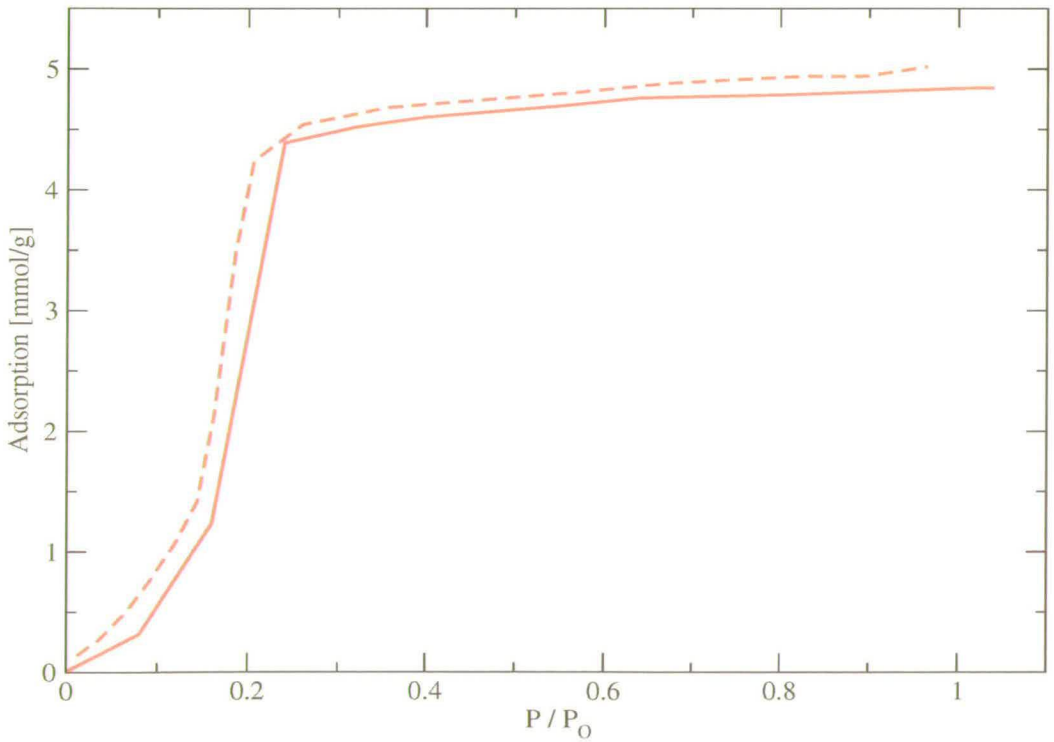

Figure 6.3: The simulated (solid line) and experimental (dashed line, taken from reference [135]) adsorption isotherms of hexane in MCM-41 at 300K (simulated) and 296K (experimental). Note that P_0 refers to the vapour pressure of hexane at 300K and has the value of 25kPa [157].

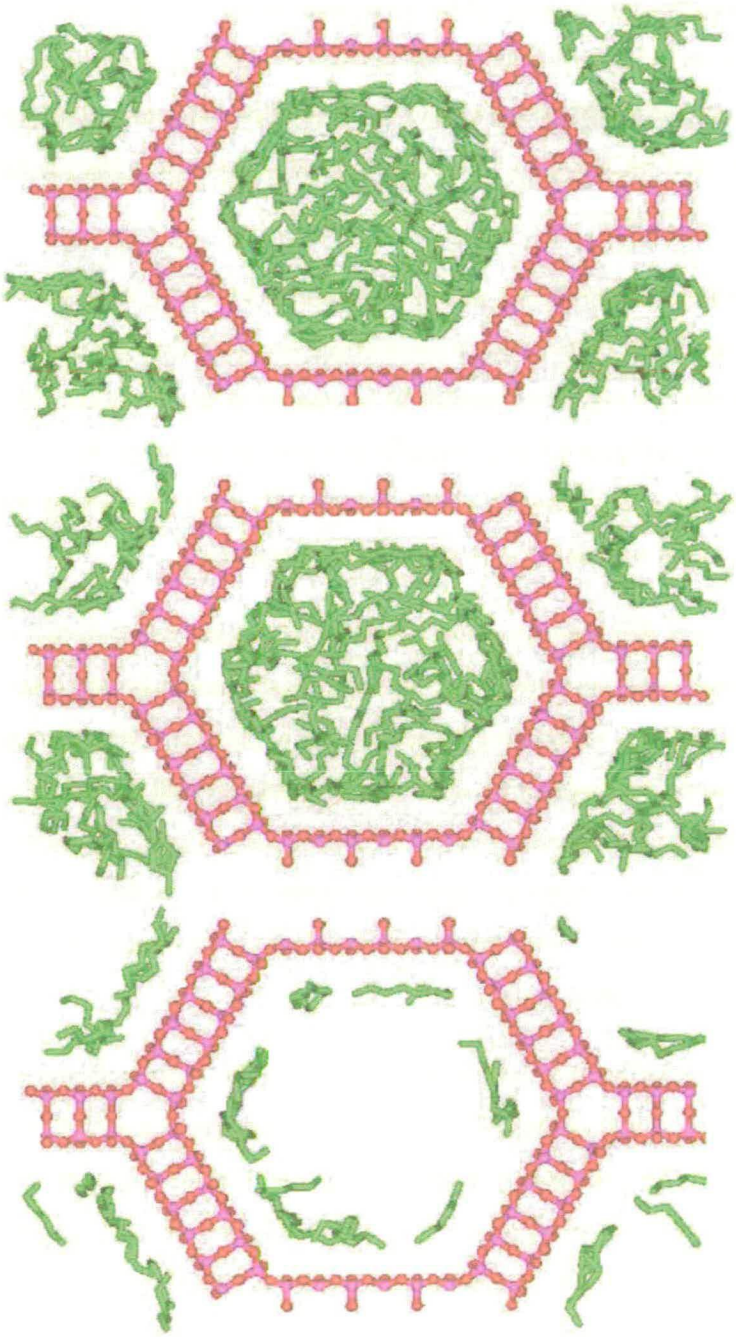

Figure 6.4: A snapshot of the positions of the hexane molecules (shown in green) in MCM-41 (red and purple structure) at P/P_0=0.12 (left), P/P_0=0.24 (middle), P/P_0=0.8 (right).

There is a small yet interesting increase in the experimental adsorption isotherm (Figure 6.3) at the highest P/P_0 values which is not present in the simulated isotherm. This slight increase is seen in all of the experimental studies (although in some [130, 133, 134, 136] it is more pronounced than others) and has been attributed, by Jänchen *et al.* [130], to adsorption of hexane molecules on the *outer* surface of MCM-41 and in the inter-particle voids (the gaps between the joins in the particles of MCM-41). This extra adsorption is not seen in this simulation study because only the pore is modelled and not the outer surface of MCM-41.

In contrast to the number of experimental studies of hexane in MCM-41, there are no studies of 2-methylpentane in MCM-41, to the author's knowledge. As a result, the simulated adsorption isotherm which is shown in Figure 6.5 cannot be compared to any experimental data. The structure of the isotherm in Figure 6.5 is very similar to that of hexane in MCM-41 (Figure 6.3), both isotherms exhibiting a large jump in uptake around $P/P_0 = 0.15$ and above this pressure the isotherms is almost flat with only a very slight increase in uptake.

It is reasonable to expect that the adsorption isotherms of hexane and 2-methylpentane are similar since both molecules share many of the same structural features: hexane is long and thin with a chain of 6 carbon atoms, whilst 2-methylpentane has a chain of 5 with a branched 'head'. Both are able to flex along the length of the chain and both interact with the mesopore oxygens via a potential with the same parameters (for all but the CH pseudo atom in 2-methylpentane). Although it is not possible to compare the adsorption isotherm of 2-methylpentane in MCM-41 with any experimental data, a comparison with the isotherm of hexane shows that the 2-methylpentane isotherm is, at least, realistic.

The simulated adsorption isotherm of cyclohexane in MCM-41 is shown in Figure 6.6 together with the only two experimental studies of cyclohexane adsorption. There are several things to note about this graph: first, the pore size of MCM-41 used in all three studies is different, with the two experimental pores being of diameter 40Å and 39.2Å whilst the simulation pore is 29.5Å in diameter. Second, the two experimental isotherms show large differences in their shape and maximum loading - despite their pore diameters differing by only 2%. Third, the relative maximum loading of the two experimental isotherms appears to be reversed - it is realistic to expect that the larger pore can accommodate more molecules than the smaller pore yet this

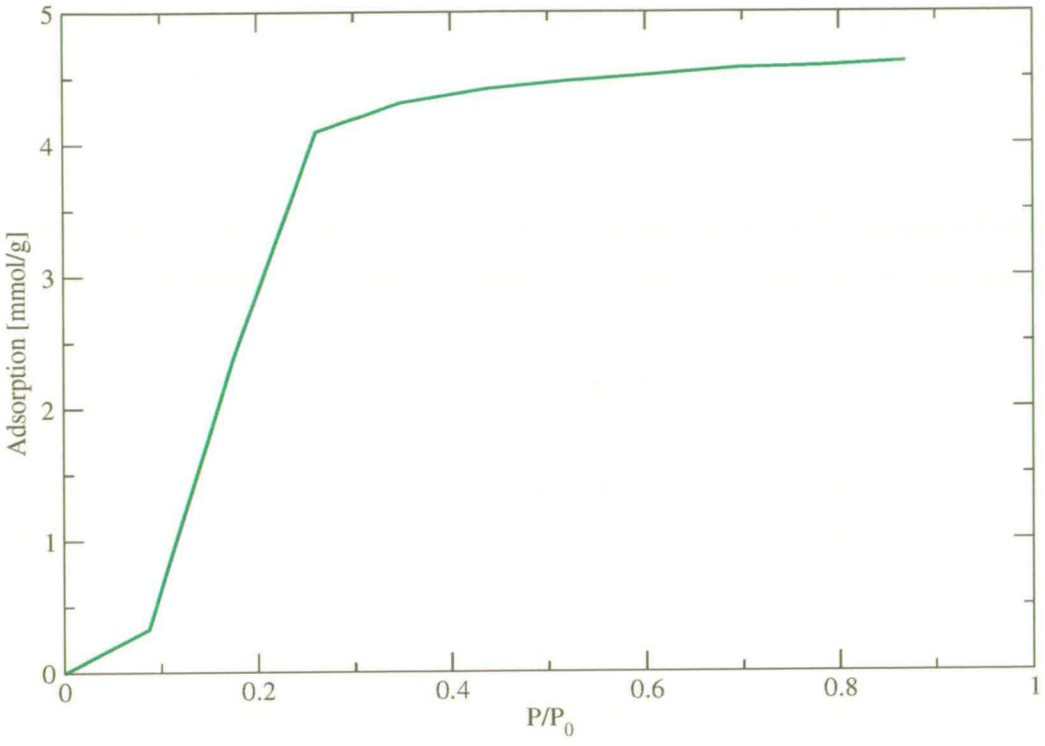

Figure 6.5: The simulated adsorption isotherm of 2-methylpentane in MCM-41 at 300K. Note that P_0 refers to the vapour pressure of 2-methylpentane at 300K and has the value of 23kPa [157].

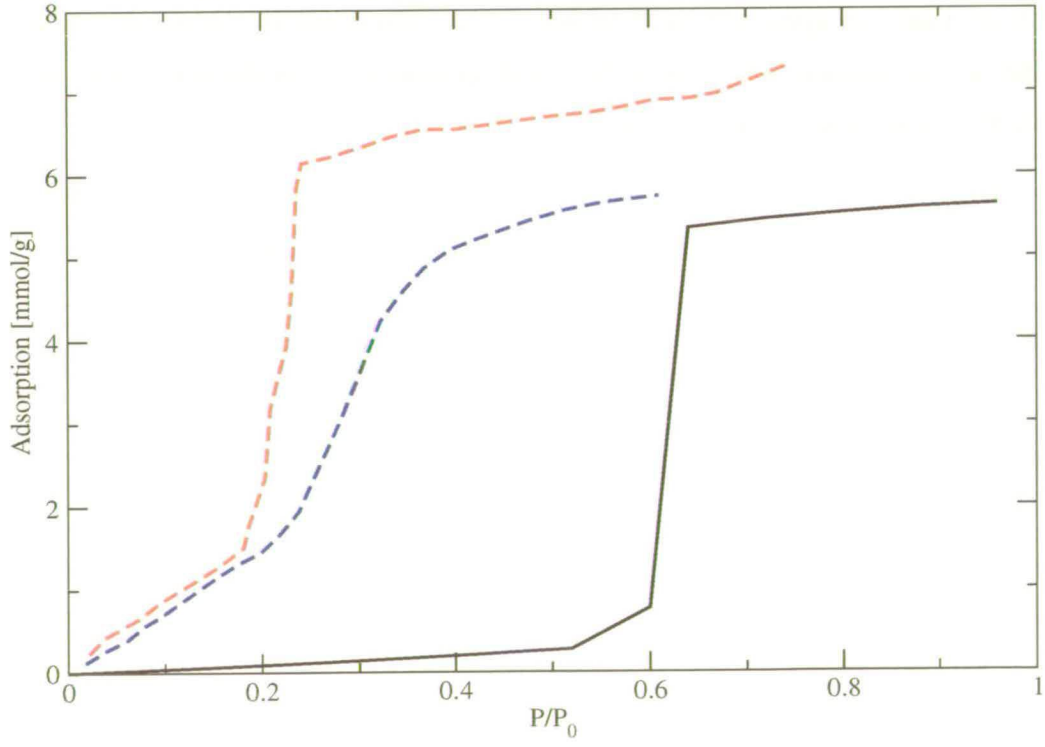

Figure 6.6: The simulated (solid line, 300K) and experimental (dashed red line is from reference [136] and dashed blue line is from reference [189], both at 298K) adsorption isotherms of cyclohexane in MCM-41. Note that P_0 refers to the vapour pressure of cyclohexane at 300K and has the value of 22kPa [157].

appears not to be the case in Figure 6.6 where the smaller pore (39.2Å) holds approximately 1 molecule per unit cell *more* than the larger pore (40.0Å). Fourth, the simulated isotherm shows a sharp increase in the loading at a much higher pressure than either of the two experimental isotherms. Finally, it is important to note that the maximum loading of cyclohexane is more than either hexane or 2-methylpentane, albeit only slightly: at 20kPa, MCM-41 can accommodate 4.8 mmol/g of hexane or 4.6 mmol/g of 2-methylpentane or 5.5 mmol/g of cyclohexane. The accommodation of more cyclohexane than hexane in MCM-41 is also seen experimentally [136] although in the experiments there was significantly more cyclohexane than hexane (approximately 50% more). The experimental work also indicated that the large increase in loading occurred in hexane at a much lower pressure than cyclohexane- this is also true of this study where the increase in hexane occurs at around 3kPa whilst at cyclohexane it is around 13kPa.

Direct comparison between the experimental and simulated adsorption isotherms in Figure 6.6 is difficult due to the large difference in pore sizes. However, the maximum loading of the simulated isotherm is less than that of either of the (larger) experimental pores, which is a realistic feature. The total loading of the simulated isotherm is larger than that of hexane in MCM-41, again, this agrees with the experiments. It would be extremely interesting to be able to compare the simulated adsorption isotherm with an experimental isotherm from adsorption in MCM-41 with a pore of similar diameter.

The macroscopic data from the simulations, namely the quantity of molecules which adsorb at a given pressure, has been compared with the available experimental data. In the next section, the microscopic data, namely the average position of the molecules within the pore, will be analysed.

6.4 Structure of adsorbed phase

The previous section introduced the adsorption isotherms for hexane, 2-methylpentane and cyclohexane in MCM-41. When it was possible to compare these to experiments using similar sized pores, the comparison was good. However, the benefit of performing computer simulations is that it is possible to analyse the microscopic nature of the adsorption. In this section,

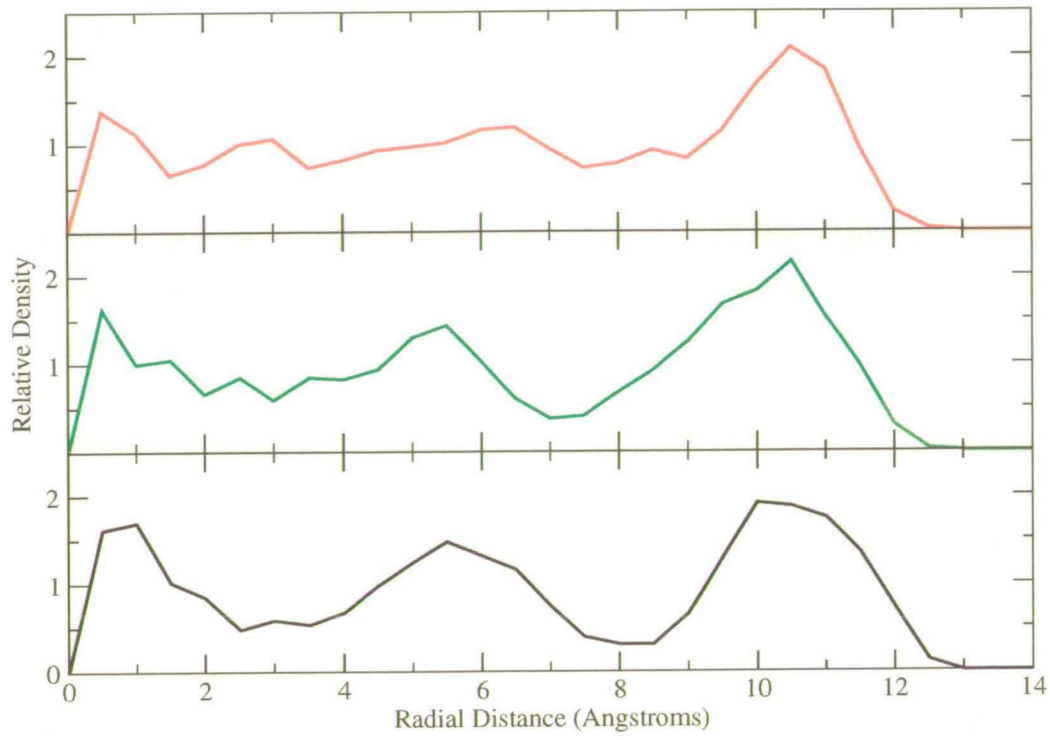

Figure 6.7: The relative density from the centre of the pore of (top to bottom) hexane, 2-methylpentane and cyclohexane in MCM-41 versus the radial distance from the central axis of the channel. The relative density is defined as the local density divided by the global density. The simulations were carried out at 300K and 10kPa.

the structure of the adsorbed phase is investigated by analysing the locations of the centre of mass of the molecules within the pore. By analysing the centre of mass positions over the duration of the simulation (after the equilibration period) a picture of the average locations of the molecules is built up, and any structure which forms can be assessed.

Figure 6.7 (top graph) shows the relative density of hexane at radial distances from the centre of the channel. The x-axis depicts the radial distance from the central axis of the channel; the y-axis is the relative density - the local density divided by the global density (total number of molecules divided by the volume of pore). By creating such a graph it is possible to determine if there are any local density fluctuations which would be indicative of any structure in the adsorbed molecules (otherwise, if there was no structure, the local density would be equivalent to the global density and Figure 6.7 would consist of three flat lines of height 1).

What Figure 6.7 does show is that there is a great deal of structure to the adsorbed phase of

all three molecules. Very close to the pore surface, above 12.5Å on the x-axis, there are no molecules. This is due to the short range repulsion between the oxygens in the mesopore and the adsorbed molecules. In all three graphs, there appear to be three peaks of high density, separated by troughs of low density. These three peaks correspond to three 'layers' of molecules. The largest, centred around 10.5Å represents the layer of molecules which is adsorbed onto the surface of the pore. The other two peaks indicate that the remaining molecules are structured, forming two regions of high density. The structure that Figure 6.7 reveals is one of concentric 'rings' of molecules separated by regions of low density where few molecules are to be found. This structure can be seen by looking at the right hand image in Figure 6.4 where there is a high density region of molecules close to the pore surface, followed by a relatively low density region slightly closer to the centre of the pore, followed by a region of higher density and finally a region of low density.

Figure 6.7 (middle graph) shows the relative density profile for 2-methylpentane in MCM-41. It is very similar to that of hexane (Figure 6.7, top graph) characterised by 3 high density regions separated by regions of a lower density. The high density peaks in the 2-methylpentane relative density profile are at approximately the same radial distance as those of hexane - this is a reasonable feature since both molecules are of a similar size and shape.

The relative density profile for cyclohexane is shown in Figure 6.7 (bottom graph) and it clearly shows three regions of high density, separated by low density regions. The high density regions appear to be more well defined that those of hexane and (to a lesser extent) 2-methylpentane.

There have been many studies focusing on the structure of hard-sphere 'molecules' in various different confined geometries [190–196]. These studies report density functions (similar to those in Figure 6.7) for small, hard 'molecules'[1] in spherical, cylindrical and slit-like pores. The density functions for small hard spheres reveal peaks of high density separated by troughs of low density. The peaks and troughs are much more well defined than those in Figure 6.7 but both density profiles show similar structure within the confined molecules. The density profiles in the literature are much more well defined because the 'molecules' are all identical and have rotational invariance. This means that the molecules can pack more efficiently since

[1] In fact, the 'molecules' are simply spherical particles which interact as hard spheres.

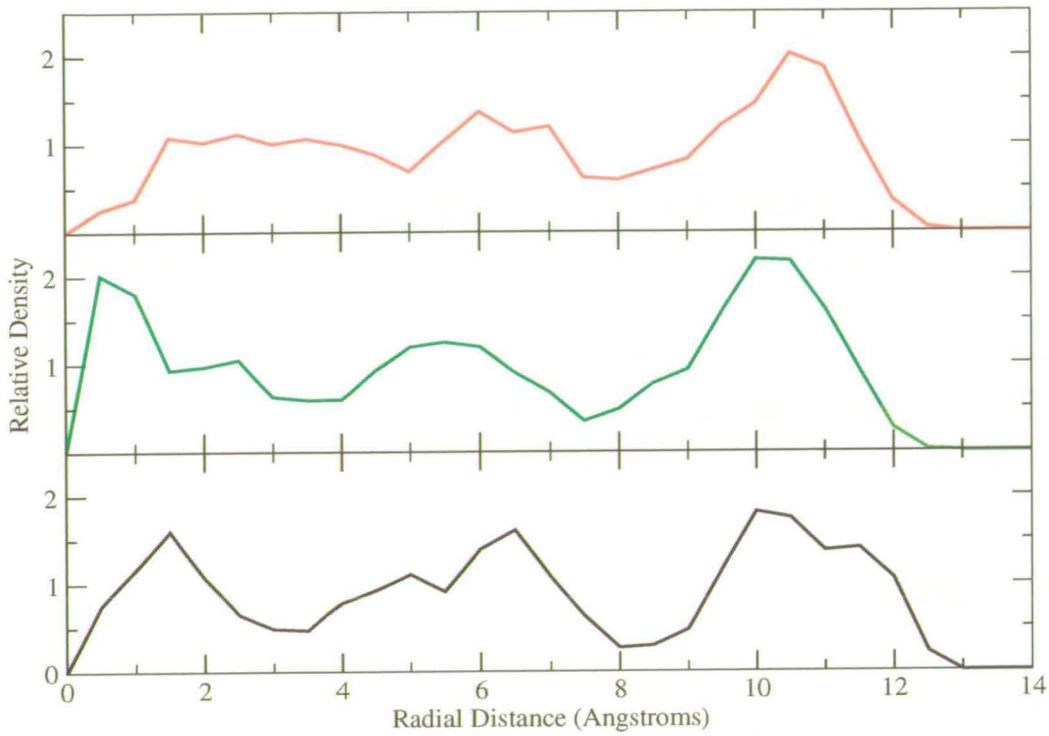

Figure 6.8: The relative density from the centre of the pore of (from top to bottom) hexane, 2-methylpentane and cyclohexane in MCM-41 at 1000kPa and 300K.

each 'molecule' does not have to take into account the orientation of its neighbours when attempting to find a suitable location close to other molecules. For molecules without rotational invariance, each molecule is affected by the orientation of its neighbours and so the molecules cannot pack as closely together and any region of high density may be spread slightly by the need for each molecule to avoid overlap with its non-spherical neighbours.

Rotational invariance can be used to explain the more distinct peaks in the literature density functions when compared to those in this work. However, it can also be used to describe the differences in the relative density profiles of hexane, 2-methylpentane and cyclohexane in MCM-41. The high pressure (1000kPa) relative density profiles for each molecule is shown in Figure 6.8. The high pressure distribution of cyclohexane centres of mass is more well defined than that of hexane or 2-methylpentane. This can be explained by the shape of the molecules - although cyclohexane is larger, its shape is more rotationally invariant than those of hexane or 2-methylpentane. This means that cyclohexane is closer to the hard-sphere 'molecule' used

in the literature to investigate structure in confined geometries. Thus, it is reasonable to expect that the more spherical a molecule is, the more well defined its density profile will be.

He *et al.* [124] have used computer simulations to investigate the adsorption of small molecules (ethane and carbon dioxide) in 3 different models of MCM-41- one is a circular cylinder and the other two are roughened cylinders. They found that that ethane adsorbed in identifiable layers in the smooth MCM-41 model with the separation between layers becoming more distinct at high pressure. However, as the roughness of MCM-41 increased, the layers became less distinct until, in the roughest model, no layering was observed, even at high pressure. In section 6.6 the effect that roughening has on the model of MCM-41 used in this work is discussed.

6.5 Mixtures

There have been no studies of the adsorption of mixtures of larger molecules (such as hexane, 2-methylpentane and cyclohexane) and so the results in this section are not compared with any other studies.

The previous chapter concluded that the adsorption of mixtures in zeolites is controlled by the ability of the adsorbed molecule to fit within the pore as well as the strength with which the molecule adsorbs onto the internal surface of the zeolite. However, MCM-41 has much larger pores than any of the zeolites studied in the previous chapter and so the adsorbates are not restricted by the pores in MCM-41 to the same degree as they were in zeolites. Thus, it would be reasonable to expect that the adsorption of mixtures in MCM-41 would be controlled by other factors, since all of the molecules can easily fit into the larger pores.

In the single component adsorption isotherms (Figure 6.3 and Figure 6.5), both hexane and 2-methylpentane have a maximum loading that is very similar: at 20kPa the loading of hexane in 4.8 mmol/g whilst that of 2-methylpentane is 4.6 mmol/g. The heats of adsorption too are very similar: 40.2 kJ/mol for hexane and 32.4kJ/mol for 2-methylpentane. Based on these observations it would be reasonable to expect that a mixture of hexane and 2-methylpentane would result in slightly more hexane adsorbing than 2-methylpentane. Figure 6.9 shows the equimolar binary mixture adsorption isotherm for hexane and 2-methylpentane in MCM-41

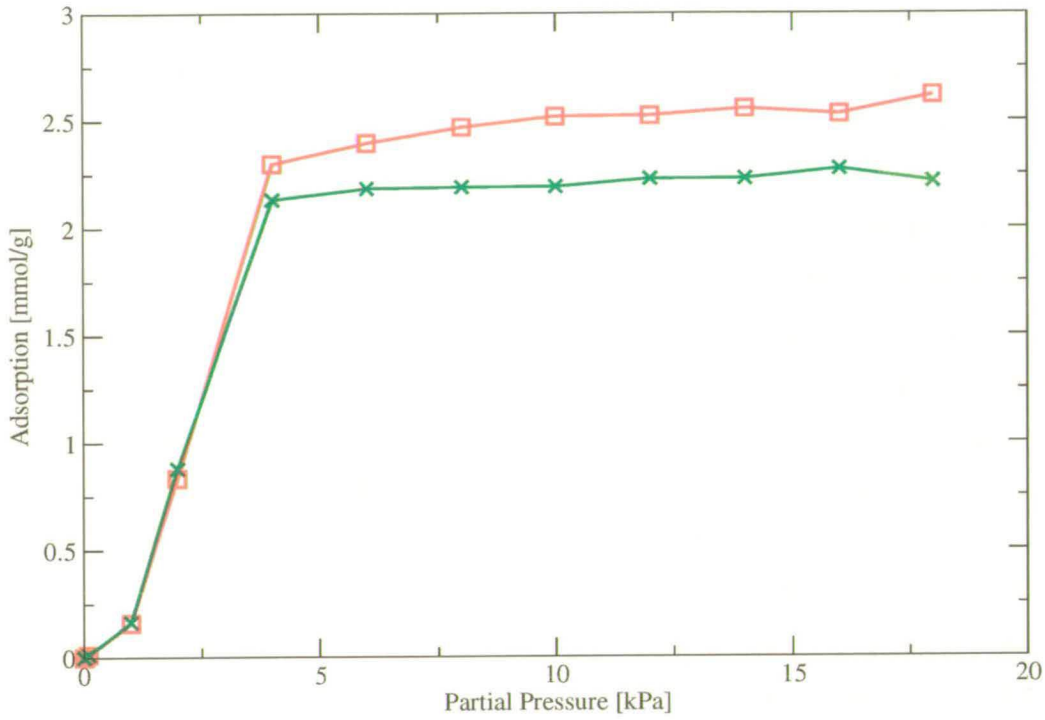

Figure 6.9: The adsorption isotherms for an equimolar binary mixture of hexane (red) and 2-methylpentane (green) in MCM-41 at 300K. Note that unlike the single component isotherm figures, this and subsequent figures show the unscaled partial pressure (i.e. not divided by P_0). This is so that the adsorption of the different mixture components can be compared at equal pressures.

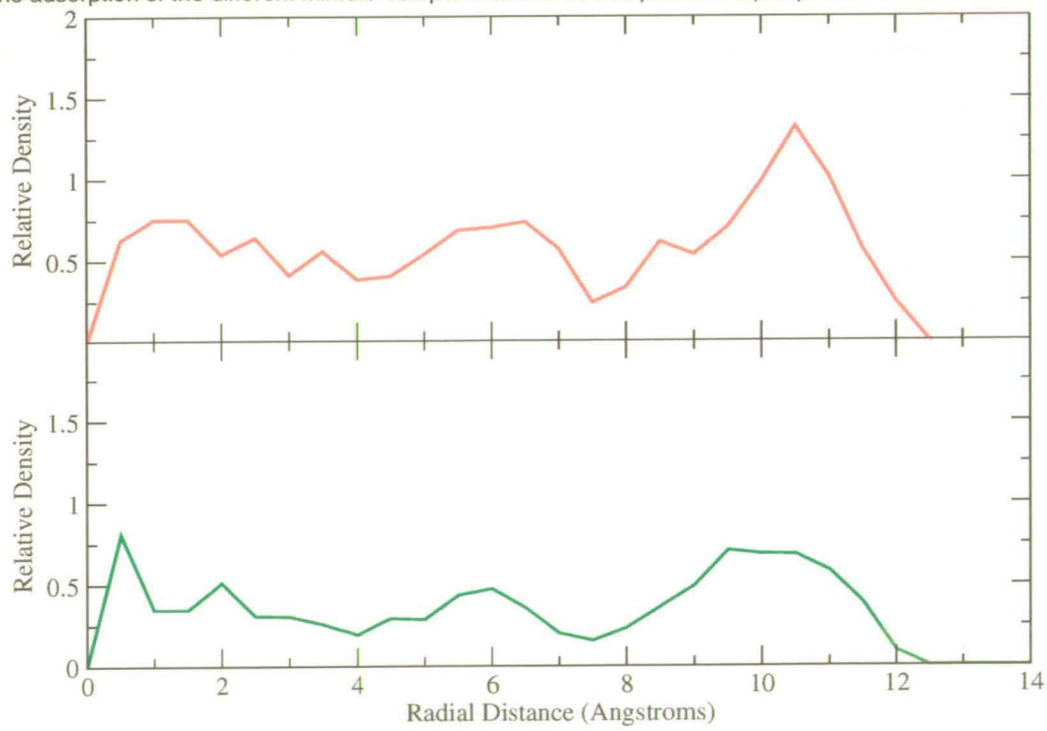

Figure 6.10: The relative density from the centre of the pore of hexane (top) and 2-methylpentane (bottom) in a equimolar binary mixture in MCM-41 at 300K.

at 300K which reveals that, at higher pressures, hexane adsorbs in slightly larger quantities than 2-methylpentane; however, the total loading of both molecules does not exceed 5 mmol/g. The structure of the adsorbed molecules in MCM-41 is shown in Figure 6.10 via the relative density plots. Note that in Figure 6.10 the density of each species is compared to the total density of the mixture - hence each plot will be slightly lower than the corresponding single component relative density plots. Figure 6.10 shows that both species are present throughout the pore and that there is a similar level of radial structure to each species. The structure of both molecular types comprises one region of high density near to the surface of the pore followed by a region of little or no structure towards the centre of the pore. The shape of the binary mixture relative density graphs for both hexane and 2-methylpentane is very similar to that of the single components, indicating that the fact that the components are in a mixture does not appear to appreciably affect their density profile. A comparison between the structure of the mixture in the pore and out of the pore is given for this mixture (and all subsequent mixtures) at the end of this section, on page 134.

The single component adsorption isotherms of hexane and cyclohexane (Figures 6.3 and 6.6) showed that not only did the maximum loadings differ (at 20kPa hexane loading was 4.8 mmol/g whilst cyclohexane was 5.5 mmol/g) but also the pressure at which the adsorption quickly increased was very different. The hexane adsorption isotherm showed a steep increase in loading at around 5kPa whilst a similar increase in loading was seen at 13 kPa in the cyclohexane adsorption isotherm. The heats of adsorption for hexane is 40.2kJ/mol whilst that of cyclohexane is 21.5 kJ/mol. Based in these facts, it it not immediately obvious what the binary mixture adsorption behaviour will be: will the fact that more cyclohexane molecules can fit within the pore be the dominant factor (at 20kPa there are, on average, 207 hexane molecules in the pore compared to 239 cyclohexane molecules at the same pressure) or will the heats of adsorption dictate the mixture adsorption?

Figure 6.11 shows the equimolar binary mixture adsorption isotherm for hexane and cyclohexane in MCM-41 at 300K. The selectivity of the mesopore is such that hexane adsorbs in much greater quantity than cyclohexane at all pressures - even at high pressures, where cyclohexane adsorbed in greater quantities than hexane in the single component adsorption isotherms. The total loading of both molecules is less than 5 mmol/g, despite the fact that on its own, more

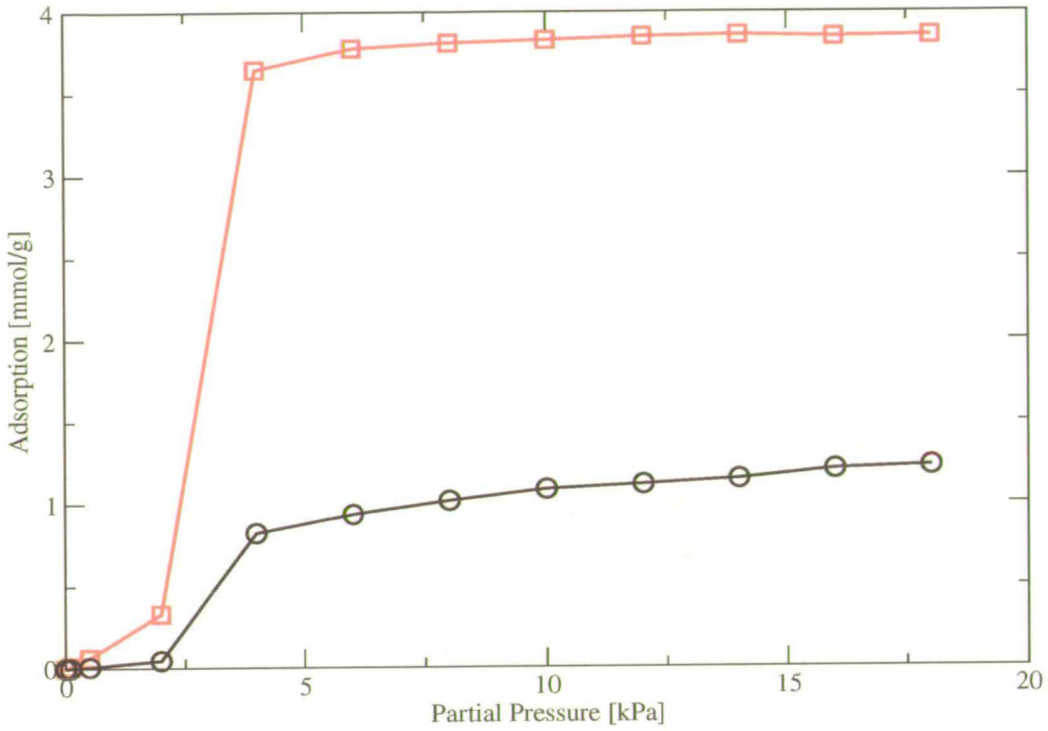

Figure 6.11: The adsorption isotherms for an equimolar binary mixture of hexane (red) and cyclohexane (black) in MCM-41 at 300K.

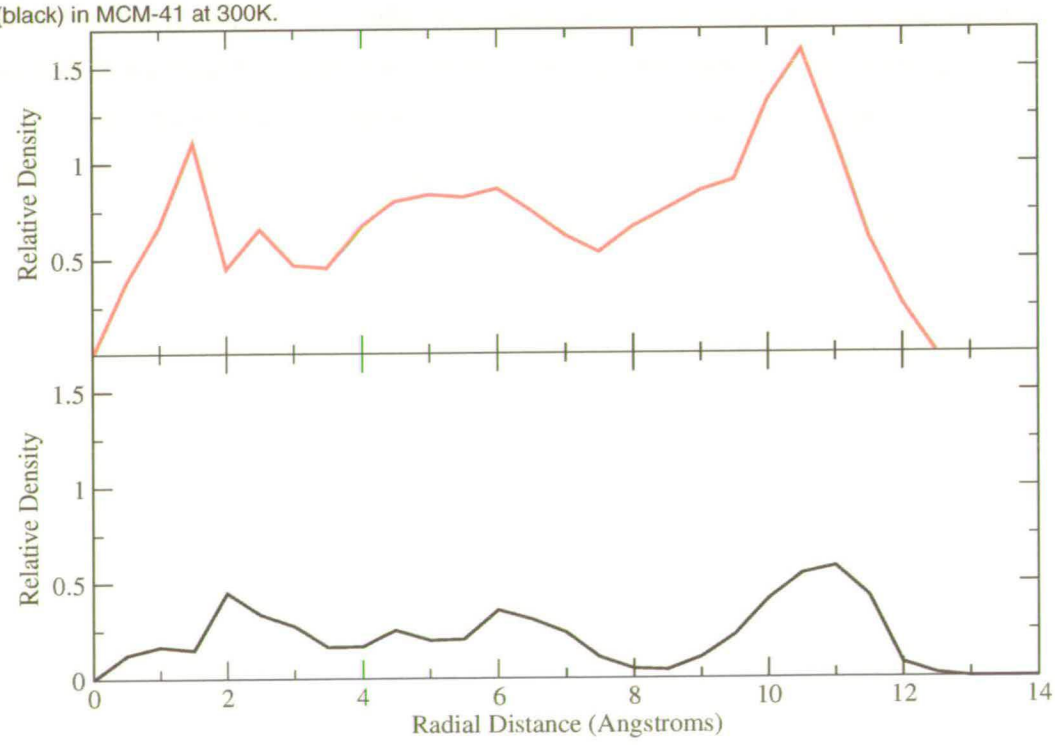

Figure 6.12: The relative density from the centre of the pore of hexane (top) and cyclohexane (bottom) in a equimolar binary mixture in MCM-41 at 300K.

than 5 mmol/g of cyclohexane is able to adsorb within the pores.

The relative density profiles of hexane and cyclohexane in the equimolar binary mixture in MCM-41 are shown in Figure 6.12. The first thing to note about these plots is that the cyclohexane relative density graph (bottom of Figure 6.12) is much lower on the vertical axis than that of hexane. This is simply due to the fact that there is less cyclohexane adsorbed within the pore and since the total density of *both* molecules is used to scale the graphs, the component with the least adsorption will have a lower relative density plot. Although adsorbing in much less quantity, cyclohexane has a relative density plot which exhibits distinct structure: close to the surface of the pore there is a region of high cyclohexane density, followed (closer to the centre) by a region, at approximately 8Åwhere almost no cyclohexane molecules are to be found throughout the duration of the simulation (the relative density plot is an average plot measured over the whole post-equilibration simulation). Closer to the centre of the pore, below the trough at 8Å, there appears to be no discernible structure to the cyclohexane density. This is probably due to the small number of cyclohexane molecules that have adsorbed - there are not sufficient molecules to impose restrictions (based on the adsorbate-adsorbate interaction) on where other cyclohexane molecules are located. The relative density plot of hexane (top of Figure 6.12) is similar to the pure hexane relative density plot shown in Figure 6.7. This is not surprising since there is very little cyclohexane in the adsorbed mixture and so the effect that it can have on the position of the hexane molecules is limited. Once again, three regions of high density are visible in the hexane relative density plot.

In Figure 6.13 the equimolar binary mixture adsorption isotherm for 2-methylpentane and cyclohexane in MCM-41 at 300K is shown. The cyclic molecule adsorbs in limited amounts, with the mixture adsorption being dominated by the branched molecule. The total maximum loading does not exceed 5 mmol/g, as is the case for the other mixture adsorption isotherms. The relative density graphs for 2-methylpentane and cyclohexane are shown in Figure 6.14 and show that both 2-methylpentane and cyclohexane have 3 regions of high density, separated by regions of low density. The 2-methylpentane graph (top of Figure 6.14) is dominated by two large peaks centred at 10Å and 5.5Å respectively. These peaks are similar in both their size and position to those seen in the single component relative density graph, indicating that 2-methylpentane is not greatly affected by the presence of the small amount of cyclohexane in

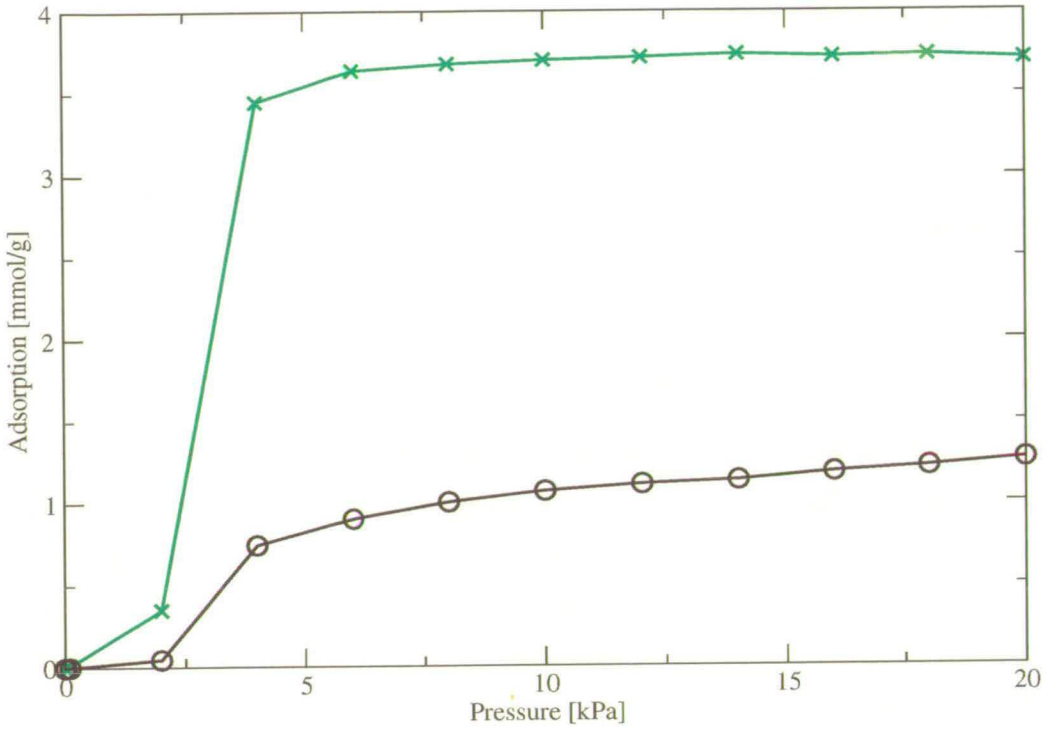

Figure 6.13: The adsorption isotherms for an equimolar binary mixture of 2-methylpentane (green) and cyclohexane (black) in MCM-41 at 300K.

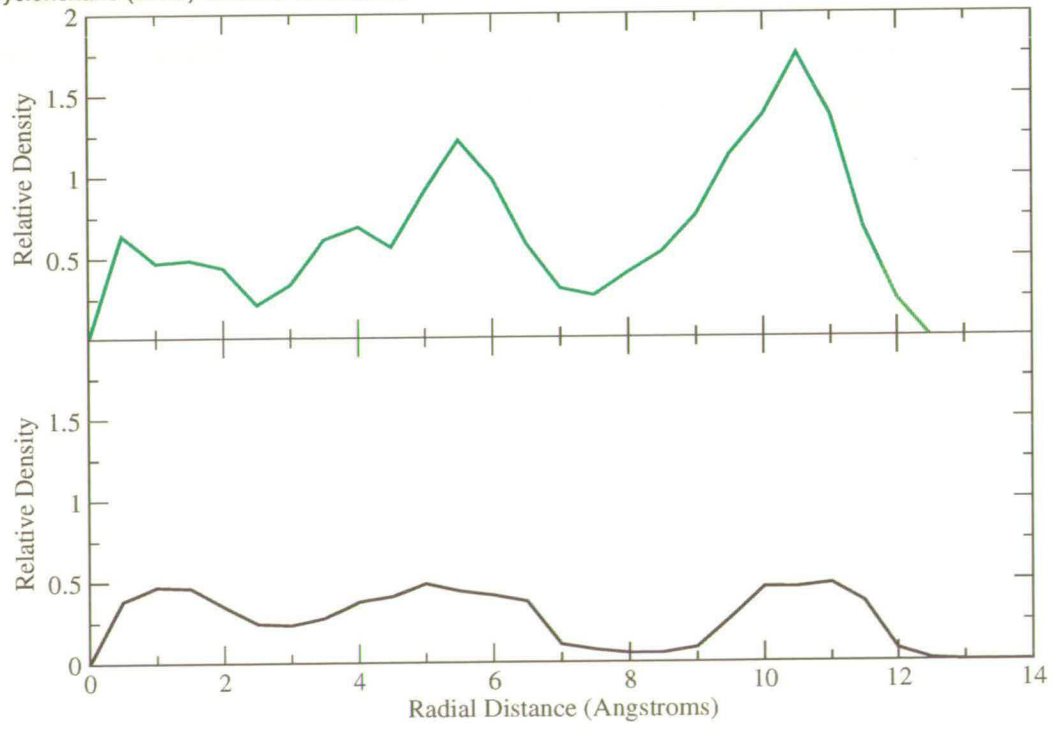

Figure 6.14: The relative density from the centre of the pore of 2-methylpentane (top) and cyclohexane (bottom) in a equimolar binary mixture in MCM-41 at 300K.

the adsorbed mixture. Despite only adsorbing in relatively small quantities, cyclohexane has a clearly visible structure to its relative density profile. There is a peak close to the pore surface (centred at around 11Å) separated from the remainder of the molecules by a region containing almost no cyclohexane molecules (between 9Å and 7Å). there are two peaks towards the centre of the channel (at 5Å and 1Å) although these are separated by only a slight dip in relative density and are not easily separable. It is interesting that, despite being present in only very small quantities, cyclohexane still manages to exhibit distinct structure and there are regions where almost no molecules are to be found (around 8Å).

The equimolar ternary mixture of hexane, 2-methylpentane and cyclohexane in MCM-41 at 300K is shown in Figure 6.15. The order of adsorption appears to follow that of the binary mixtures: hexane adsorbs in greatest numbers, closely followed by 2-methylpentane and finally, with much fewer molecules adsorbing, cyclohexane. Based on the heats of adsorption, this would be the predicted order of adsorption. However, based on the maximum loadings of the single components, the order would be: cyclohexane followed by hexane and finally, 2-methylpentane. This indicates that despite the fact that more cyclohexane than 2-methylpentane or hexane is able to adsorb within the pore, it is the interaction between the pore and the adsorbate which determines which molecule is adsorbed from a mixture of several different species. The structure of the adsorbed molecules, shown in Figure 6.16, reveals that all three molecules maintain their structure, even when adsorbed as part of a mixture. All three molecules have three regions of high density separated by regions of low density. Both 2-methylpentane and cyclohexane relative density plots have regions where almost no molecules are to be found - at 8Å and (for cyclohexane) between 2Å and 4Å. The structure of the relative density plots for the molecules in the mixture do not differ greatly from those of the pure component plots, shown in Figure 6.7.

All of the relative density plots for binary and ternary mixtures within the mesopore have shown that each component has a significant amount of structure, brought about by the adsorption onto the surface and the subsequent layers of adsorption made by the molecules further form the pore surface. However, none of the mixtures exhibit any structure that indicates that they are not ideal. If the mixture was not ideal, it would be reasonable to expect that the relative density plots of each component in the mixture would have a different structure to those of the

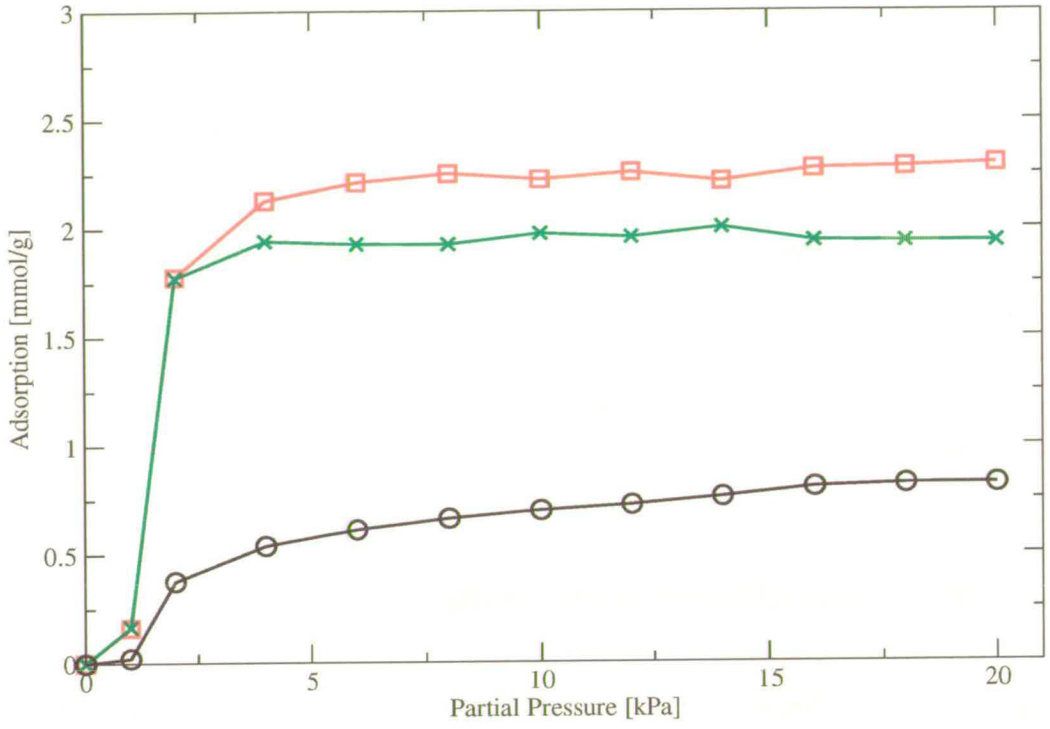

Figure 6.15: The adsorption isotherms for an equimolar ternary mixture of hexane (red) 2-methylpentane (green) and cyclohexane (black) in MCM-41 at 300K.

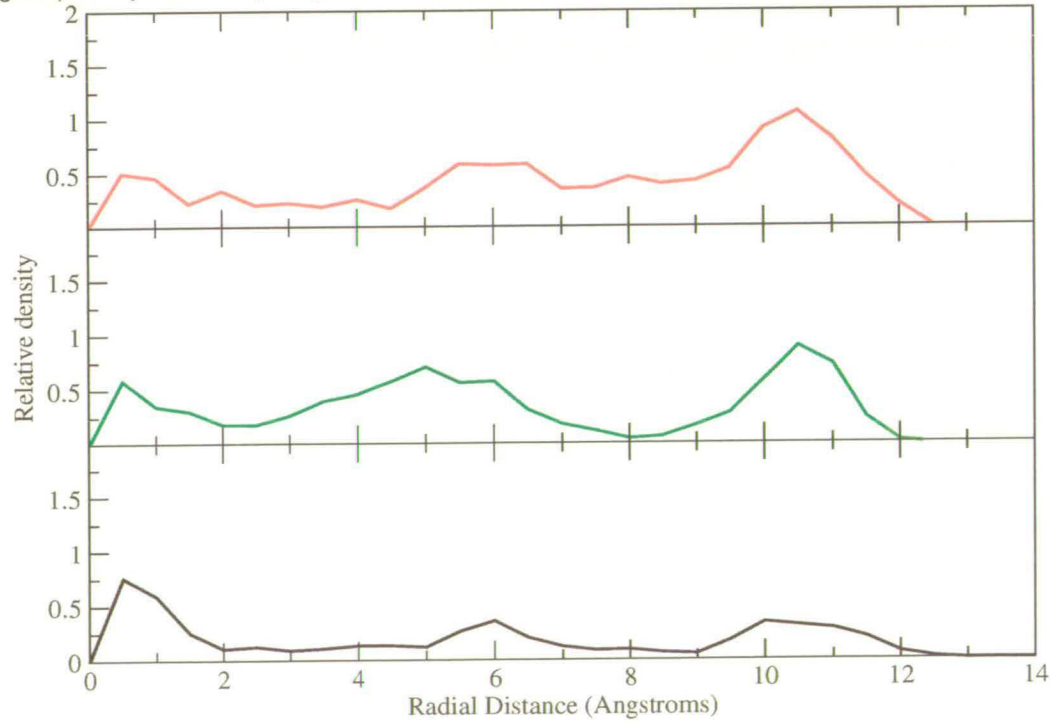

Figure 6.16: The relative density from the centre of the pore of hexane (top), 2-methylpentane (middle) and cyclohexane (bottom) in a equimolar ternary mixture in MCM-41 at 300K.

pure components within the pore. This is not the case: all of the mixture relative density plots are similar in shape (i.e. the location of the peaks and toughs) to those of the pure components. This indicates that the adsorbed mixtures are indeed approximately ideal and do not exhibit any regions where only one species is excluded.

This section has covered the adsorption of mixtures of the three molecules within the pores of MCM-41 and has analysed the structure of the adsorbed phase. There has been no comparison with experiment since no experimental data could be found. The next section discussed possible refinements to the model of MCM-41 and any affect that such refinements would be expected to have.

6.6 Possible refinements to model

Whilst the model of MCM-41 presented in Section 6.2 provides adsorption data which compares favourably with the available experimental data, it does not incorporate some of the more subtle features of MCM-41. These features, along with ways in which they may be included in a revised computational model, are discussed in the following sections.

6.6.1 Non-crystalline model

Whilst the precise location of the atoms which comprise MCM-41 are not experimentally known, it is true that the structure is *not* crystalline and so the present computational model of MCM-41 is deficient in this aspect. However, the crystalline model does work well and is an important step in the ongoing study of MCM-41. One way of adding heterogeneity to the model of MCM-41 is to randomly displace the atoms by some small amount with the result that the surface of MCM-41 becomes roughened. This technique has been used by others [122] to incorporate surface roughness. The roughness of the surface of MCM-41 been shown [124] to affect the adsorption of small adsorbates, such as ethane and carbon dioxide. However, the effect that surface roughness has on the adsorption of larger molecules, such as those used in this work, has not previously been studied.

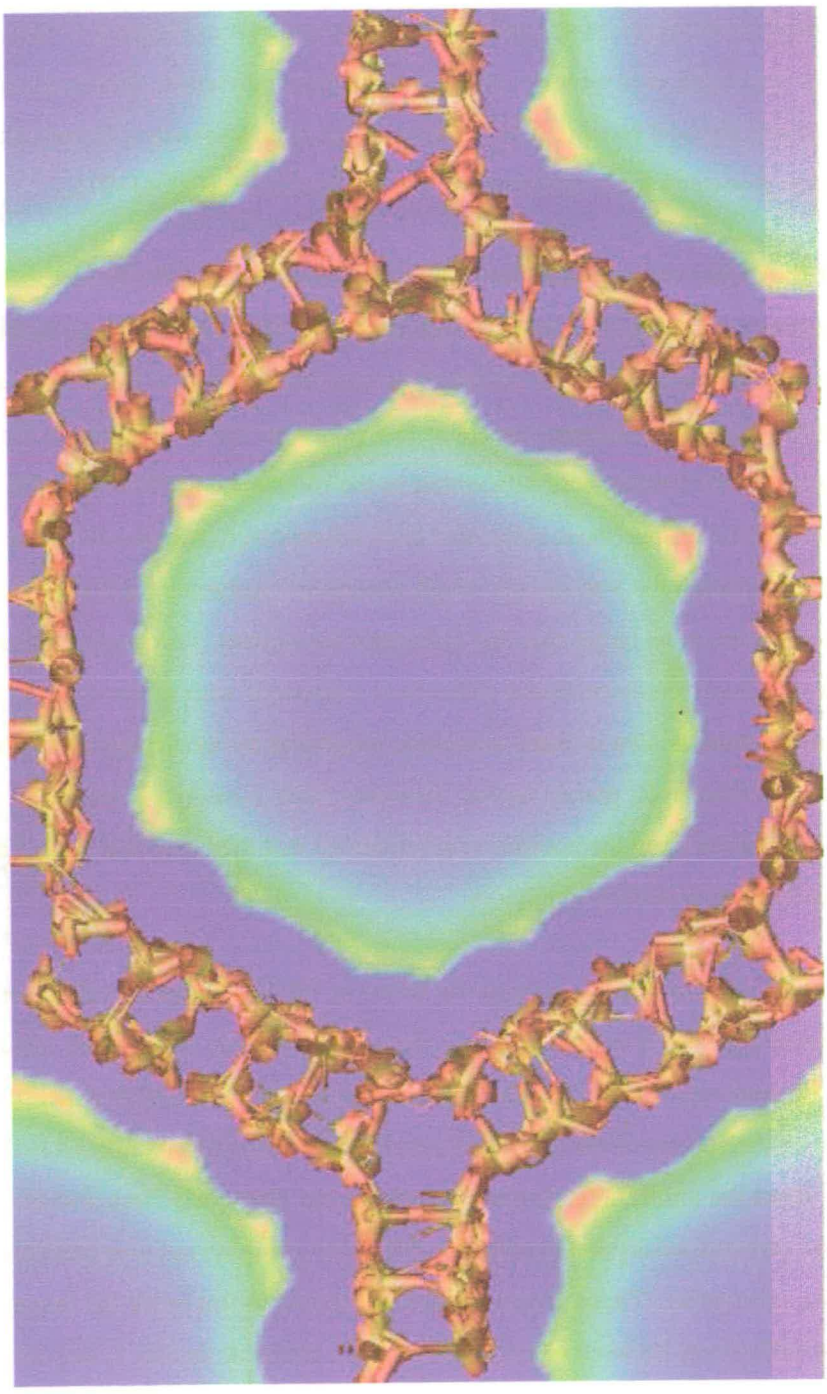

Figure 6.17: The roughened model of MCM-41 (made by randomly displacing the atoms by up to 1Å) together with a slice through the adsorbate-mesopore potential energy isosurface for the roughened model of MCM-41. Red areas indicate regions of strongest adsorbate-mesopore attraction, through orange, yellow, green and light blue which indicates regions of weakest attraction. Dark blue areas indicate adsorbate-mesopore repulsion.

The roughened model of MCM-41 used in this study is shown in Figure 6.17 and was formed by randomly displacing each atom by up to 1Å in a random direction. Whilst this method does not represent any physical process of roughening, it has been shown to give very similar results to a relaxation procedure for roughening such as Molecular Dynamics [197].

Figure 6.18 shows the comparison between the adsorption isotherms for hexane, 2-methylpentane and cyclohexane in both the smooth and rough models of MCM-41. All three isotherms of adsorption in the roughened MCM-41 model show very little deviation from the corresponding smooth MCM-41 model isotherms, except at low pressure. At low pressures, the roughened isotherms (that is, the isotherms of adsorption in the roughened MCM-41 model) lie slightly below the smooth isotherms (those calculated from adsorption in the smooth MCM-41 model). The difference between the smooth and rough adsorption isotherms for 2-methylpentane and cyclohexane appears to be larger than the difference for hexane. This could be due to the fact that hexane has fewer conformational restrictions compared with either 2-methylpentane or cyclohexane. Hexane is able to react to surface roughness by modifying its structure, by altering the angle between its pseudo atoms. However, both 2-methylpentane and cyclohexane have more restrictions upon the possible conformations that they may take, thus limiting their ability to easily react to surface roughness.

The fact that the random displacement of the atoms in MCM-41 does not affect the high pressure adsorption capacity is not surprising - the overall volume of the pore remains almost unchanged by randomly moving the atoms by a small amount in a random direction. However, at low pressure the volume of the pore does not play such an important role - it is the topology which will affect the adsorption. Surface roughness has previously been shown to (slightly) affect the low pressure adsorption of ethane in MCM-41 [124] but not to appreciably affect the high pressure adsorption. These characteristics are shown in this work for larger molecules, although the differences between adsorption in the two different models is very small. Surface roughness can affect the low pressure adsorption by creating areas on the internal surface of the pore which have different adsorption characteristics to those of the smooth pore surface. Such differences arise due to the energetically different landscape caused by the movement of the surface atoms.

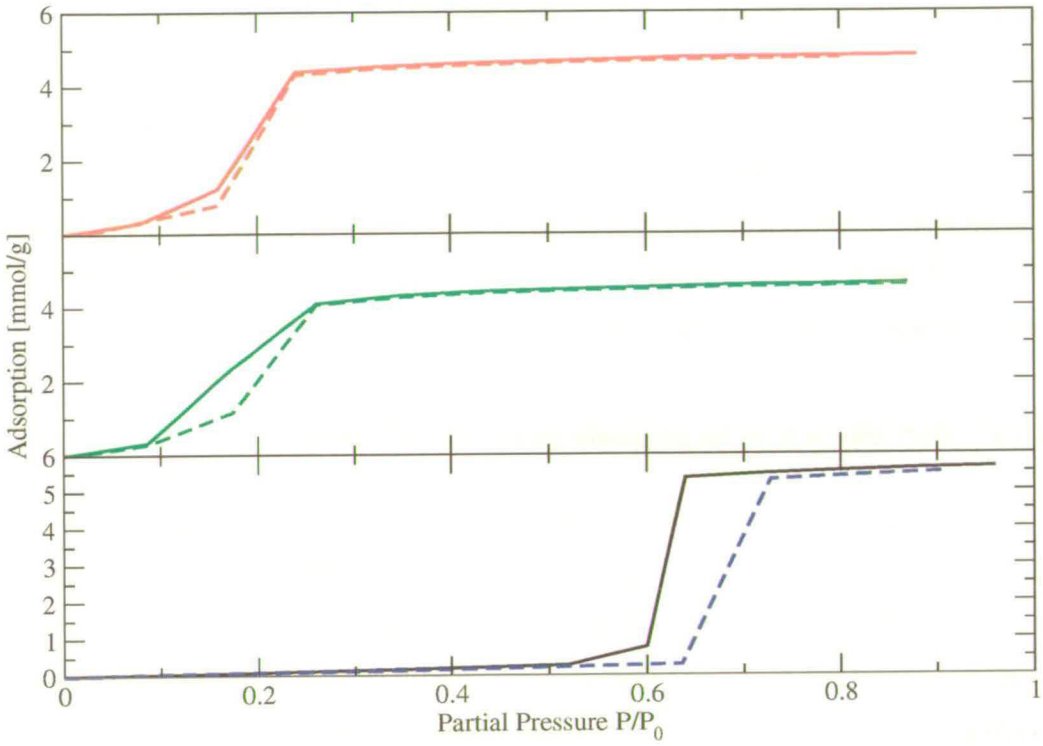

Figure 6.18: The adsorption isotherms in the smooth and roughened (dashed lines) MCM-41 model. From top to bottom: hexane, 2-methylpentane and cyclohexane.

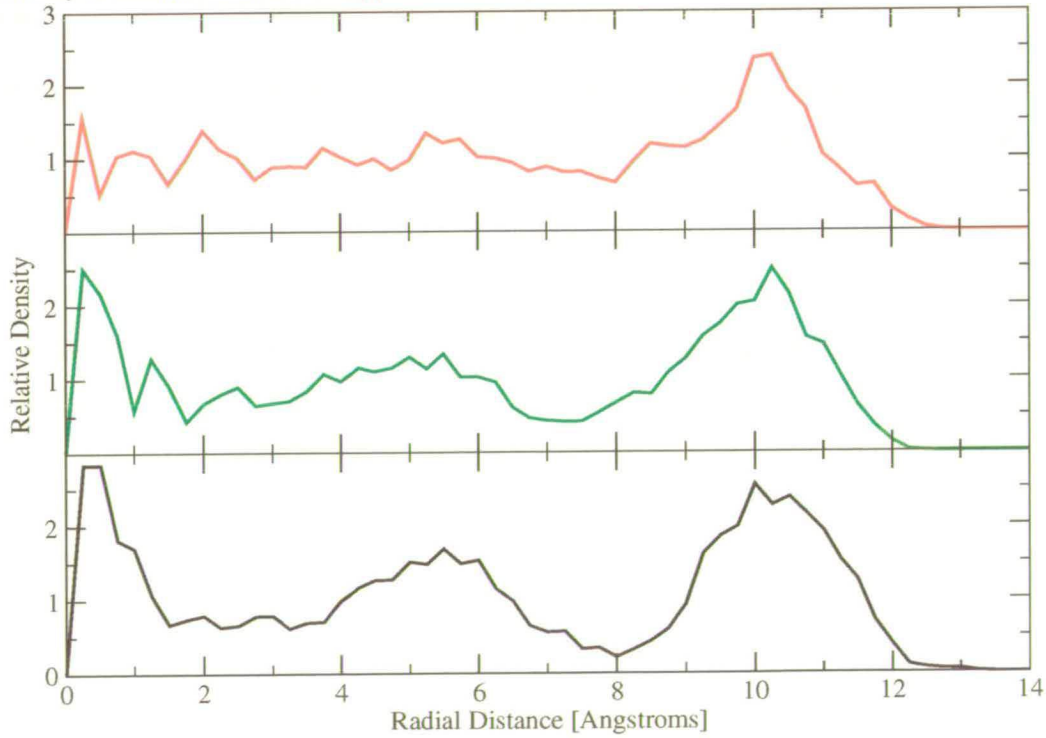

Figure 6.19: The relative density plots of (from top to bottom) hexane, 2-methylpentane and cyclohexane in the roughened model of MCM-41 at 20kPa.

The relative density plots of hexane, 2-methylpentane and cyclohexane at 20kPa in the roughened MCM-41 model are shown in Figure 6.19 and reveal that, despite the surface of MCM-41 being roughened, the relative density profiles are very similar to those of the molecules within the smooth model of MCM-41. It would be reasonable to expect the effect that surface roughness has on molecules near the centre of the pore (far from the walls) would be small. However, based on Figure 6.19 the roughness of the wall does not appreciably affect the structure of the adsorbed (large) molecules at high pressure, even close to the wall.

6.6.2 Hydroxyls and large scale pore restrictions

Both the smooth and rough model of MCM-41 are composed of only silicon and oxygen atoms. However, it is known that MCM-41 contains hydroxyl groups (OH), both on the internal surface and in the bulk. These hydrogen atoms compensate for the charge imbalance when a silicon atom is bound to 3 or fewer silanol (OSi) groups (instead of the usual 4, as part of the tetrahedral building block). The ratio of silicon, oxygen and charge compensating hydrogen atoms can be classified using the following formula,

$$\mathrm{Si(OSi)_nOH_{(4-n)}} \tag{6.1}$$

where n is 1, 2, 3 or 4. Experimental studies have put the number of hydroxyl groups present in MCM-41 between 2 and 8 per nm^2 [122, 198]. The hydrogen atoms may cause MCM-41 to exhibit different adsorption properties due to both the topological and compositional changes. Previous simulations have used different models, both including [122, 125] and ignoring [120, 121, 123, 124, 126, 128] the contribution from the surface hydrogen atoms. Both types of model have been shown to predict the adsorption properties of MCM-41 with good agreement with experimental data, although none of the simulations used adsorbates which were larger than ethane. It would be interesting to determine if the presence of surface hydrogen atoms affects the adsorption of larger molecules. He *et al.* [124] find that small topological changes affect the adsorption of ethane at low pressure, particularly the structure of the adsorbed molecules whilst Coasne *et al.* [122] find that surface corrugation such as surface hydrogen atoms, does not significantly affect the adsorption of argon in MCM-41. They found that it took much larger scale structural changes (such as restriction to the pore on the 10Å scale) to affect the

adsorption of argon. This suggests that the adsorption of larger molecules such as hexane, 2-methylpentane and cyclohexane would only be affected by large scale pore topology changes.

Larger scale pore restrictions can be realised by reducing the pore diameter at some point in the pore producing an approximate hourglass shape. However, such restrictions are difficult to implement since there is no physical basis for redesigning the pore and so any pore restriction is man-made and may not be indicative of the true restrictions within MCM-41. It may be possible to include large scale pore restrictions using a model which is constructed from first principles, whereby the *experimental* procedure for producing MCM-41 is repeated *computationally* to produce a model for MCM-41 which, if the simulations are performed correctly, should both resemble the experimental product, as well as sharing its adsorption properties. Such models are currently being investigated by the group of Prof. Seaton at Edinburgh University.

6.7 Conclusions

This chapter has introduced a new computational model for the mesopore MCM-41. Using this model, simulations of the adsorption of hexane, 2-methylpentane and cyclohexane, along with mixtures of these molecules, were carried out. The single component adsorption of hexane was in excellent agreement with the experimental data from a pore of almost identical size. There was no experimental data available to compare with the simulated adsorption of 2-methylpentane - although the shape of the isotherm and the maximum loading were similar to that of hexane, indicating that the 2-methylpentane isotherm was, at least, realistic. Experimental data was found for the adsorption isotherm of cyclohexane in MCM-41 with much larger pores than the computational model (experimental pores size was 40Å whilst simulation model pores size was 29Å). However, a comparison between the simulated and experimental adsorption isotherms revealed that fewer molecules were able to adsorb in the simulation model compared with the experiments - which is a reasonable prediction. The shape of the isotherms were similar, although the simulated isotherm indicated that it took higher pressures to fill the pore compared with the experimental study of the larger pore. The high pressure loading of cyclohexane was found to be more than either hexane or 2-methylpentane.

The heats of adsorption were found to be 40.2kJ/mol for hexane, 32.4kJ/mol for 2-methylpentane and 21.5kJ/mol for cyclohexane. The value for hexane was very close to that of the experimental data (39, 38.1 and 37kJ/mol) whilst no data could be found for 2-methylpentane or cyclohexane.

An analysis of the structure of the adsorbed phase of each species was made by examining the relative radial density from the centre of the pore to the pore surface. The relative density plots of all three species revealed ring-like structures within the pore. This comprised three regions of high density separated by regions of low density - in the case of cyclohexane the low density regions were much lower than those of hexane and 2-methylpentane. This may be explained by examining the structure of the three species. Both hexane and 2-methylpentane are long, thin molecules whilst cyclohexane is relatively short and fat - the molecule is more like a spherical particle than either hexane or 2-methylpentane. Spherical particles have been shown [190–196] to exhibit a high degree of structure when adsorbed within large pores and therefore it is reasonable to expect that the more spherical molecule (cyclohexane) will have more structure compared with the less spherical molecules (hexane and 2-methylpentane). An analysis of the adsorbed structure at high pressure did not reveal any deviations from these findings - the structure of all three species remained.

The adsorption binary mixtures of the three species revealed some interesting properties. The adsorption isotherms were dominated by the heats of adsorption - hexane always adsorbed in greater quantities, regardless of the other mixture component, whilst cyclohexane always adsorbed in least number, regardless of the other mixture component. However, the relative density plots of the adsorbed mixture revealed that all of the adsorbed molecules exhibited similar structures to those seen in the pure component adsorption. Even when one species adsorbed in relatively small quantities (such as cyclohexane in the cyclohexane and hexane mixture) the relative density plots showed a high degree of structure. Furthermore, in the case of cyclohexane in mixture with 2-methylpentane, there were regions in the pore where almost no cyclohexane would be found throughout the entire simulation. This structure arose even though there were relatively few cyclohexane molecules in the pore which was filled with many more 2-methylpentane molecules than cyclohexane molecules. The distinct structure of the molecules was also seen in the ternary mixture adsorption - which was dominated by

hexane and 2-methylpentane with much less cyclohexane adsorbing. For the case of ternary mixture adsorption, all three of the relative density plots revealed three distinct regions of high density, separated by regions of very low density.

A roughened model was introduced in an effort to capture some of the non-crystalline features of MCM-41. The model affected the low pressure adsorption of each of the three species whilst leaving the high pressure adsorption unchanged. This could be explained by the surface roughness causing local fluctuations in the adsorbate-mesopore surface which would affect the adsorption at low pressure. However, at high pressure, these local atomic corrugations did not affect the adsorption because they were softened by a layer of adsorbed molecules which would reside between the pore surface and the remaining adsorbing molecules. The relative density plots of the molecules adsorbed in the roughened pore indicate the surface heterogeneity does not appreciably affect the structure of the adsorbed phase, which is unchanged from the structure in the smooth model.

A model was proposed for the inclusion of surface hydrogen atoms within MCM-41- these are known to exist to compensate for the charge imbalance which arises when an oxygen atom is bonded to a silicon which only has three oxygens bonded to it. It was though that the inclusion of surface hydrogen atoms would not greatly affect the adsorption of large molecules (such as hexane, 2-methylpentane and cyclohexane) since the inclusion of surface hydrogen atoms would only alter the structure of MCM-41 on a small scale (relative to the size of the adsorbing molecules).

Possible further refinements to the model could include larger pore restrictions, such as a change in the local pore diameter, creating an hourglass shape. Such constrictions may affect the adsorption of larger molecules but their inclusion is not based on any physical process - it is simply a 'man-made' obstacle within the model of MCM-41. An improvement to this technique would be to model the procedure used to experimentally form MCM-41- such simulations are currently in use at Edinburgh University.

This chapter has shown that it is possible to use the potentials for the interaction between hydrocarbons and *zeolites* to model the interaction between the hydrocarbons and a *mesopore*. The order of magnitude increase in the size of the pores allows many more molecules to adsorb,

Chapter 7

Conclusions and future work

In this thesis the adsorption of mixtures of linear, branched and cyclic hydrocarbon molecules within zeolites and mesopores has been investigated using Monte Carlo simulations. The fluid properties of the hydrocarbons were simulated and compared with experimental data to ensure that the simulation model was correct. Adsorption isotherms of each of the molecules in the porous materials were calculated and were found to agree well with the available experimental data. To further probe the interaction between the molecules and the porous materials, the microscopic level of detail available from the simulations was used to build up a picture of the strength of the interaction between the molecules and the zeolites/mesopore. The adsorbate-porous material potential energy was calculated at points within the porous network to build up an energetic landscape that the molecules would 'see' as they moved through the pores. This was useful to get an approximate idea of where in the zeolite/mesopore each molecule was most likely to be found.

The level of complexity was increased by investigating the adsorption of mixtures of different molecules. In the zeolites, relatively few molecules adsorbed compared with the mesopores where the pore filled with many hundreds of molecules. Within the pores of the zeolites the shape of the molecule was important when determining which component of a mixture would adsorb in the greatest quantity. The temperature was found to play an important role: an increase in temperature was seen to reverse the selectivity of some of the zeolites for some of the mixtures. Ideal Adsorption Solution Theory was used to predict the mixture adsorption

isotherms in the zeolites, based on the single component adsorption isotherms, and these were found to agree well with the simulated isotherms.

A new model for the mesopore was proposed and found to predict adsorption isotherms which agreed well with the limited experimental data. The adsorbed molecules within the mesopore were analysed and found to exhibit structure comprising layers of high density separated by regions of lower density. This structure persisted even when the molecules were adsorbed sparingly as part of a mixture. The mesopore model was modified to include surface roughness by randomly moving the atoms by a small amount. The surface roughness was not found to appreciably affect the high pressure adsorption and only slightly altered the low pressure adsorption.

This work has shown that computer simulations can play an important role in investigating the properties of linear, branched and cyclic molecules in porous materials. Using one set of forcefield parameters, four different porous materials have been studied, including a new model for the structure of the mesopore and a zeolite which has only recently been synthesised and is yet to be the subject of an experimental study.

7.1 Future work

Whilst this work makes a significant contribution, by performing simulations of mixtures which include cyclic molecules and by introducing a model of the mesopore which is used to study the adsorption of larger molecules, it is only a small step in the much larger field of computer simulations of porous materials. Future work in this field would include the following:

- incorporating flexibility into the model of the zeolites and mesopore - this would allow for a more realistic simulation of the porous materials but would greatly increase the length of time of the simulation.
- modifying the model of the mesopore to include hydrogen atoms, which are known to exist in the structure of the pore, to determine if these make an appreciable difference to the adsorption of hydrocarbons.

- including acid sites: industrial uses of porous materials include catalysis - which relies on the porous material having acid sites within its structure. It would be interesting to incorporate such acid sites into the model of the porous structures to determine the behaviour of molecules which will interact with these acid sites.

Finally, to attempt to come closer to the simulation of a real industrial process, such as the catalytic cracking of hydrocarbons, the length scale of the simulations together with the number of components which make up the mixture being studied could be increased. However, this would involve bringing together different simulations techniques since it would be necessary to use quantum mechanical simulations to model the chemical interaction between the adsorbed molecules and the porous structure, whilst using classical techniques to simulate the movement and preferred adsorption locations of the molecules.

Appendix A

Properties of MCM-41

In this appendix, a comparison is made between the experimental physical properties of MCM-41 and the same properties measured from the simulation model.

Table A.1 compares the experimental and simulation model values of pore size, pore surface area and pore volume density of MCM-41. The table lists the experimental data in order of increasing pore diameter. The experimental values for both the surface area and the pore volume density vary greatly, even for pores with the same diameter. The values calculated from the simulation model are in reasonable agreement with the experimental values for pores of a similar size.

Table A.1: Structural properties of MCM-41: a comparison between experiment and the simulation model. The experimental data is found by using the BJH method [187] for the pore size and the pore volume density whilst the BET method [199] is used to determine the surface area.

Reference	Pore Size (Å)	Pore Surface Area (m^2/g)	Pore Volume Density (cm^3/g)
[124]	26.96	1013.7	–
[131]	28	1000	0.73
[127]	29	755.0	0.34
[200]	29	1180	–
[201]	29.2	1072	0.658
[135]	29.5	985	0.815
[130]	30	900	1.12
[132]	30.41	1151	0.6736
[188]	31	965	0.73
[126]	31.43	1195.93	0.921
[133]	32.3	1066	0.87
[134]	32.7	963	0.45
[7]	34	1340	1.01
[136]	34.8	875	0.916
[6]	36.5	1087	0.85
[6]	39	1157	0.98
[136]	39.2	1139	1.33
[189]	40.0	970	–
[2]	$\approx$40	$\geq$1000	0.79
[123]	40.9	1023	0.92
This Work	29	1167	0.845

Appendix B

Publications

- J. P. Fox, V. Rooy, and S. P. Bates. Simulating the adsorption of linear, branched and cyclic alkanes in silicalite-1 and $AlPO_4$-5. *Microporous Mesoporous Mater.*, 69(1-2):9–18, 2004.
- J. P. Fox and S. P. Bates. Simulating the adsorption of binary and ternary mixtures of linear, branched and cyclic alkanes in zeolites. *J. Phys. Chem. B.* 108: 17136–17142, 2004.
- J. P. Fox and S. P. Bates. The adsorption and structure of hydrocarbons in MCM-41: a computational study. *Langmuir Submitted.*, 2004.
- L. Dougan, S. P. Bates, R. Hargreaves, J. P. Fox, J. Crain, J. L. Finney, V. Réat, and A. K. Soper. Methanol-water solutions: A bi-percolating liquid mixture. *J. Chem. Phys*, 121:6456–6462, 2004.
- S. K. Allison, J. P. Fox, R. Hargreaves, and S. P. Bates. Clustering and Micro-immiscibility in Alcohol-Water Mixtures: Evidence from Molecular Dynamics Simulations. *Phys. Rev. B Submitted.*, 2004.

List of Figures

List of Tables

Bibliography

[1] http://winnie.chem-eng.northwestern.edu/~todd/.

[2] C. T. Kresge, M. E. Leonowicz, W. J. Roth, J. C. Vartuli, and J. S. Beck. Ordered mesoporous molecular sieves synthesized by a liquid-crystal template mechanism. *Nature*, 359:710–712, 1992.

[3] http://www.criontheweb.com/zeolite.htm.

[4] http://www.coolsystem.de/.

[5] M. Vallet-Regí, A. Rámila, R.P del Real, and J. Pérez-Pariente. A new property of MCM-41: Drug delivery system. *Chem. Mater.*, 13:308, 2001.

[6] P. Horcajada, A. Rámila, J. Pérez-Pariente, and M. Vallet-Regí. Influence of pore size of MCM-41 matrices on drug delivery rate. *Microporous Mesoporous Mater.*, 68:105–109, 2004.

[7] A. Sayari. Catalysis by crystalline mesoporous molecular sieves. *Chem. Mater.*, 8:1840–1852, 1996.

[8] W. Xu, Q. Luo, H. Wang, L. C. Francesconi, R. E. Stark, and D. L. Akins. Polyoxoanion occluded within modified MCM-41: Spectroscopy and structure. *J. Phys. Chem. B*, 107:497–501, 2003.

[9] V. R. Choudhary and K. Mantri. Adsorption of aromatic hydrocarbons on highly siliceous MCM-41. *Langmuir*, 16:7031–7037, 2000.

[10] W. Chae, I. Hwang, J. Jung, and Y. Kim. Optical and magnetic properties induced by structural confinement of ternary chalcogenide in AlMCM-41 nanotube. *Chem. Phys. Lett.*, 341:279–284, 2001.

[11] E. R. Cooper, C. D. Andrews, P. S. Wheatley, P. B. Webb, P. Wormald, and R. E. Morris. Ionic liquids and euctectic mixtures as solvent and template in synthesis of zeolite analogues. *Nature*, 430:1012–1016, 2004.

[12] http://www.umich.edu/~becklab/research.html/.

[13] The octane number of fuel is a measure of its performance. A high octane number corresponds to a fuel which is resistant to pre-ignition - this is where the fuel ignites when it is compressed, before it is ignited by the spark plug, resulting in a reduction in performance. Higher octane numbers are achieved by increasing the fraction of branched molecules in the fuel. The term *octane* comes from 2,2,4,tri-methylpentane, also called iso-octane, which has an octane rating of 100 (by definition).

[14] B. Smit. Phase diagrams of Lennard-Jones fluids. *J. Chem. Phys.*, 96:8639–8640, 1992.

[15] B. Smit, S. Karaborni, and J I. Siepmann. Computer simulations of vapour-liquid phase equilibria of *n*-alkanes. *J. Chem. Phys.*, 102(5):2126–2140, 1995.

[16] J. J. Potoff and A. Z. Panagiotopoulos. Critical point and phase behaviour of the pure fluid and a Lennard-Jones mixuture. *J. Chem. Phys.*, 109(24):10914–10920, 1999.

[17] J. I. Siepmann, S. Karaborni, and B. Smit. Simulating the critical behaviour of complex fluids. *Nature*, 365:330–332, 1993.

[18] A. L. Rodriguez, C. Vega, J. J. Freire, and S. Lago. Improved results for the potential parameters of methyl and methylene obtained from second virial coefficients of *n*-alkanes. *Mol. Phys.*, 80(6):1565–1567, 1993.

[19] B. Neubauer, A. Boutin, B. Tavitian, and A. H. Fuchs. Gibbs ensemble simulations of vapour-liquid phase equilibria of cyclic alkanes. *Mol. Phys.*, 97(6):769–776, 1999.

[20] A. L. Rodriguez, C. Vega, J. J. Freire, and S. Lago. Potential parameters of methyl and methylene obtained from second virial coefficients of *n*-alkanes. *Mol. Phys.*, 73(3):691–701, 1991.

[21] C. D. Wick, M. G. Martin, and J. I. Siepmann. Transferable potentials for phase equilibria. 4. united atom description of linear and branched alkanes and alkylbenzenes. *J. Phys. Chem. B*, 107:8008–8016, 2000.

[22] M. D. Foster, A. Simperler, R. G. Bell, O. D. Friedrichs, F. A. A. Paz, and J. Klinowski. Chemically feasible hypothetical crystalline networks. *Nature Materials*, 3:234–238, 2004.

[23] M. D. Foster, O. D. Friedrichs, R. G. Bell, F. A. A. Paz, and J. Klinowski. Chemical evaluation of hypothetical uninodal Zeolites. *J. Am. Chem. Soc.*, 126:9769–9775, 2003.

[24] A. Simperler, M. D. Foster, R. G. Bell, and J. Klinowski. Hypothetical Uninodal Zeolite Structures: Comparison of $AlPO_4$ and SiO_2 Compositions Using Computer Simulation. *J. Phys. Chem. B*, 108:869–879, 2004.

[25] J. R. Errington and A. Z. Panagiotopoulos. A new intermolecular potential model for the *n*-alkane homologous series. *J. Phys. Chem. B*, 103:6314–6322, 1999.

[26] W. L. Jorgensen, J. D. Madura, and C. J. Swenson. Optimized intermolecular potential functions for liquid hydrocarbons. *J. Am. Chem. Soc.*, 106:6638–6646, 1984.

[27] M. G. Martin and J. I. Siepmann. Transferable potentials for phase equilibria. 1. United atom description of *n*-alkanes. *J. Phys. Chem. B*, 102:2569–2577, 1998.

[28] S. K. Nath, F. A. Escobedo, and J. J. de Pablo. On the simulation of vapour-liquid equilibria for alkanes. *J Chem. Phys.*, 108(23):9905–9911, 1998.

[29] P. Ungerer, C. Beauvais, J. Delhommelle, A. Boutin, B. Rousseau, and A. H. Fuchs. Optimisation of the anisotropic united atoms intermolecular potential for n-alkanes. *J. Chem. Phys.*, 112(12):5499–5510, 2000.

[30] A. K. Rappé and W. A. Goddard III. Charge equilibrium for molecular dynamics simulations. *J. Phys. Chem.*, 95:3358–3363, 1991.

[31] J. I. Siepmann, M. G. Martin, C. J. Mundy, and M. L. Klein. Intermolecular potentials for branched alkanes and the vapour-liquid phase equilibria of *n*-heptane, 2-methylhexane, and 3-ethylpentane. *Mol. Phys.*, 90(5):687–693, 1997.

[32] M. G. Martin and J. I. Siepmann. Novel Configurational-Bias Monte Carlo method for branched molecules. Transferable potentials for phase equilibria. 2. United atom description of branched alkanes. *J. Phys. Chem. B*, 103:4508–4517, 1999.

[33] S. K. Nath and J. J. de Pablo. Simulation of vapour-liquid equilibria for branched alkanes. *Mol. Phys.*, 98(4):231–238, 2000.

[34] E. Bourasseau, P. Ungereer, and A. Boutin. Prediction of equilibrium properties of cyclic alkanes by Monte Carlo simulation - new anisotropic united atoms intermolecular potential- new transfer bias method. *J. Phys. Chem. B*, 106:5483–5491, 2002.

[35] S. Chempath, L. A. Clark, and R. Q. Snurr. Two general methods for grand canonical ensemble simulation of molecules with internal flexibility. *J. Chem. Phys.*, 118(16):7635–7643, 2003.

[36] Z. Chen and F. A. Escobedo. A Configurational-Bias approach for the simulation of inner sections of linear and cyclic molecules. *J. Chem. Phys.*, 113(24):11382–11392, 2000.

[37] J. R. Errington and A. Z. Panagiotopoulos. New intermolecular potential models for benzene and cyclohexane. *J. Chem. Phys.*, 111(21):9731–9738, 1999.

[38] R. L. Hilderbrandt, J. D. Wieser, and L. K. Montgomery. The conformations and structures of cyclodecane as determined by electron diffraction and molecular mechanics calculations. *J. Am. Chem. Soc.*, 95:8598–8605, 1973.

[39] C. Lee. Energetics of cyclohexane isomers: A density functional study. *J. Korean Chem. Soc.*, 35(4):370–373, 1999.

[40] C. D. Wick and J. I. Siepmann. Self-Adapting Fixed-End-point Configurational-Bias Monte Carlo method for the regrowth of interior segments of chain molecules with strong intramolecular interactions. *MacroMol.*, 33:7207–7218, 2000.

[41] B. Smit. Grand Canonical Monte Carlo simulations of chain molecules: adsorption isotherms of alkanes in zeolites. *Mol. Phys.*, 85(1):153–172, 1995.

[42] S. P. Bates, W. J. M. van Well, R. A. van Santen, and B. Smit. Location and conformation of *n*-alkanes in zeolites: An analysis of Configurational Bias Monte Carlo calculations. *J. Phys. Chem.*, 100:17573–17581, 1996.

[43] S. P. Bates, W. J. M. van Well, R. A. van Santen, and B. Smit. Energetics of *n*-alkanes in zeolites: A Configurational Bias Monte Carlo investigation into pore size dependence. *J. Am. Chem. Soc.*, 118:6753–6759, 1996.

[44] P. Demontis, G. B. Suffritti, S. Quartieri, E. S. Fois, and A. Gamba. Molecular Dynamics studies of Zeolites. 3. Dehydrated Zeolite A. *J. Phys. Chem.*, 92:867–871, 1998.

[45] P. Demontis and G. B. Suffritti. Structure and dynamics of Zeolites investigated by Molecular Dynamics. *Chem. Rev.*, 97:2845–2878, 1997.

[46] P. Demontis, G. B. Suffritti, S. Bordiga, and R. Buzzoni. Atom pair potential for Molecular Dynamics simulations of structural and dynamical properties of Aluminosilicates: Test on Silicalite and Anhydrous Na-A and Ca-A Zeolites and comparison with experimental data. *J. Chem. Soc. Faraday Trans.*, 95(3):525–533, 1995.

[47] J. D. Gale. Analytical free energy minimisation of silica ploymorphs. *J. Phys. Chem. B*, 102:5423–5431, 1998.

[48] G. J. Kramer and R. A. van Santen. Theoretical determination of proton affinity differences in Zeolites. *J. Am. Chem. Soc.*, 155:2887–2897, 1993.

[49] M. Mabilia, R. A. Pearlstein, and A. J. Hopfinger. Molecular modelling of Zeolite structure. 1. Properties of the sodalite cage. *J. Am. Chem. Soc.*, 109:7960–7968, 1987.

[50] J. B. Nicholas, A. J. Hopfinger, F. R. Trouw, and L. E. Iton. Molecular modelling of Zeolite structure. 2. Structure and dynamics of silica sodalite and silicate force field. *J. Am. Chem. Soc.*, 113:4792–4800, 1991.

[51] M. J. Sanders, M. Leslie, and C. R. A. Catlow. Interatomic potentials for SiO_2. *J. Chem. Soc. Chem. Commun.*, pages 1271–1273, 1984.

[52] K. S. Smirnov and D. Bougeard. Molecular Dynamics study of the virational spectra of siliceous zeolites built from Sodalite cages. *J. Phys. Chem.*, (97):9434–9440, 1993.

[53] B. W. H. van Beest, G. J. Kramer, and R. A. van Santen. Force fields for Silicas and Aluminophosphates based on *ab initio* calculations. *Phys. Rev. Let.*, 64(16):1955–1958, 1990.

[54] S. M. Auerbach. Analytical theory of benzene diffusion in Na-Y zeolite. *J. Chem. Phys.*, 106(18):7810–7815, 1997.

[55] S. Bandyopadhyay and S. Yashonath. Diffusion anomoly in Silicalite and VPI-5 from molecular dynamics simulations. *J. Phys. Chem.*, 99:4286–4292, 1995.

[56] C. Blanco and S. M. Auerbach. Nonequilibrium Molecular Dynamics of microwave driven Zeolite-Guest systems: Loading dependence of athermal effects. *J. Phys. Chem. B*, 107:2490–2499, 2003.

[57] C. R. A. Catlow, C. M. Freeman, B. Vessal, S. M. Tomlinson, and M. Leslie. Molecular Dynamics studies of hydrocarbon diffusion in Zeolites. *J. Chem. Soc. Faraday. Trans.*, 87(13):1947–1950, 1991.

[58] D. Dubbeldam and B. Smit. Computer simulation of incommensurate diffusion in Zeolites: Understanding window effects. *J. Phys. Chem. B*, 107:12138–12152, 2003.

[59] R. L. June, A. T. Bell, and D. N. Theodorou. Molecular dynamics studies of butane and hexane in silicalite. *J. Phys. Chem.*, 96:1051–1060, 1992.

[60] D. I. Kopelevich and H-C. Chang. Diffusion of inert gases in silica sodalite: Importance of lattice flexibility. *J. Chem. Phys.*, 115(20):9519–9527, 2001.

[61] F. Leroy, B. Rousseau, and A. H. Fuchs. Self-diffusion of *n*-alkanes in silicalite using molecular dynamics simulation: A comparison between rigid and flexible frameworks. *Phys. Chem. Chem. Phys.*, 6:775–783, 2004.

[62] J.M.D. MacElroy and S.H. Suh. Equilibruim and nonequilibrium molecular dynamics studies of diffusion in model one-dimensional micropores. *Micopor. Mesopor. Mat.*, 48:195–202, 2001.

[63] T. Mosell, G. Schrimpf, and J. Briskmann. Diffusion of aromatic molecules in Zeolite NaY. 1. contrained reaction coordinate dynamics. *J. Phys. Chem. B*, 101:9476–9484, 1997.

[64] T. Mosell, G. Schrimpf, and J. Briskmann. Diffusion of aromatic molecules in Zeolite NaY. 2. dynamical corrections. *J. Phys. Chem. B*, 101:9485–9494, 1997.

[65] M. A. C. Nascimento. Computer simulations of the adsorption process of light alkanes in high silica zeolites. *J. Mol. Struct.*, 464:239–247, 1999.

[66] S. D. Pickett, A. K. Nowak, J. M. Thomas, B. K. Peterson, J. F. P. Swift, A. K. Cheethams, C. J. J. den Ouden, and M. F. M. Post. Mobility of adsorbed species in Zeolites: a molecular dynamics simulation of Xenon in Silicalite. *J. Phys. Chem.*, 94:1233–1236, 1990.

[67] R. Runnebaum and E. Maginn. Molecular dynamics simulations of alkanes in the zeolite Silicalite: Evidence for resonant diffusion effects. *J. Phys. Chem. B*, 101:6394–6408, 1997.

[68] G. Sastre, N. Raj, C. R. A. Catlow, R. Roque-Malherbe, and A. Corma. Selective diffusion of C8 aromitics in a 10 and 12 MR zeolite. a molecular dynamics study. *J. Phys. Chem. B*, 102:3198–3209, 1998.

[69] D. Schuring, A. P. J. Jansen, and R. A van Santen. Concentration and chainlength dependence of the diffusivity of alkanes in Zeolites studied with MD simulations. *J. Phys. Chem. B*, 104:941–948, 2000.

[70] L. Song, Z-L. Sun, and L. V.C. Rees. Experimental and molecular simulation studies of adsorption and diffusion of cyclic hydrocarbons in silicalite-1. *Microporous Mesoporous Mater*, 55:31–49, 2002.

[71] E. B. Webb III, G. S. Crest, and M. Mondello. Intracrystalline diffusion of linear and branched alkanes in the zeolites TON, EUO and MFI. *J. Phys. Chem. B*, 103:4949–4959, 1999.

[72] S. Yashonath and P. Santikary. Diffusion of sorbates in zeolites Y and A: Novel dependence on sorbate size and strength of sorbate-zeolite interaction. *J. Phys. Chem.*, 98:6368–6376, 1994.

[73] L. Song and L. V. C. Rees. Adsorption and diffusion of cyclic hydrocarbons in MFI-type zeolites studied by gravimetric and frequency-response techniques. *Microporous Mesoporous Mater.*, 35-36:301–314, 2000.

[74] D. Frenkel and B. Smit. *Understanding Molecular Simulation. From Algorithms to Applications*. Academic Press, 2nd edition, 2002.

[75] L. R. Pratt. A statistical method for identifying transition states in high dimensional problems. *J. Chem. Phys.*, 85:5045–5048, 1986.

[76] M. C. Payne, M. Hytha, I. Stich, J. D. Gale, and K. Terakura. First principles calculation of the free energy barrier for the reaction of methanol in a zeolite catalyst. *Microporous Mesoporous Mater.*, 48:375–381, 2001.

[77] K. Schwarz, E. Nusterer, and P. E. Blöchl. First-principles molecular dynamics study of small molecules in zeolites. *Catal. Today*, 3-4(50):501–509, 1999.

[78] P. Adhangale and D. Keffer. A grand canonical Monte Carlo study of the adsorption of Methane, Ethane, and their mixtures in one-dimensional nanoporous materials. *Langmuir*, 18:10455–10461, 2002.

[79] S. P. Bates and R. A. van Santen. The molecular basis of zeolite catalysis: A review of theoretical simulations. *Advances in Catalysis*, 42:1–114, 1998.

[80] E. Beerdsen, D. Dubbeldam, B. Smit, T. J. H. Vlugt, and S. Calero. Simulating the effect of nonframework cations on the adsorption of alkanes in MFI-type zeolites. *J. Phys. Chem. B*, 107:12088–12096, 2003.

[81] E. Beerdsen, B. Smit, and S. Calero. The influence of non-framework sodium cations on the adsorption of alkanes in MFI and MOR-type zeolites. *J. Phys. Chem. B*, 106:10659–10667, 2002.

[82] L. A. Clark and R. Q. Snurr. Adsorption isotherm sensitivity to small changes in zeolite structure. *Chem. Phys. Lett.*, 308:155–159, 1999.

[83] J. P. Fox, V. Rooy, and S. P. Bates. Simulating the adsorption of linear, branched and cyclic alkanes in silicalite-1 and $AlPO_4$-5. *Microporous Mesoporous Mater.*, 69(1-2):9–18, 2004.

[84] K. Esselink, L. D. J. C. Loyens, and B. Smit. Parallel Monte Carlo simulations. *Phys. Rev. E*, 51(2):1560–1568, 1995.

[85] T. J. Grey, K. P. Travis, J. D. Gale, and D. Nicholson. A comparative simulation study of the adsorption of nitrogen and methane in siliceous heulandite and chabazite. *Micopor. Mesopor. Mat.*, 48:203–209, 2001.

[86] A. Gupta, L. A. Clark, and R. Q. Snurr. Grand Canonical Monte Carlo simulations of nonrigid molecules: Siting and segregation in silicalite zeolite. *Langmuir*, 16:3910–3919, 2000.

[87] I. Halasz, S. Kim, and B. Marcus. Uncommon adsorption isotherms of methanol on a hydrophobic Y zeolite. *J. Phys. Chem. B*, 105:10788–10796, 2001.

[88] I. Halasz, S. Kim, and B. Marcus. Hydrophilic and hydrophobic adsorption on Y zeolites. *Mol. Phys.*, 100(19):3123–3132, 2002.

[89] N. J. Henson, A. K. Cheetham, M. Stockenhuber, and J. A. Lercher. Modelling aromiatics in siliceous zeolites: a new forcefield from thermochemical studies. *J. Chem. Soc. Faraday. Trans.*, (94):3759–3786, 1998.

[90] R. L. June, A. T. Bell, and D. N. Theodorou. Prediction of low occupancy sorption of alkanes in silicalite. *J. Phys. Chem.*, 94:1508–1516, 1990.

[91] T. L. M. Maesen, S. Calero, M. Schenk, and B. Smit. Alkane hydrocracking: shape selectivity or kinetics? *J. Catal.*, 221:241–251, 2004.

[92] E. J. Maginn, A. T. Bell, and D. N. Theodorou. Sorption thermodynamics, siting, and conformation of long *n*-alkanes in silicalite as predicted by configurational bias Monte Carlo integration. *J. Phys. Chem.*, 99:2057–2079, 1995.

[93] T. Maris, T. J. H. Vlugt, and B. Smit. Simulation of alkane adsorption in the aluminophosphate molecular sieve $AlPO_4$-5. *J. Phys. Chem. B*, 102:7183–7189, 1998.

[94] J. B. Ndjaka, G. Zwanenburg, B. Smit, and M. Schenk. Molecular simulations of adsorption isotherms of small alkanes in FER-, TON-, MTW- and DON- type zeolites. *Microporous Mesoporous Mater.*, 68:37–43, 2004.

[95] N. Raj, G. Sastre, and C. R. A. Catlow. Diffusion of octane in silicalite: A molecular dynamics study. *J. Phys. Chem. B*, 103:11007–11015, 1999.

[96] B. Smit and T. L. M. Maesen. Commensurate 'freezing' of alkanes in the channels of a zeolite. *Nature*, 374:42–44, 1995.

[97] B. Smit, L. D. J. C. Loyens, and G. L. M. M. Verbist. Simulation of adsorption and diffusion of hydrocarbons in zeolites. *Faraday Discuss.*, 106:93–104, 1997.

[98] B. Smit and R. Krishna. Monte Carlo simulations in zeolites. *Curr. Opin. Solid St. M.*, pages 455–461, 2001.

[99] B. Smit and R. Krishna. Molecular simulations in zeolitic process design. *Chem. Eng. Sci.*, 58:557–568, 2003.

[100] B. Smit and J. I. Sipemann. Computer simulations of the energetics and siting of *n*-alkanes in zeolites. *J. Phys. Chem.*, 98:8442–8452, 1994.

[101] B. Smit and J. I. Siepmann. Simulating the adsorption of alkanes in Zeolites. *Science*, 264:1118–1120, 1994.

[102] R. Q. Snurr, A. T. Bell, and D. N. Theodorou. Prediction of adsorption of aromatic hydrocarbons in silicalite from grand canonical Monte Carlo simulations with biased insertions. *J Phys. Chem.*, 97:13742–13752, 1993.

[103] T. J. H. Vlugt and M. Schenk. Influence of framework flexibility on the adsorption properties of hydrocarbons in the zeolite silicalite. *J. Phys. Chem. B*, 106:12757–12763, 2002.

[104] T. J. H. Vlugt, W. Zhu, F. Kapteijn, J. A. Moulijn, B. Smit, and R. Krishna. Adsorption of linear and branched alkanes in the zeolite Silicalite-1. *J. Am. Chem. Soc.*, 120:5599–5600, 1998.

[105] S. Calero, B. Smit, and R. Krishna. Configurational entropy effects during sorption of hexane isomers in silicalite. *J. Catal.*, 202:395–401, 2001.

[106] S. Calero, B. Smit, and R. Krishna. Separation of linear, mono-methyl and di-methyl alkanes in the 5-7 carbon atom range by exploiting configurational entropy effects during sorption on silicalite-1. *Phys. Chem. Chem. Phys.*, 3:4390–4398, 2001.

[107] S. Chempath, J. F. M. Denayer, K. M. A. De Meyer, G. V. Baron, and R. Q. Snurr. Adsorption of liquid-phase alkane mixtures in silicalite: simulations and experiments. *Langmuir*, 20:150–156, 2004.

[108] L. A. Clark, A. Gupta, and R. Q. Snurr. Siting and segregation effects of simple molecules in zeolites MFI, MOR and BOG. *J. Phys. Chem. B*, 102:6720–6731, 1998.

[109] J. P. Fox and S. P. Bates. Simulating the adsorption of binary and ternary mixtures of linear, branched and cyclic alkanes in zeolites. *J. Phys. Chem. B*, 108:17136–17142, 2004.

[110] A. H. Fuchs and A. K. Cheetham. Adsorption of guest molecules in zeolitic materials: Computational aspects. *J. Phys. Chem. B*, 105(31):7375–7383, 2001.

[111] R. Krishna. Exploiting configurational entropy effects for separation of hexane isomers using Silicalite-1. *Trans. IChemE.*, 79:182–194, 2001.

[112] R. Krishna, S. Calero, and B. Smit. Investigation of entropy effects during sorption of mixtures of alkanes in MFI zeolite. *Chem. Eng. J.*, 88(1-3):81–94, 2002.

[113] R. Krishna, B. Smit, and S. Calero. Entropy effects during sorption of alkanes in zeolites. *Chem. Soc. Rev.*, 31:185–194, 2002.

[114] R. Krishna, B. Smit, and T. J. H. Vlugt. Sorption induced diffusion selective separation of hydrocarbon isomers using silicalite. *J. Phys. Chem. A*, 102(40):7727–7730, 1998.

[115] L. Lu, Q. Wang, and Y. Liu. Adsorption and separation of ternary and quaternary mixtures of short linear alkanes in zeolites by Molecular simulation. *Langmuir*, 19:10617–10623, 2003.

[116] M. Schenk, S. Calero, T. L. M. Maesen, L. L. van Benthem, M. G. Verbeek, and B. Smit. Understanding zeolite catalysis: Inverse shape selectivity revisited. *Angew. Chem. Int. Ed*, 41(14):2500–2502, 2002.

[117] M. Schenk, S. L. Vidal, T. J. H. Vlugt, B. Smit, and R. Krishna. Separation of alkane isomers by exploiting entropy effects during adsorption on silicalite-1. a Configurational Bias Monte Carlo simulation study. *Langmuir*, 17:1558–1570, 2001.

[118] D. Schuring, A. O. Koriabkina, A. M. de Jong, B. Smit, and R. A. van Santen. Adsorption and diffusion of *n*-Hexane/2-Methylpentane mixtures in zeolite Silicalite: Experiments and modelling. *J. Phys. Chem. B*, 105:7690–7698, 2001.

[119] T. J. H. Vlugt, R. Krishna, and B. Smit. Molecular simulations of adsorption isotherms for linear and branched alkanes and their mixtures in silicalite. *J. Phys. Chem. B*, 103:1102–1118, 1999.

[120] M. W. Maddox, J. P. Olivier, and K. E. Gubbins. Characterization of MCM-41 using Molecular simulation: heterogeneity effects. *Langmuir*, 13:1737–1745, 1997.

[121] B. P. Feuston and J. B. Higgins. Model structures for MCM-41 materials: A Molecular Dynamics simulation. *J. Phys. Chem.*, 98:4459–4462, 1994.

[122] B. Coasne and R. J-M. Pellenq. Grand canonical Monte carlo simulation of argon adsorption at the surface of silica nanopores: Effect of pore size, pore morphology, and surface roughness. *J. Chem. Phys.*, 120(6):2913–2922, 2004.

[123] J. Yun, T. Duren, F. J. Keil, and N. A. Seaton. Adsorption of methane, ethane and their binary mixtures on MCM-41: Experimental evaluation of methods for the prediction of adsorption equilibriation. *Langmuir*, 18:2693–2701, 2002.

[124] Y. He and N. A. Seaton. Experimental and computer simulation studies of the adsorption of ethane, carbon dioxide, and their binary mixtures in MCM-41. *Langmuir*, 19:10132–10138, 2003.

[125] C. A. Koh, R. F. Westacott, R. I. Nooney, V. Boissel, S. F. Tahir, and V. Tricarico. Separation of dichloromethane-nitrogen mixtures by adsorption: experimental and molecular simulation studies. *Mol. Phys.*, 100(13):2087–2095, 2002.

[126] D. Cao, Z. Shen, J. Chen, and X. Zhang. Experiment, molecular simulation and density functional theory for investigation of fluid confined in MCM-41. *Microporous Mesoporous Mater.*, 67:159–166, 2004.

[127] J. Wloch, M. Rozwadowski, M. Lezanska, and K. Erdmann. Analysis of the pore structure of the MCM-41 materials. *Appl. Surf. Sci.*, 191:368–374, 2002.

[128] C. A. Koh, T. Montanari, R. I. Nooney, S. F. Tahir, and R. E. Westacott. Experimental and computer simulation studies of the removal of carbon dioxide from mixtures with methane using $AlPO_4$-5 and MCM-41. *Langmuir*, 15:6043–6049, 1999.

[129] S. Kallus, A. Hahn, and J. D. F. Ramsay. Gas adsorption in mcm-41 porous silicas dynamics measurements using sans. *Eur. Phys. J. E*, S01:S31–S33, 2003.

[130] J Jänchen, H. Stach, M. Busio, and J. H. M. C. van Wolput. Microcalorimetric and spectroscopic studies of the acidic- and physisiorption characteristics of MCM-41 and zeolites. *Thermochim. Acta.*, 312:33–45, 1998.

[131] D. Kumar, G. K. Dey, and N. M. Gupta. Nanoparticles of uranium oxide occluded in MCM-41 silica host: influence of synthesis condition on the size and the chemisorption behaviour. *Phys. Chem. Chem. Phys.*, 5:5477–5484, 2003.

[132] S. Z. Qiao, S. K. Bhatia, and D. Nicholson. Study of hexane adsorption in nanoporous MCM-41 silica. *Langmuir*, 20:389–395, 2004.

[133] X. S. Zhao, Q. Ma, and G. Q. Lu. VOC removal: Comparison of MCM-41 with hydrophobic zeolites and activated carbon. *Energ. Fuel.*, 12:1051–1054, 1998.

[134] M. M. L. Ribeiro Carrott, A. J. E. Candeias, P. J. M. Carrott, P. I. Ravikovitch, A. V. Neimark, and A. D. Sequeira. Adsorption of nitrogen, neopentane, *n*-hexane, benzene and methanol for the evaluation of pore sizes in silica grades of MCM-41. *Microporous Mesoporous Mater.*, 47:323–337, 2001.

[135] X. S. Zhao, G. Q. Lu, and X. Hu. Organophilicity of MCM-41 adsorbents studied by adsorption and temperature-programmed desorption. *Colloids Surf., A*, 179:261–269, 2001.

[136] Y. Long, T. Xu, Y. Sun, and W. Dong. Adsorption behaviour on defect structure of mesoporous molecular sieve MCM-41. *Langmuir*, 14:6173–6178, 1998.

[137] J. Li and O. Talu. Structural effect on molecular simulations of tight-pore systems. *J. Chem. Soc. Faraday Trans.*, 89(11):1683–1687, 1993.

[138] J. S. Beck, J. C. Vartuli, W. J. Roth, M. E. Leonowicz, C. T. Kresge, K. D. Schmitt, C. T-W. Chu, D. H. Olson, E. W. Sheppard, S. B. McCullen, J. B. Higgins, and J. L. Schlenker. A new family of mesoporous molecular sieves prepared with liquid crystal templates. *J. Am. Chem. Soc.*, 114:10834–10843, 1992.

[139] M. P. Allen and D. J. Tildesley. *Computer Simulations of liquids*. Clarendon Press, 2nd edition, 1987.

[140] S. Brunauer. *The adsorption of gases and vapours*. Oxford University Press, 1944.

[141] D. M. Ruthven. *Principles of adsorption and adsorption processes*, page 91. John Wiley, 1984.

[142] R. Shah, J. D. Gale, and M. C. Payne. Methanol adsorption in zeolites - a first principles study. *J. Phys. Chem.*, 100:11688, 1996.

[143] R. Shah, J. D. Gale, and M. C. Payne. In situ study of reaction intermediates of methanol in zeolites from first principles calculations. *J. Phys. Chem. B*, 101:4787–4797, 1997.

[144] R. Shah, M. C. Payne, M-H. Lee, and J. D. Gale. Understanding the catalytic behaviour of zeolites: a first-principles study of the adsorption of methanol. *Science*, 271:1395–1397, 1996.

[145] A. L. Myers and J. M. Prausnitz. Thermodynamics of mixed-gas adsorption. *A.I.Ch.E. J*, 11(1):121–127, 1965.

[146] B. Smit, Ph. de Smedt, and D. Frenkel. Computer simulations in the gibbs ensemble. *Mol. Phys.*, 68:931–950, 1989.

[147] J. S. Rowlinson and B. Widom. *Molecular Theory of capillarity*, page 261. Oxford University Press, 1989.

[148] J. S. Rowlinson and F. L. Swinton. *Liquids and Liquid mixtures*, pages 70–75. Butterworth, 1982.

[149] L. Dougan, S. P. Bates, R. Hargreaves, J. P. Fox, J. Crain, J. L. Finney, V. Réat, and A. K. Soper. Methanol-water solutions: A bi-percolating liquid mixture. *J. Chem. Phys*, 121:6456–6462, 2004.

[150] S. K. Allison, J. P. Fox, R. Hargreaves, and S. P. Bates. Clustering and Micro-immiscibility in Alcohol-Water Mixtures: Evidence from Molecular Dynamics Simulations. *Phys. Rev. B*, 2004.

[151] D. R. Lide and H. V. Kehiaian. *CRC Handbook of thermophysical and thermochemical data.* CRC Press, 994.

[152] http://www.csc.fi/gopenmol.

[153] http://www.opendx.org.

[154] H. A. Lorentz. *Ann. Phys.*, 12:127, 1881.

[155] D. C Berthelot. *C. R. Acad. Sci., Paris*, 126:1703, 1898.

[156] K. Palmö, N. G. Mirkin, L.-O Pietilä, and S. Krimm. Spectroscopically determined force fields for macromolecules. 1 *n*-alkane chains. *MacroMol.*, 26:6831–6840, 1993.

[157] D. R. Lide, editor. *Handbook of Chemistry and Physics.* CRC, 73rd edition, 1992.

[158] A.G. Bezus, A.V. Kiselev, A.A. Lopatkin, and P. Quang Du. *J. Chem. Soc. Faraday Trans.2*, 74:367–379, 1978.

[159] D. H Olson and W. O. Haag. *Structure selectivity relationship in xylene isomerization and selective toluene disproportionation*, volume 248. ACS Symposium Series, 1984.

[160] G. Xomeritakis, S. Nair, and M. Tsapatsis. Transport properties of alumina-supported MFI membranes made by secondary (seeded) growth. *Microporous Mesoporous Mater.*, 38:61–73, 2000.

[161] http://molsim.chem.uva.nl/bigmac/.

[162] T. J. H. Vlugt and B. Smit. BIGMAC, a configurational bias Monte Carlo program. University of Amsterdam, 1998.

[163] L. N. Canjar and F. S. Manning. *Thermodynamic properties and reduced correlations for gases*. Gulf, 1967.

[164] R. E. Richards and L. V. C. Rees. Sorption and packing of *n*-alkane molecules in ZSM-5. *Langmuir*, 3:335–340, 1987.

[165] H. Stach, U. Lohse, H. Thamm, and W. Schriner. Adsorption equilibria of hydrocarbons on highly dealuminated zeolites. *Zeolites*, 6:74–90, 1985.

[166] M. S. Sun, O. Talu, and D. B. Shah. Adsorption equilibria of C_5-C_{10} normal alkanes in silicalite crystals. *J. Phys. Chem.*, 100:17276–17280, 1996.

[167] C. L. Cavalcante Jr and D. M. Ruthven. Adsorption of branched and cyclic paraffins in silicalite. 2. Kinetics. *Ind. Eng. Chem. Res.*, 34:185–191, 1995.

[168] F. Eder and J. A. Lercher. Alkane sorption in molecular sieves: the contribution of ordering, intermolecular interactions, and sorption on Brønsted acid sites. *Zeolites*, 18:75–81, 1997.

[169] B. L. Newalkar, R. V. Jasra, V. Kamath, and S. G. T Bhat. Sorption of C_6 alkanes in Aluminophosphate molecular sieve, $AlPO_4$-5. *Adsorption*, 5:345–357, 1999.

[170] C. L. Cavalcante(Jr) and D. M. Ruthven. Adsorption of branched and cyclic paraffins in silicalite. *Ind. Eng. Chem. Res.*, 34:177–184, 1995.

[171] S.Ashtekar, J. J. Hastings, and L. F. Gladden. FT-Raman studies of single component and binary adsorption in silicalite-1. *J. Chem. Soc. Faraday. Trans.*, 94(8):1157–1161, 1998.

[172] B. Paweewan, P. J. Barrie, and L. F. Gladden. Coking and deactivation during *n*-hexane cracking in ultrastable zeolite Y. *Appl. Catal. A*, 185:259–268, 1999.

[173] B. Paweewan, P. J. Barrie, and L. F. Gladden. Coking during ethene conversion on ultrastable zeolite Y. *Appl. Catal. A*, 167:353–362, 1998.

[174] D. M. Nace. Catalytic cracking over crystalline aluminosilicates. I. *I and EC produce Research and Development*, 8(1):24–31, 1969.

[175] D. M. Nace. Catalytic cracking over crystalline aluminosilicates. II. *I and EC produce Research and Development*, 8(1):31–38, 1969.

[176] J. Abbot. Cracking reactions of C_6 paraffins on HZSM-5. *Appl. Catal.*, 57:105–125, 1990.

[177] S. Jolly, J. Saussey, M. M. Bettahar, J. C. Lavalley, and E. Benazzi. Reaction mechanicsms and kinetics in the *n*-hexane cracking over zeolites. *Appl. Catal. A*, 156:71–96, 1997.

[178] L. V. C. Rees, J. Hampson, and P. Brückner. Sorption of single gases and their binary mixtures in zeolites. In *Zeolites Microporous solids: Synthesis , Structure and Reactivity*, page 13. Kluwer Academic, 1992.

[179] H. H. Funke, A. M. Argo, J. L. Falconer, and R. D. Noble. Separations of Cyclic, Branched, and Linear Hydrocarbon mixtures through Silicalite membranes. *Ind. Eng. Chem. Res.*, 36:137–143, 1997.

[180] H. H. Funke, M. G. Kovalchick, J. L. Falconer, and R. D. Noble. Separation of hydrocarbon isomer vapours with Silicalite zeolite membranes. *Ind. Eng. Chem. Res.*, 35:1575–1582, 1996.

[181] S. Sommer, T. Melin, J. L. Falconer, and R. D. Noble. Transport of C_6 isomers through ZSM-5 zeolite membranes. *J. Membr. Sci.*, 224:51–67, 2003.

[182] a gauche bond has a dihedral angle of $\pm$ 120 degrees.

[183] Y. Huang and H. Wang. An investigation of the conformational behaviour of *n*-hexane adsorbed in zeolites by FT-Raman spectroscopy. *Langmuir*, 19:9706–9713, 2003.

[184] S. K. Gade, V. A. Tuan, C. J. Gump, R. D. Noble, and J. L. Falconer. Highly selective separation of *n*-hexane from branched, cyclic and aromatic hydrocarbons using B-ZSM-5 membranes. *Chem. Commun.*, pages 601–602, 2001.

[185] C. J. Gump, R. D. Noble, and J. L. Falconer. Separation of Hexane isomers throught Nonzeolite pores in ZSM-5 Zeolite membranes. *Ind. Eng. Chem. Res.*, 38:2775–2781, 1999.

[186] V. Gusev. http://boba.boom.ru.

[187] E. P. Barrett, L. G. Joyner, and P. P. Halenda. The Determinations of Pore Volume and Area Distributions in Porous Substances. I. Computations from Nitrogen Isotherms. *J. Am. Chem. Soc.*, 73:373–380, 1951.

[188] P. Trens, N Tanchoux, D. Maldonado, A. Galarneua, F. Di Renzo, and F. Fajula. Study of *n*-hexane adsorption in MCM-41 mesoporous materials: a scaling effect approach of capillary condensation processes. *New. J. Chem.*, 28:874–879, 2004.

[189] C-Y. Chen, S-Q. Xiao, and M. E. Davis. Studies on ordered mesoporous materials III. Comparison of MCM-41 to mesoporous materials derived from kanemite. *Microporous Mater.*, 4:1–20, 1995.

[190] M. Schoen, D. J. Diestler, and J. H. Cushman. Fluids in micropores. i. structure of a simple classical fluid in a slit-pore. *J. Chem. Phys.*, 87:5464–5476, 1987.

[191] W-J. Ma, J. R. Banavar, and J. Koplik. A molecular dynamics study of freezing in a confined geometry. *J. Chem. Phys.*, 97:485–493, 1992.

[192] A. Papadopoulou, F. van Swol, and U. Marconi. Pore-end effects on adsorption hysteresis in cylindrical and slitlike pores. *J. Chem. Phys.*, 97:6942–6952, 1992.

[193] Y. Zhou and G. Stell. Nonlocal integral-equation approximations. i. the zeroth order (hydrostatic) approximation with applications. *J. Chem. Phys.*, 92:5533–5544, 1990.

[194] S. Sokolowski and J. Fischer. Relation between Born-Green-Yvon solutions and chemical potential for a fluid inside a pore. *J. Chem. Phys.*, 93:6787–6792, 1990.

[195] D. Henderson and S. Sokolowski. Adsorption in a spherical cavity. *Phys. Rev. E*, 52(1):758–762, 1995.

[196] Y. Duda, S. Sokolowski, P. Bryk, and O. Pizio. Structure and adsorption of a hard sphere fluid in a cylindrical and spherical pore filled by a disordered matrix: A Monte Carlo study. *J. Phys. Chem. B*, 102:5490–5494, 1998.

[197] R. J. M. Pellenq and P. E. Levitz. Capillary condensation in a disordered mesoporous medium: a grand canonical Monte Carlo study. *Mol. Phys.*, 13:2059–2077, 2002.

[198] C. Schumacher. *Private Communcication.*

[199] S. Brunauer, P. H. Emmett, and E. Teller. Adsorption of gases in Multimolecular layers. *J. Am. Chem. Soc*, 60:309, 1938.

[200] M-A. Springuel-Huet, K. Sun, and J. Fraissard. On the roughness of the internal surface of MCM-41 materials studies by ^{129}Xe NMR. *Micropor. Mesopor. Mater.*, 33:89–95, 1999.

[201] O. Franke, G. Scultz-Elkoff, J. Rathouský, J. Stárek, and A. Zukal. Unusual type of adsorption isotherm describing capillary condensation without hysteresis. *J. Chem. Soc., Chem. Commun.*, pages 724–726, 1993.